IntechOpen

# Ultrasound Elastography

*Edited by Monica Lupsor-Platon*

# Ultrasound Elastography

*Edited by Monica Lupsor-Platon*

Published in London, United Kingdom







IntechOpen






*Supporting open minds since 2005*

Ultrasound Elastography
http://dx.doi.org/10.5772/intechopen.80108
Edited by Monica Lupsor-Platon

Contributors
Binafsha Manzoor Syed, Jawaid Naeem Qureshi, Bikha Ram Devrajani, Ahmed Ghandour, Roxana Sirli, Alina Popescu, Ioan Sporea, Roxana Pintican, Angelica Chiorean, Diana Feier, Dan Eniu, Maria Magdalena Duma, Samuel Nguku Gitau, Issa Menge, Michael Pykov, Natalya Kuzmina, N. M. Rostovtsev, A. Yu. Kinzersky, Monica Lupsor-Platon, Lidia Ciobanu



First published in London, United Kingdom, 2020 by IntechOpen
IntechOpen is the global imprint of INTECHOPEN LIMITED, registered in England and Wales, registration number: 11086078, 7th floor, 10 Lower Thames Street, London, EC3R 6AF, United Kingdom
Printed in Croatia

British Library Cataloguing-in-Publication Data
A catalogue record for this book is available from the British Library

Additional hard and PDF copies can be obtained from orders@intechopen.com

Ultrasound Elastography
Edited by Monica Lupsor-Platon
p. cm.
Print ISBN 978-1-78985-709-2
Online ISBN 978-1-78985-710-8
eBook (PDF) ISBN 978-1-83880-015-4

# Meet the editor

Monica Lupşor-Platon MD, PhD is an Associate Professor of Medical Imaging at the Iuliu-Hatieganu University of Medicine and Pharmacy, Cluj-Napoca, Romania. She is currently working in the Department of Ultrasonography and Elastography of the Institute of Gastroenterology and Hepatology in Cluj. She is involved in the medical education of students and residents and she teaches postgraduate courses in abdominal ultrasonography and elastography. She has carried out important research activity, especially in the field of non-invasive evaluation of fibrosis and steatosis in diffuse liver diseases using ultrasonographic and elastographic methods, resulting in several scientific papers, with currently over 3000 citations and many national and international awards. She is the author of 3 books and 16 chapters. She is a member of many Romanian and European scientific societies.

# Contents

# Preface

Elastography, the science of creating noninvasive images of mechanical characteristics of tissues, has been rapidly evolving in recent years. The advantage of this technique is its ability to rapidly detect and quantify the changes in soft tissue stiffness resulting from specific pathological or physiological processes. Ultrasound elastography is nowadays applied especially on the liver and breast, but the technique has been increasingly used for other tissues including the thyroid, lymph nodes, spleen, pancreas, gastrointestinal tract, kidney, prostate, and the musculoskeletal and vascular systems.

This book presents some of the applications of strain and shear-wave ultrasound elastography in hepatic, pancreatic, breast and musculoskeletal conditions.

Most of the book is focused on diffuse liver conditions, since the evaluation of diffuse liver disease is the best validated application of ultrasound elastography and has been widely adopted for non-invasive detection and staging of liver fibrosis and steatosis, for the diagnosis of cirrhosis and its complications, as well as for monitoring disease progression. The main elastographic techniques in these conditions are reviewed, namely Vibration Controlled Transient Elastography (VCTE), point-Shear Waves Elastography, and 2D Share Wave Elastography.

The use of elastography in breast conditions is also discussed; specifically, the technique is used for differentiating benign focal lesions from suspicious focal lesions (in general, benign lesions have low stiffness, while malignant lesions have high stiffness). Both strain and shear-wave methods have been evaluated for improving the generally high sensitivity and specificity of the Breast Imaging Reporting and Data System (BIRADS) and it is recommended that they are used to enhance the usual ultrasound examination.

Another chapter reviews pancreatic elastography, a challenging new procedure used for inflammatory and tumoral conditions. Certain technical difficulties, such as the deep location of the organ, impede the accurate assessment of pancreatic stiffness, but the new software for both conventional and endoscopic ultrasound offer promise for the differential diagnosis between malignant tumors and different forms of chronic pancreatitis.

The last chapter includes some preliminary data on the strain-based elastography assessment of patients with De Quervain tenosynovitis.

Evidently, further research with unbiased large-scale studies is still required, but ultrasound elastography holds immense potential for various clinical applications, and its continued development will warrant its widespread clinical use in the upcoming years.

**Monica Lupşor-Platon**
Associate Professor,
Department of Medical Imaging,
Iuliu Hatieganu University of Medicine and Pharmacy,
Cluj-Napoca, Romania

Regional Institute of Gastroenterology and Hepatology "Prof. Dr. Octavian Fodor",
Cluj-Napoca, Romania

Section 1

# Liver Elastography

Chapter 1

# Noninvasive Assessment of Diffuse Liver Diseases Using Vibration-Controlled Transient Elastography (VCTE)

*Monica Lupsor-Platon*

## Abstract

Because of the limitations and invasive nature of liver biopsy, other noninvasive means are being tested for the evaluation of diffuse liver diseases. One of these methods is vibration-controlled transient elastography (VCTE). This chapter reviews the principle of VCTE, the examination technique, the normal range for liver stiffness values, the pathological changes that may influence liver stiffness, as well as the diagnostic performance in several diffuse liver diseases, especially chronic hepatitis C, chronic hepatitis B, nonalcoholic steatohepatitis, and alcoholic liver disease. Apart from the assessment of fibrosis stages, we will also discuss the diagnosis of cirrhosis and its complications as well as other applications of VCTE, reviewing its advantages and limitations.

**Keywords:** diffuse liver disease, fibrosis, noninvasive, vibration-controlled transient elastography, Fibroscan

## 1. Introduction

Chronic liver diseases are an important public health issue. Extensive research has been made lately on the development of noninvasive diagnostic methods, able to accurately assess fibrosis and steatosis. Among these, an important place is reserved for elastographic techniques and especially vibration-controlled transient elastography (Fibroscan).

## 2. Principle

Vibration-controlled transient elastography is performed with the Fibroscan® equipment (Echosens, Paris) [1]. The transducer of the device is placed in an intercostal space above the right liver lobe, in a point of maximal hepatic dullness. A mechanical vibrator is mounted on the axis of the device; the vibrator generates a painless vibration, inducing a train of elastic waves, which propagate through the skin and subcutaneous tissue to the liver. In parallel to the vibration, the transducer performs ultrasound acquisitions, at a frequency of 4 kHz [1–3] By comparing the ultrasonographic signals thus obtained, tissue deformation records, induced by the propagation of the elastic wave, can be drawn. The time necessary for the train of waves to propagate along the interest

area, as well as the velocity of propagation, is recorded. The liver stiffness can afterwards be calculated using the formula: $E = 3\rho Vs2$ (E, the elasticity module; ρ, density; Vs, the elastic wave velocity in the liver parenchyma). The stiffer the tissue, the higher the velocity of the wave train [1–3].

On the other hand, knowing that fat impairs ultrasound propagation and induces attenuation, the producers of the Fibroscan equipment have developed a software able to precisely quantify the ultrasound attenuation. This controlled attenuation parameter (CAP) is expressed in dB/m and is calculated using the same radio-frequency data, and the same region of interest, as the region used to assess the liver stiffness [4, 5].

## 3. Examination technique

The patient is placed in a dorsal decubitus position, with the right arm in maximum abduction above the head, in order to best expose the right abdominal quadrant, perpendicularly to the intercostal space, in an area of maximal dullness, free of any large vascular structure [1, 3]. When pressing the transducer button, the vibration is generated and transmitted to the liver. The software of the equipment analyzes the tissue deformation records and measures the stiffness of the parenchyma. The results are expressed in kilopascals (kPa) and represent the median value of 10 valid measurements. The equipment can measure values ranging between 2.5 and 75 kPa [1, 3]. At the same time, the software can measure both the liver stiffness (for the assessment of fibrosis) and the controlled attenuation parameter, CAP (for the assessment of steatosis).

It is important to choose the correct transducer for the examinations (S, M, or XL). The choice is made according to the circumference of the thorax: if below 75 cm, the S probe is chosen (either S1 < 45 cm or S2 for 45–75 cm and the M probe for a thoracic circumference above 75 cm). The XL transducer will be chosen if the distance between the skin and the liver capsule exceeds 25 mm. It is worth mentioning that, when measured with the XL probe, the median liver stiffness is significantly lower than that measured with the M probe [6].

The examination should be performed after an overnight fast, or at least 2 hours after a meal, because a postprandial examination would raise the stiffness value due to increased hepatic blood flow [7, 8]. In addition, the patient should remain at rest for 10 minutes before the examination [9] and hold his or her breath during the examination [10].

A proper measurement can be performed even by a technician after a training period (approximately 100 cases) [6, 10], but the clinical interpretation of results must always be issued by an expert taking into account the demographic data, disease etiology, and biochemical profile at the moment of the examination [3, 11].

Following the manufacturer's recommendation, the assessment is reliable only when 10 valid readings and an IQR ≤ 30% of the median (IQR/M ≤ 30%) are obtained [9].

## 4. Normal range of liver stiffness

The mean value of liver stiffness in healthy subjects, without any known liver disease and with normal biochemistry and hematology tests, is 5.5 ± 1.6 kPa according to some authors [12] and 4.8 ± 1.3 kPa according to others [13]. Age does not appear to influence this value, but stiffness is higher in men than in women (5.8 ± 1.6 kPa vs. 5.2 ± 1.6 kPa) as well as in subjects with a BMI > 30 $kg/m^2$

(6.3 ± 1.9 kPa vs. 5.4 ± 1.5 kPa) [14]. It is very difficult to establish the normal range of liver stiffness without biopsy, but the reverse is not feasible. In a group of HCV patients, without pathological changes on the biopsy sample, the liver stiffness was 4.84 ± 1.49 kPa [15]. In our unit, values of or above 5.3 kPa have a positive predictive value of 90% for the prediction of a fibrosis stage of at least F1.

## 5. Pathological changes influencing liver stiffness

Although liver stiffness correlates very well with fibrosis, just a single physical parameter (stiffness) cannot be used to completely describe a complex biological system, in which fibrosis is just a part [2]. Liver stiffness is increased by hepatic inflammation (often but not exclusively revealed by an elevated transaminase level) [16–18], obstructive cholestasis [19], hepatic congestion [20], amyloidosis, lymphomas, and extramedullary hematopoiesis [9]. These error factors must be taken into consideration when interpreting the liver stiffness values.

*Necroinflammatory activity* leads to an increase in liver stiffness alongside the degree of histologic activity [21–23]. For instance, the tissue changes occurring during an acute hepatitis can associate a rise in liver stiffness reaching sometimes cirrhotic values, due to cellular intumescence and sometimes to severe cholestasis [24]. The contribution of these non-fibrotic alterations on stiffness has been demonstrated by recording the progressive decrease in stiffness alongside the decrease in transaminase levels [17, 18]. On the other hand, in patients with relapsed chronic hepatitis, the higher stiffness values are caused not only by pre-existing fibrosis but also to the superimposed cellular intumescence [16]. Therefore, caution is advised when interpreting the liver stiffness values in patients with increased ALT: if the ALT values exceed a 2.5-fold increase, there is a risk of overestimating the fibrosis stage which should be specified in the written report [15].

*Extrahepatic cholestasis* can increase the stiffness independently from fibrosis [19], and after biliary drainage, the liver stiffness values decrease at a mean rate of 1.2 ± 0.56 kPa for every 1 g/dL decrease in bilirubin levels. It would therefore be prudent to exclude a possible cholestasis through imaging and lab tests before interpreting liver stiffness values in order to avoid overestimating the fibrosis stage.

*Congestive heart failure* may lead to increased liver stiffness reaching even cirrhotic levels, due to a higher liver blood volume, in up to 60% of patients [25–27].

*Liver steatosis* influence on liver stiffness values remains controversial. In some studies, steatosis did not significantly affect stiffness values, even after adjusting for fibrosis stage, but the proportion of patients with severe steatosis was too low to allow accurate quantification of a potential influence [1, 21, 28]. Other studies, however, have proven that, for the same fibrosis stage and the same necroinflammation grade, the presence of steatosis leads to a significant increase in liver stiffness [29]; furthermore, the morphometric analysis of biopsy samples has proven that steatosis does change liver stiffness independently from fibrosis. This influence is negligible in cirrhotic patients, but significant in non-cirrhotic patients. Further studies are however required to clarify this issue [28].

## 6. Diagnostic performance of VCTE

### 6.1 Chronic hepatitis C (CHC)

The first patients to have benefited from vibration-controlled transient elastography were those diagnosed with chronic C viral hepatitis (HCV). Studies performed

on large groups of HCV patients indicate that the liver stiffness values are strongly correlated with fibrosis stage, but there is some degree of overlap between adjacent stages. The practical utility of the method is based on establishing certain threshold stiffness values for each fibrosis stage. The diagnosis of stages F ≥ 2, F ≥ 3, and cirrhosis is based on the following stiffness values: 5.2–9.5 kPa, 9.5–9.6 kPa, and 11–15 kPa, respectively, as proposed by certain studies [15, 21, 30–34]. As suggested by studies assessing other noninvasive methods [35], the difference between these values can be explained by the varying prevalence of each fibrosis stage in the analyzed groups as well as by the different aims of the investigation (screening strategy vs. exclusion strategy). Therefore, although the already-defined cutoffs may be relevant to a certain population, they may not be applicable in another population with different prevalence of fibrosis stage and with another diagnostic aim for performing VCTE. In any case, according to the EFSUMB guidelines, "TE can be used as the first-line assessment for the severity of liver fibrosis in patients with chronic viral hepatitis C. It performs best with regard to the ruling out of cirrhosis" [9].

### 6.2 Chronic hepatitis B (CHB)

In patients with CHB, VCTE has a similar performance as in CHC patients [9]. For this type of patients, Marcellin and collaborators [36], considering the METAVIR scoring system, have suggested as early as 2009 the 7.2 kPa stiffness value as the cutoff for the prediction of F ≥ 2 (Se 70%, Sp 83%, PPV 80%, NPV 73%, AUROC 0.81), 8.1 kPa for F ≥ 3 (Se 86%, Sp 85%, PPV 65%, NPV 95%, AUROC 0.93), and 11 kPa for the prediction of cirrhosis (Se 93%, Sp 87%, PPV 38%, NPV 99%, AUROC 0.93).

Other articles [37–42] have confirmed the performance of the method, yielding AUROC values raging between 0.80 and 0.90 (for the prediction of significant fibrosis) and liver stiffness cutoffs varying between 6.6 and 8.8 kPa [9, 43–47]. With regard to the prediction of cirrhosis, AUROCs vary between 0.81 and 0.97 and the cutoffs between 9.4 and 13.4 kPa [44, 45]. The meta-analyses have suggested that a liver stiffness above 11.7 kPa should raise the suspicion of cirrhosis in patients with CHB [9, 45].

Generally, the cutoff value used for the cirrhosis prediction is lower in CHB than in CHC patients. One explanation could be the fact that HBV infection is one of the causes of macronodular cirrhosis, so that the predominant macronodular regeneration and the fine fibrous septa surrounding the nodules mean a smaller quantity of fibrosis than in micronodular cirrhosis with thick fibrous septa. It follows that, generally, liver stiffness is lower in macronodular than in micronodular cirrhosis.

On the other hand, liver stiffness values below 5 kPa in patients with normal ALT and low serum HBV DNA levels (<2000 IU/ml) are characteristic for inactive HBV carriers [9, 48, 49]. VCTE can be used to rule out significant fibrosis and cirrhosis in HBV inactive carriers, which is the best indication for VCTE in HBV.

According to the EFSUMB guidelines, "TE is useful in patients with CHB to identify those with cirrhosis, but concomitant assessment of transaminases is required to exclude flare-ups (elevation > 5 times upper limit of normal)". In addition, TE is useful in inactive HBV carriers to rule out fibrosis, in case the liver stiffness is below 5 kPa [9].

### 6.3 Nonalcoholic steatohepatitis (NASH)

In NASH patients, the correlation between stiffness and fibrosis is weaker than in patients with chronic viral hepatitis, because of a different fibrosis distribution

pattern (in chronic viral hepatitis, fibrosis appears early in the periportal areas and gives rise to a dense, stellate, and regularly distributed portal fibrosis; in steatohepatitis, however, the fibrosis is located in the perisinusoidal space of the centrilobular area and in the walls of the centrilobular vein) [28, 50]. There is a direct proportion between the amount of dense, stellate portal fibrosis and liver stiffness, whereas perisinusoidal fibrosis distributed preferentially in the centrilobular areas does not proportionally increase the liver stiffness values, as was proven by morphometric studies [28].

A meta-analysis including 854 NASH patients examined with the M probe [51] has proven the very good performance of VCTE in diagnosing stages F ≥ 3 (Se 82%, Sp 82%) and F4 (Se 92%, Sp 92%) and its moderate performance in diagnosing significant fibrosis F ≥ 2 (Se 79%, Sp 75%). The cutoff yielded by various studies varies between 6.6 and 7.7 kPa (for F ≥ 2), 8–10.4 kPa (for F ≥ 3), and 10.3–17.5 kPa (for the prediction of cirrhosis) [50, 52–57].

The available data indicate that, in patients with NAFLD, VCTE is a highly accurate, noninvasive method for the exclusion of advanced fibrosis and a moderately accurate method for the exclusion of significant fibrosis. According to the EFSUMB and EASL Guidelines and Recommendations on the clinical use of liver ultrasound elastography, "TE can be used in NAFLD patients to confidently exclude severe fibrosis and especially cirrhosis," with a high negative predictive value (around 90%) [9, 34].

### 6.4 Alcoholic liver disease (ALD)

There is no consensus regarding the optimal cutoffs for the prediction of fibrosis stages in ALD patients [9, 58]. In various studies, the cutoffs range between 7.8 and 9.6 kPa for significant fibrosis, 8.0–17.0 kPa for severe fibrosis, and 7.15–34.9 kPa for cirrhosis prediction; the explanation for this variation lies in the difference in prevalence of fibrosis stages in the analyzed groups, as well as in the different patient selection methods (with or without exclusion of acute alcoholic hepatitis or of patients with decompensated disease) [59–62].

In a meta-analysis by Pavlov, the cutoffs used for the prediction of fibrosis stages were the following: 5.9 kPa for ≥F1 (Se 83%, Sp 86%, PPV 97.6%, NPV 35.3%, and AUROC 0.84), 7.5 kPa for ≥F2 (Se 94%, Sp 89%, positive likelihood ratio 8.2, negative likelihood ratio 0.07), and 9.5 kPa for ≥F3 (Se 92%, Sp 68%, positive likelihood ratio 2.9, negative likelihood ratio 0.11) [63]. For the prediction of cirrhosis, the proposed 12.5 kPa cutoff had a 95% sensitivity and 71% specificity, a 3.3 positive likelihood ratio, and a 0.07 negative likelihood ratio [63].

The proposed cutoff values for the different stages of hepatic fibrosis may be used in clinical practice, but with caution, since those reported values were simply the most common cutoff values used by the study authors and are insufficiently validated while, additionally, there is always the risk of overestimation of LS values in patients who are not abstinent from alcohol consumption.

It is also important to consider the AST levels when using VCTE to assess fibrosis in ALD patients. For AST levels above 100 U/L, the liver stiffness may increase independently from fibrosis, as a result of steatohepatitis, leading to interpretation errors [59]. On the other hand, liver stiffness decreased significantly after alcohol cessation over a long period of follow-up. It follows that liver stiffness measurements in alcoholic liver disease should be interpreted with caution and assessed in regard to the current alcohol consumption. Large-scale prospective studies should be performed to determine the different optimal cutoff values according to alcohol consumption, and more data are required to determine the best delay after alcohol cessation prior to VCTE evaluation.

VCTE is more suited to rule out than to rule in cirrhosis. At a Young's modulus of 12.5 kPa, VCTE may rule out cirrhosis with a negative likelihood ratio of 0.07 if the disease prevalence is 50% or lower.

In conclusion, according to the EFSUMB guidelines, "TE can be used to exclude cirrhosis in patients with alcoholic liver disease, provided that acute alcoholic hepatitis is not present" [9]. The current alcohol drinking status is also relevant.

### 6.5 Other chronic liver diseases

The performance of VCTE in identifying significant fibrosis was also assessed in other chronic liver diseases, such as HCV-HIV coinfection [64, 65], post liver transplantation status [66–69], cholestatic liver diseases (primitive biliary cirrhosis or primary sclerosing cholangitis) [70], and hemochromatosis [71]: the results yielded AUROC values between 0.74 and 0.93 for the prediction of significant fibrosis, at cutoffs ranging between 4 and 10.1 kPa.

### 6.6 The diagnosis of cirrhosis and its complications

One of the most important applications of VCTE is the noninvasive diagnosis of liver cirrhosis. The diagnostic accuracy of VCTE is far better in the prediction of cirrhosis than that of other stages of fibrosis, with areas under the ROC curve (AUROCs) ranging between 0.90 and 0.99 at cutoffs between 9 and 26.6 kPa. In a meta-analysis performed by Friedrich-Rust [72], the mean AUROC for the diagnosis of cirrhosis was 0.94, and the optimal cutoff for cirrhosis prediction proved to be 13.01 kPa. In Stebbing's meta-analysis [73], the 15.08 kPa cutoff had 84.45% sensitivity and 94.69% specificity for the prediction of cirrhosis. Tsochatzis [74] assessed the diagnostic accuracy of VCTE in the prediction of cirrhosis in a meta-analysis of 30 studies, which yielded a LS optimal cutoff of 15 ± 4.1 kPa (median, 14.5 kPa, ranging between 9 and 26.5 kPa in the various studies analyzed), with 83% sensitivity and 89% specificity. It is however important to keep in mind that the cutoffs proposed by the various studies were chosen based on the AUROCs providing the maximal sum between sensitivity and specificity. As was suggested in certain studies performed for the assessment of other noninvasive methods, the difference between these values can, however, be explained by the difference in prevalence of cirrhosis in the analyzed groups [35].

On the other hand, interpreting the LS value as compatible with the diagnosis of cirrhosis can only be made after excluding some other conditions: significant cytolysis, significant cholestasis, right heart failure, or performing the examination after a meal. Nevertheless, even if the liver stiffness values are not typical for cirrhosis, cirrhosis may however be present in 3% of cases. This is the case of macronodular cirrhosis (more frequent in HBV infection, but also in other liver diseases) where the nodules are surrounded by fine fibrous septa, which do not increase the liver stiffness to "cirrhotic" levels.

#### *6.6.1 Portal hypertension screening*

Various studies have reported on the correlation between the LS value and portal hypertension (PHT), identified either through the presence of esophageal varices (EV) during upper digestive endoscopy [75–77] or by measuring the hepatic venous pressure gradient (HVPG), considered the gold standard in the assessment of portal hypertension [66, 77–79].

Despite an excellent correlation at HVPG values below 10 or 12 mm Hg, the comparison did not yield valuable results at HVPG values > 10 mm Hg (which is

the HVPG threshold for the prediction of varices) or > 12 mm Hg (threshold for the prediction of other complications, such as variceal effraction or ascites).

When analyzing the relationship between liver stiffness and the presence of esophageal varices, the area under the ROC curve for the prediction of varices varied between 0.74 and 0.85. When using the 13.9 kPa, 17.6 kPa, and 21.3 kPa cutoff values, the authors found high sensitivity for the prediction of varices (95%, 90%, and 79%, respectively) but relatively low specificity (43, 43, and 70%, respectively) [3, 75–77].

Some authors claim that there is a correlation between liver stiffness values and variceal size [75, 76, 78], while others could find no proof of this correlation [77]. For the prediction of grade 2 and 3 varices, TE had a high sensitivity (91% and 76%) at the 19 kPa and 30.5 kPa cutoffs, respectively, but with low specificity (60% and 80%, respectively) and positive predictive value (48% and 54%, respectively) [75, 76].

According to the Baveno VI criteria [80], in patients with compensated chronic liver diseases of viral etiology, the noninvasive methods may predict the clinically significant portal hypertension, identifying the proportion of patients at risk of having endoscopic markers of PHT. For that purpose, liver stiffness measurements above 20–25 kPa can be used alone or in combination with platelet levels and spleen size. Liver stiffness below 20 kPa and platelet levels above 150,000 indicate a very low risk of esophageal varices requiring treatment, and therefore endoscopic screening can be avoided. These patients must be followed-up annually (VCTE and platelet levels), and an endoscopy must be performed in case of increasing stiffness or decreasing platelets.

The assessment of spleen stiffness has emerged as a new technique in hepatology, which may provide useful information on the presence and degree of portal hypertension and the prediction of its complications.

### *6.6.2 Prognostic significance of LS in patients with liver cirrhosis*

Some studies suggested that VCTE could be used as a risk marker for the development of a hepatocarcinoma in patients with hepatitis C [81, 82], who have a fivefold increase in risk at liver stiffness values above 25 kPa. On the other hand, in our experience, in patients with hepatitis C-related cirrhosis, a liver stiffness value > 38 kPa and an IQR > 30% of the median value (after previous exclusion of gross technical errors) are important markers which suggest the need for further imaging investigations in search of a possible hepatocarcinoma (HCC) [83]. Some authors have found that an increase in LS of more than 1 kPa at 3 years is correlated with a worse prognosis and with an increase in mortality rate in the next 2 years; for every 1 kPa increase over the median LS found in any given patient, the relative risk for a severe clinical event in that particular patient increases: 1.07 for hepatic decompensation, 1.11 for HCC, and 1.22 for death [84]. Nevertheless, these results require confirmation through prospective studies performed on large groups of patients, in order to confirm whether liver stiffness can indeed predict complications in decompensated cirrhosis [11]. In case it does, elastography may serve as a method of fast noninvasive screening, in order to classify each patient in a risk category [85].

## 6.7 Other applications of VCTE

The assessment of liver stiffness using VCTE is useful in the monitoring of adverse effects of hepatotoxic medication [86] as well as that of the effect of

antiviral therapy. Of course, in the latter situation, it is difficult to establish with certainty to what extent the decrease in liver stiffness is caused by a regression in fibrosis, a stabilization of necroinflammation, or both: however, a decrease in LS values in parallel with antiviral treatment exhibited favorable short- and long-term outcomes in patients with chronic viral hepatitis.

## 7. Advantages of VCTE

The technique is easy to use, painless, noninvasive and does not require hospitalization. It can measure at the same time liver stiffness (for the prediction of fibrosis) and the controlled attenuation parameter (CAP) for the prediction of steatosis, in a volume 100 times larger than that examined during a liver biopsy.

## 8. Limitations of VCTE

Liver fibrosis cannot be evaluated by VCTE in 5–8% of the cases [3], especially in the case of obesity, ascites, or narrow intercostal spaces. In the case of obesity, using the XL probe helps to lower the measurement failure. The measurement failure is significantly less frequent when using the XL probe than the standard M probe [54]. The XL probe can still yield unreliable results, but only in 25%, as opposed to 50% of cases with the M probe [87]. The main limiting factors for the XL probe are a skin-to-liver capsule distance > 3.4 cm and extreme obesity (BMI > 40 kg/m$^2$) [54].

## 9. Conclusions

In conclusion, vibration-controlled transient elastography (VCTE) is a useful method in the assessment and monitoring of diffuse liver diseases. It is important to perform the technique correctly and to interpret the results considering the clinical context, disease etiology, and laboratory results.

## Conflict of interest

Nothing to declare.

## Author details

Monica Lupsor-Platon[1,2]

1 Department of Medical Imaging, Iuliu Hatieganu University of Medicine and Pharmacy, Cluj-Napoca, Romania

2 Regional Institute of Gastroenterology and Hepatology "Prof. Dr. Octavian Fodor", Cluj-Napoca, Romania

*Address all correspondence to: monica.lupsor@umfcluj.ro

## References

[1] Sandrin L, Fourquet B, Hasquenoph JM, Yon S, Fournier C, Mal F, et al. Transient elastography: A new noninvasive method for assessment of hepatic fibrosis. Ultrasound in Medicine and Biology. 2003;**29**(12):1705-1713. DOI: 10.1016/j.ultrasmedbio

[2] Yeh WC, Li PC, Jeng YM, Hsu HC, Kuo PL, Li ML, et al. Elastic modulus measurements of human liver and correlation with pathology. Ultrasound in Medicine and Biology. 2002;**28**(4):467-474

[3] Lupsor M, Stefanescu H, Feier D, Badea R. Non-invasive evaluation of liver steatosis, fibrosis and cirrhosis in hepatitis C virus infected patients using unidimensional transient elastography (Fibroscan®). In: Tagaya N, editor. Liver Biopsy—Indications, Procedures, Results. Croatia: Intech; 2012. pp. 209-234. DOI: 10.5772/52621

[4] Sasso M, Beaugrand M, de Ledinghen V, Douvin C, Marcellin P, Poupon R, et al. Controlled attenuation parameter (CAP): A novel VCTE™ guided ultrasonic attenuation measurement for the evaluation of hepatic steatosis: Preliminary study and validation in a cohort of patients with chronic liver disease from various causes. Ultrasound in Medicine and Biology. 2010;**36**(11):1825-1835. DOI: 10.1016/j.ultrasmedbio.2010.07.005

[5] Sasso M, Miette V, Sandrin L, Beaugrand M. The controlled attenuation parameter (CAP): A novel tool for the non-invasive evaluation of steatosis using Fibroscan. Clinics and Research in Hepatology and Gastroenterology. 2012;**36**(1):13-20. DOI: 10.1016/j.clinre.2011.08.001

[6] Kettaneh A, Marcellin P, Douvin C, Poupon R, Ziol M, Beaugrand M, et al. Features associated with success rate and performance of FibroScan measurements for the diagnosis of cirrhosis in HCV patients: A prospective study of 935 patients. Journal of Hepatology. 2007;**46**(4):628-634. DOI: 10.1016/j.jhep.2006.11.010

[7] Mederacke I, Wursthorn K, Kirschner J, Rifai K, Manns MP, Wedemeyer H, et al. Food intake increases liver stiffness in patients with chronic or resolved hepatitis C virus infection. Liver International. 2009;**29**(10):1500-1506. DOI: 10.1111/j.1478-3231.2009.02100.x

[8] Arena U, Lupsor Platon M, Stasi C, Moscarella S, Assarat A, Bedogni G, et al. Liver stiffness is influenced by a standardized meal in patients with chronic HCV hepatitis at different stages of fibrotic evolution. Hepatology. 2013;**58**(1):65-72. DOI: 10.1002/hep.26343

[9] Dietrich CF, Bamber J, Berzigotti A, Bota S, Cantisani V, Castera L, et al. EFSUMBguidelinesandrecommendations on the clinical use of liver ultrasound elastography, update 2017 (long version). Ultraschall in der Medizin. 2017;**38**(4):e16-e47. DOI: 10.1055/s-0043-103952

[10] Boursier J, Konate A, Guilluy M, Gorea G, Sawadogo A, Quemener E, et al. Learning curve and interobserver reproducibility evaluation of liver stiffness measurement by transient elastography. European Journal of Gastroenterology and Hepatology. 2008;**20**(7):693-701. DOI: 10.1097/MEG.0b013e3282f51992

[11] Castera L, Forns X, Alberti A. Non-invasive evaluation of liver fibrosis using transient elastography. Journal of Hepatology. 2008;**48**(5):835-847

[12] Roulot D, Czernichow S, Le Clésiau H, Costes JL, Vergnaud AC,

Beaugrand M. Liver stiffness values in apparently healthy subjects: Influence of gender and metabolic syndrome. Journal of Hepatology. 2008;**48**(4):606-613

[13] Sirli R, Sporea I, Tudora A, Deleanu A, Popescu A. Transient elastographic evaluation of subjects without known hepatic pathology: Does age change the liver stiffness? Journal of Gastrointestinal and Liver Diseases. 2009;**18**(1):57-60

[14] Corpechot C, El Naggar A, Poupon R. Gender and liver: Is the liver stiffness weaker in weaker sex? Hepatology. 2006;**44**(2):513-514

[15] Lupsor Platon M, Stefanescu H, Feier D, Maniu A, Badea R. Performance of unidimensional transient elastography in staging chronic hepatitis C. Results from a cohort of 1,202 biopsied patients from one single center. Journal of Gastrointestinal and Liver Diseases. 2013;**22**(2):157-166

[16] Coco B, Oliveri F, Maina AM, Ciccorossi P, Sacco R, Colombatto P, et al. Transient elastography: A new surrogate marker of liver fibrosis influenced by major changes of transaminases. Journal of Viral Hepatitis. 2007;**14**(5):360-369. DOI: 10.1111/j.1365-2893.2006.00811.x

[17] Sagir A, Erhardt A, Schmitt M, Häussinger D. Transient elastography is unreliable for detection of cirrhosis in patients with acute liver damage. Hepatology. 2008;**47**(2):592-595. DOI: 10.1002/hep.22056

[18] Arena U, Vizzutti F, Corti G, Ambu S, Stasi C, Bresci S, et al. Acute viral hepatitis increases liver stiffness values measured by transient elastography. Hepatology. 2008;**47**(2):380-384. DOI: 10.1002/hep.22007

[19] Millonig G, Reimann FM, Friedrich S, Fonouni H, Mehrabi A, Büchler MW, et al. Extrahepatic cholestasis increases liver stiffness (FibroScan) irrespective of fibrosis. Hepatology. 2008;**48**(5):1718-1723. DOI: 10.1002/hep.22577

[20] Millonig G, Friedrich S, Adolf S, Fonouni H, Golriz M, Mehrabi A, et al. Liver stiffness is directly influenced by central venous pressure. Journal of Hepatology. 2010;**52**(2):206-210. DOI: 10.1016/j.jhep.2009.11.018

[21] Arena U, Vizzutti F, Abraldes JG, Corti G, Stasi C, Moscarella S, et al. Reliability of transient elastography for the diagnosis of advanced fibrosis in chronic hepatitis C. Gut. 2008;**57**(9):1288-1293. DOI: 10.1136/gut.2008.149708

[22] Fraquelli M, Rigamonti C, Casazza G, Conte D, Donato MF, Ronchi G, et al. Reproducibility of transient elastography in the evaluation of liver fibrosis in patients with chronic liver disease. Gut. 2007;**56**(7):968-973

[23] Chan HL, Wong GL, Choi PC, Chan AW, Chim AM, Yiu KK, et al. Alanine aminotransferase-based algorithms of liver stiffness measurement by transient elastography (Fibroscan) for liver fibrosis in chronic hepatitis B. Journal of Viral Hepatitis. 2009;**16**(1):36-44. DOI: 10.1111/j.1365-2893.2008.01037.x

[24] Kim SU, Han KH, Park JY, Ahn SH, Chung MJ, Chon CY, et al. Liver stiffness measurement using FibroScan is influenced by serum total bilirubin in acute hepatitis. Liver International. 2009;**29**(6):810-815. DOI: 10.1111/j.1478-3231.2008.01894.x

[25] Pozzoni P, Prati D, Berzuini A, et al. Liver stiffness values measured by transient elastography are increased in patients with acutely decompensated heart failure. Digestive and Liver Disease. 2009;**41**(3):A39

[26] Lebray P, Varnous S, Charlotte F, Varaut A, Poynard T, Ratziu V. Liver stiffness is an unreliable marker of liver fibrosis in patients with cardiac insufficiency. Hepatology. 2008;**48**(6):2089. DOI: 10.1002/hep.22594

[27] Bioulac-Sage P, Couffinhal T, Foucher J, Balabaud CP. Interpreting liver stiffness in the cirrhotic range. Journal of Hepatology. 2009;**50**(2):423-424. DOI: 10.1016/j.jhep.2008.11.003

[28] Ziol M, Kettaneh A, Ganne-Carrié N, Barget N, Tengher-Barna I, Beaugrand M. Relationships between fibrosis amounts assessed by morphometry and liver stiffness measurements in chronic hepatitis or steatohepatitis. European Journal of Gastroenterology and Hepatology. 2009;**21**(11):1261-1268. DOI: 10.1097/MEG.0b013e32832a20f5

[29] Lupşor M, Badea R, Stefănescu H, Grigorescu M, Sparchez Z, Serban A, et al. Analysis of histopathological changes that influence liver stiffness in chronic hepatitis C. Results from a cohort of 324 patients. Journal of Gastrointestinal and Liver Diseases. 2008;**17**(2):155-163

[30] Ziol M, Handra-Luca A, Kettaneh A, Christidis C, Mal F, Kazemi F, et al. Noninvasive assessment of liver fibrosis by measurement of stiffness in patients with chronic hepatitis C. Hepatology. 2005;**41**(1):48-54

[31] Castéra L, Vergniol J, Foucher J, Le Bail B, Chanteloup E, Haaser M, et al. Prospective comparison of transient elastography, Fibrotest, APRI, and liver biopsy for the assessment of fibrosis in chronic hepatitis C. Gastroenterology. 2005;**128**(2):343-350

[32] Sporea I, Sirli R, Deleanu A, Tudora A, Curescu M, Cornianu M, et al. Comparison of the liver stiffness measurement by transient elastography with the liver biopsy. World Journal of Gastroenterology. 2008;**14**(42):6513-6517

[33] Nitta Y, Kawabe N, Hashimoto S, Harata M, Komura N, Kobayashi K, et al. Liver stiffness measured by transient elastography correlates with fibrosis area in liver biopsy in patients with chronic hepatitis C. Hepatology Research. 2009;**39**(7):675-684. DOI: 10.1111/j.1872-034X.2009.00500.x

[34] European Association for Study of Liver, Asociacion Latinoamericana para el Estudio del Higado. EASL-ALEH clinical practice guidelines: Non-invasive tests for evaluation of liver disease severity and prognosis. Journal of Hepatology. 2015;**63**(1):237-264. DOI: 10.1016/j.jhep.2015.04.006

[35] Poynard T, Halfon P, Castera L, Munteanu M, Imbert-Bismut F, Ratziu V, et al. Standardization of ROC curve areas for diagnostic evaluation of liver fibrosis markers based on prevalences of fibrosis stages. Clinical Chemistry. 2007;**53**(9):1615-1622

[36] Marcellin P, Ziol M, Bedossa P, Douvin C, Poupon R, de Lédinghen V, et al. Non-invasive assessment of liver fibrosis by stiffness measurement in patients with chronic hepatitis B. Liver International. 2009;**29**(2):242-247. DOI: 10.1111/j.1478-3231.2008.01802.x

[37] Degos F, Perez P, Roche B, Mahmoudi A, Asselineau J, Voitot H, et al. Diagnostic accuracy of FibroScan and comparison to liver fibrosis biomarkers in chronic viral hepatitis: A multicenter prospective study (the FIBROSTIC study). Journal of Hepatology. 2010;**53**(6):1013-1021. DOI: 10.1016/j.jhep.2010.05.035

[38] Cardoso AC, Carvalho-Filho RJ, Stern C, Dipumpo A, Giuily N, Ripault MP, et al. Direct comparison of diagnostic performance of transient

elastography in patients with chronic hepatitis B and chronic hepatitis C. Liver International. 2012;**32**(4):612-621. DOI: 10.1111/j.1478-3231.2011.02660.x

[39] Viganò M, Paggi S, Lampertico P, Fraquelli M, Massironi S, Ronchi G, et al. Dual cut-off transient elastography to assess liver fibrosis in chronic hepatitis B: A cohort study with internal validation. Alimentary Pharmacology and Therapeutics. 2011;**34**(3):353-362. DOI: 10.1111/j.1365-2036.2011.04722.x

[40] Oliveri F, Coco B, Ciccorossi P, Colombatto P, Romagnoli V, Cherubini B, et al. Liver stiffness in the hepatitis B virus carrier: A non-invasive marker of liver disease influenced by the pattern of transaminases. World Journal of Gastroenterology. 2008;**14**(40):6154-6162

[41] Lesmana CR, Salim S, Hasan I, Sulaiman AS, Gani RA, Pakasi LS, et al. Diagnostic accuracy of transient elastography (FibroScan) versus the aspartate transaminase to platelet ratio index in assessing liver fibrosis in chronic hepatitis B: The role in primary care setting. Journal of Clinical Pathology. 2011;**64**(10):916-920. DOI: 10.1136/jclinpath-2011-200044

[42] Verveer C, Zondervan PE, ten Kate FJ, Hansen BE, Janssen HL, de Knegt RJ. Evaluation of transient elastography for fibrosis assessment compared with large biopsies in chronic hepatitis B and C. Liver International. 2012;**32**(4):622-628. DOI: 10.1111/j.1478-3231.2011.02663.x

[43] Seo YS, Kim MN, Kim SU, Kim SG, Um SH, Han KH, et al. Risk assessment of hepatocellular carcinoma using transient elastography vs. liver biopsy in chronic hepatitis B patients receiving antiviral therapy. Medicine (Baltimore). 2016;**95**:e2985. DOI: 10.1097/MD.0000000000002985

[44] Meng F, Zheng Y, Zhang Q, Mu X, Xu X, Zhang H, et al. Noninvasive evaluation of liver fibrosis using real-time tissue elastography and transient elastography (FibroScan). Journal of Ultrasound in Medicine. 2015;**34**:403-410. DOI: 10.7863/ultra.34.3.403

[45] Chon YE, Choi EH, Song KJ, Park JY, Kim DY, Han KH, et al. Performance of transient elastography for the staging of liver fibrosis in patients with chronic hepatitis B: A meta-analysis. PLoS One. 2012;**7**:e44930. DOI: 10.1371/journal.pone.0044930

[46] Xu X, Su Y, Song R, Sheng Y, Ai W, Wu X, et al. Performance of transient elastography assessing fibrosis of single hepatitis B virus infection: A systematic review and meta-analysis of a diagnostic test. Hepatology International. 2015;**9**:558-566. DOI: 10.1007/s12072-015-9643-z

[47] Li Y, Huang YS, Wang ZZ, Yang ZR, Sun F, Zhan SY, et al. Systematic review with meta-analysis: The diagnostic accuracy of transient elastography for the staging of liver fibrosis in patients with chronic hepatitis B. Alimentary Pharmacology and Therapeutics. 2016;**43**:458-469. DOI: 10.1111/apt.13488

[48] Castéra L, Bernard PH, Le Bail B, Foucher J, Trimoulet P, Merrouche W, et al. Transient elastography and biomarkers for liver fibrosis assessment and follow-up of inactive hepatitis B carriers. Alimentary Pharmacology and Therapeutics. 2011;**33**:455-465. DOI: 10.1111/j.1365-2036.2010.04547.x

[49] Dong CF, Xiao J, Shan LB, Li HY, Xiong YJ, Yang GL, et al. Combined acoustic radiation force impulse, aminotransferase to platelet ratio index and Forns index assessment for hepatic fibrosis grading in hepatitis B. World Journal of Hepatology. 2016;**8**:616-624. DOI: 10.4254/wjh.v8.i14.616

[50] Lupsor M, Badea R, Stefanescu H, Grigorescu M, Serban A, Radu C, et al. Performance of unidimensional transient elastography in staging non-alcoholic steatohepatitis. Journal of Gastrointestinal and Liver Diseases. 2010;**19**(1):53-60

[51] Kwok R, Tse YK, Wong GL, Ha Y, Lee AU, Ngu MC, et al. Systematic review with metaanalysis: Non-invasive assessment of non-alcoholic fatty liver disease—The role of transient elastography and plasma cytokeratin-18 fragments. Alimentary Pharmacology and Therapeutics. 2014;**39**(3):254-269. DOI: 10.1111/apt.12569

[52] Kumar R, Rastogi A, Sharma MK, Bhatia V, Tyagi P, Sharma P, et al. Liver stiffness measurements in patients with different stages of nonalcoholic fatty liver disease: Diagnostic performance and clinicopathological correlation. Digestive Diseases and Sciences. 2013;**58**(1):265-274. DOI: 10.1007/s10620-012-2306-1

[53] Gaia S, Carenzi S, Barilli AL, Bugianesi E, Smedile A, Brunello F, et al. Reliability of transient elastography for the detection of fibrosis in non-alcoholic fatty liver disease and chronic viral hepatitis. Journal of Hepatology. 2011;**54**(1):64-71. DOI: 10.1016/j.jhep.2010.06.022

[54] Myers RP, Pomier-Layrargues G, Kirsch R, Pollett A, Duarte-Rojo A, Wong D, et al. Feasibility and diagnostic performance of the FibroScan XL probe for liver stiffness measurement in overweight and obese patients. Hepatology. 2012;**55**(1):199-208. DOI: 10.1002/hep.24624

[55] Petta S, Vanni E, Bugianesi E, Di Marco V, Cammà C, Cabibi D, et al. The combination of liver stiffness measurement and NAFLD fibrosis score improves the noninvasive diagnostic accuracy for severe liver fibrosis in patients with nonalcoholic fatty liver disease. Liver International. 2015;**35**:1566-1573. DOI: 10.1111/liv.12584

[56] Wong VW, Vergniol J, Wong GL, Foucher J, Chan HL, Le Bail B, et al. Diagnosis of fibrosis and cirrhosis using liver stiffness measurement in nonalcoholic fatty liver disease. Hepatology. 2010;**51**(2):454-462. DOI: 10.1002/hep.23312

[57] Yoneda M, Yoneda M, Mawatari H, Fujita K, Endo H, Iida H, et al. Noninvasive assessment of liver fibrosis by measurement of stiffness in patients with nonalcoholic fatty liver disease (NAFLD). Digestive and Liver Disease. 2008;**40**(5):371-378. DOI: 10.1016/j.dld.2007.10.019

[58] Lupsor-Platon M, Badea R. Noninvasive assessment of alcoholic liver disease using unidimensional transient elastography (Fibroscan(®)). World Journal of Gastroenterology. 2015;**21**(42):11914-11923. DOI: 10.3748/wjg.v21.i42.11914

[59] Mueller S, Millonig G, Sarovska L, Friedrich S, Reimann FM, Pritsch M, et al. Increased liver stiffness in alcoholic liver disease: Differentiating fibrosis from steatohepatitis. World Journal of Gastroenterology. 2010;**16**:966-972. DOI: 10.3748/wjg.v16.i8.966

[60] Nahon P, Kettaneh A, Tengher-Barna I, Ziol M, de Lédinghen V, Douvin C, et al. Assessment of liver fibrosis using transient elastography in patients with alcoholic liver disease. Journal of Hepatology. 2008;**49**:1062-1068. DOI: 10.1016/j.jhep.2008.08.011

[61] Janssens F, de Suray N, Piessevaux H, Horsmans Y, de Timary P, Stärkel P. Can transient elastography replace liver histology for determination of advanced fibrosis in alcoholic patients: A real-life study. Journal of Clinical Gastroenterology.

2010;**44**:575-582. DOI: 10.1097/MCG.0b013e3181cb4216

[62] Thiele M, Detlefsen S, Sevelsted Møller L, Madsen BS, Fuglsang Hansen J, Fialla AD, et al. Transient and 2-dimensional shear-wave elastography provide comparable assessment of alcoholic liver fibrosis and cirrhosis. Gastroenterology. 2016;**150**:123-133. DOI: 10.1053/j.gastro.2015.09.040

[63] Pavlov CS, Casazza G, Nikolova D, Tsochatzis E, Burroughs AK, Ivashkin VT, et al. Transient elastography for diagnosis of stages of hepatic fibrosis and cirrhosis in people with alcoholic liver disease. Cochrane Database of Systematic Reviews. 2015;**1**:CD010542. DOI: 10.1002/14651858.CD010542.pub2

[64] de Lédinghen V, Douvin C, Kettaneh A, Ziol M, Roulot D, Marcellin P, et al. Diagnosis of hepatic fibrosis and cirrhosis by transient elastography in HIV/hepatitis C virus-coinfected patients. Journal of Acquired Immune Deficiency Syndromes. 2006;**41**(2):175-179

[65] Vergara S, Macías J, Rivero A, et al. The use of transient elastometry for assessing liver fibrosis in patients with HIV and hepatitis C virus coinfection. Clinical Infectious Diseases. 2007;**45**(8):969-974. DOI: 10.1086/521857

[66] Carrion JA, Navasa M, Bosch J, Bruguera M, Gilabert R, Forns X. Transient elastography for diagnosis of advanced fibrosis and portal hypertension in patients with hepatitis C recurrence after liver transplantation. Liver Transplantation. 2006;**12**(12):1791-1798. DOI: 10.1002/lt.20857

[67] Rigamonti C, Donato MF, Fraquelli M, Agnelli F, Ronchi G, Casazza G, et al. Transient elastography predicts fibrosis progression in patients with recurrent hepatitis C after liver transplantation. Gut. 2008;**57**(6):821-827. DOI: 10.1136/gut.2007.135046

[68] Corradi F, Piscaglia F, Flori S, D'Errico-Grigioni A, Vasuri F, Tamé MR, et al. Assessment of liver fibrosis in transplant recipients with recurrent HCV infection: Usefulness of transient elastography. Digestive and Liver Disease. 2009;**41**(3):217-225. DOI: 10.1016/j.dld.2008.06.009

[69] Harada N, Soejima Y, Taketomi A, Yoshizumi T, Ikegami T, Yamashita Y, et al. Assessment of graft fibrosis by transient elastography in patients with recurrent hepatitis C after living donor liver transplantation. Transplantation. 2008;**85**(1):69-74. DOI: 10.1097/01.tp.0000297248.18483.16

[70] Corpechot C, El Naggar A, Poujol-Robert A, Ziol M, Wendum D, Chazouillères O, et al. Assessment of biliary fibrosis by transient elastography in patients with PBC and PSC. Hepatology. 2006;**43**(5):1118-1124. DOI: 10.1002/hep.21151

[71] Adhoute X, Foucher J, Laharie D, Terrebonne E, Vergniol J, Castéra L, et al. Diagnosis of liver fibrosis using FibroScan and other noninvasive methods in patients with hemochromatosis: A prospective study. Gastroentérologie Clinique et Biologique. 2008;**32**(2):180-187

[72] Friedrich-Rust M, Ong MF, Martens S, et al. Performance of transient elastography for the staging of liver fibrosis: A meta-analysis. Gastroenterology. 2008;**134**(4):960-974

[73] Stebbing J, Farouk L, Panos G, Anderson M, Jiao LR, Mandalia S, et al. A meta-analysis of transient elastography for the detection of hepatic fibrosis. Journal of Clinical Gastroenterology. 2010;**44**(3):214-219. DOI: 10.1097/MCG.0b013e3181b4af1f

[74] Tsochatzis EA, Gurusamy KS, Ntaoula S, Cholongitas E, Davidson BR, Burroughs AK. Elastography for the diagnosis of severity of fibrosis in chronic liver disease: A meta-analysis of diagnostic accuracy. Journal of Hepatology. 2011;**54**(4):650-659. DOI: 10.1016/j.jhep.2010.07.033

[75] Castéra L, Le Bail B, Roudot-Thoraval F, Bernard PH, Foucher J, Merrouche W, et al. Early detection in routine clinical practice of cirrhosis and oesophageal varices in chronic hepatitis C: Comparison of transient elastography (FibroScan) with standard laboratory tests and non-invasive scores. Journal of Hepatology. 2009;**50**(1):59-68. DOI: 10.1016/j.jhep.2008.08.018

[76] Kazemi F, Kettaneh A, N'kontchou G, Pinto E, Ganne-Carrie N, Trinchet JC, et al. Liver stiffness measurement selects patients with cirrhosis at risk of bearing large oesophageal varices. Journal of Hepatology. 2006;**45**(2):230-235. DOI: 10.1016/j.jhep.2006.04.006

[77] Vizzutti F, Arena U, Romanelli RG, Rega L, Foschi M, Colagrande S, et al. Liver stiffness measurement predicts severe portal hypertension in patients with HCV-related cirrhosis. Hepatology. 2007;**45**(5):1290-1297. DOI: 10.1002/hep.21665

[78] Bureau C, Metivier S, Peron JM, Selves J, Robic MA, Gourraud PA, et al. Transient elastography accurately predicts presence of significant portal hypertension in patients with chronic liver disease. Alimentary Pharmacology and Therapeutics. 2008;**27**(12):1261-1268. DOI: 10.1111/j.1365-2036.2008.03701.x

[79] Lemoine M, Katsahian S, Ziol M, Nahon P, Ganne-Carrie N, Kazemi F, et al. Liver stiffness measurement as a predictive tool of clinically significant portal hypertension in patients with compensated hepatitis C virus or alcohol-related cirrhosis. Alimentary Pharmacology and Therapeutics. 2008;**28**(9):1102-1110. DOI: 10.1111/j.1365-2036.2008.03825.x

[80] de Franchis R, editor. Portal hypertension VI. In: Proceedings of the Sixth Baveno Consensus Workshop: Stratifying Risk and Individualizing Care. Switzerland: Springer International Publishing; 2016. DOI: 10.1007/978-3-319-23018-4

[81] Masuzaki R, Tateishi R, Yoshida H, Yoshida H, Sato S, Kato N, et al. Risk assessment of hepatocellular carcinoma in chronic hepatitis C patients by transient elastography. Journal of Clinical Gastroenterology. 2008;**42**(7):839-843

[82] Masuzaki R, Tateishi R, Yoshida H, Goto E, Sato T, Ohki T, et al. Prospective risk assessment for hepatocellular carcinoma development in chronic hepatitis C patients by transient elastography. Hepatology. 2009;**49**(6):1954-1961. DOI: 10.1002/hep.22870

[83] Feier D, Lupsor Platon M, Stefanescu H, Badea R. Transient elastography for the detection of hepatocellular carcinoma in viral C liver cirrhosis. Is there something else than increased liver stiffness? Journal of Gastrointestinal and Liver Diseases. 2013;**22**(3):283-289

[84] Tapper EB, Castera L, Afdhal NH. FibroScan (vibration-controlled transient elastography): Where does it stand in the United States practice. Clinical Gastroenterology and Hepatology. 2015;**13**(1):27-36. DOI: 10.1016/j.cgh.2014.04.039

[85] Pinzani M. Non-invasive evaluation of hepatic fibrosis: Don't count your chickens before they're hatched. Gut. 2006;**55**(3):310-312. DOI: 0.1136/gut.2005.068585

[86] Laharie D, Zerbib F, Adhoute X, Boué-Lahorgue X, Foucher J, Castéra L, et al. Diagnosis of liver fibrosis by transient elastography (FibroScan) and non-invasive methods in Crohn's disease patients treated with methotrexate. Alimentary Pharmacology and Therapeutics. 2006;**23**(11):1621-1628. DOI: 10.1111/j.1365-2036.2006.02929.x

[87] Castera L, Vilgrain V, Angulo P. Noninvasive evaluation of NAFLD. Nature Reviews. Gastroenterology and Hepatology. 2013;**10**(11):666-675. DOI: 10.1038/nrgastro.2013

Chapter 2

# Liver Fibrosis Assessment by Point Shear-Wave Elastography Techniques

*Roxana Șirli, Alina Popescu and Ioan Sporea*

## Abstract

Point shear-wave elastographic (pSWE) techniques use acoustic radiation force impulse (ARFI) to stimulate the liver tissue and to generate shear waves that propagate into the liver. The shear-wave velocity (SWV) increases with the severity of fibrosis. The first type of pSWE was Virtual Touch Quantification (VTQ) developed by Siemens, followed by ElastPQ by Philips, and nowadays pSWE is available on other systems (Hitachi, Esaote, Samsung). To evaluate liver fibrosis by pSWE, ten valid measurements are performed in the right liver lobe; a median value is calculated, with the results expressed in meters/second or in kilopascals (kPa) (if the operator chooses). VTQ is a reproducible method, the intraclass correlation coefficient (ICC) for inter- and intraobserver measurements ranging from 0.81 to 0.87. Confounding factors for VTQ are non-fasting conditions, elevated aminotransferases, congestive heart failure, and extrahepatic cholestasis. In patients with chronic hepatopathies, the AUROCs for predicting significant fibrosis range between 0.75 and 0.85 and for predicting cirrhosis between 0.85 and 0.95. There were promising results regarding the value of VTQ to predict liver cirrhosis complications, especially portal hypertension. ElastPQ is a newly developed point shear-wave elastographic method (from Philips). Only few data were published but with promising results.

**Keywords:** liver fibrosis, liver elastography, point shear-wave elastography, Virtual Touch Quantification, ElastPQ

## 1. Introduction

Evaluation of liver fibrosis severity is essential in chronic hepatopathies, especially for prognosis, but also for decision regarding treatment in some cases or for follow-up [1]. For a long time, liver biopsy was considered to be the reference method for fibrosis assessment. Not only mainly due to its invasiveness [2] but also due to issues regarding inter-observer variability and sampling errors [3], noninvasive methods have been developed to assess the severity of liver fibrosis. These methods can be either biological or elastographic [1].

Elastographic techniques are based on an intrinsic property of tissue elasticity. When an extrinsic force is applied to a tissue, it deforms more or less according to its elasticity. Less elastic, stiffer tissue deforms less when subjected to an external force. Elastographic techniques measure tissue displacement when subjected to

an external force. In chronic hepatopathies, as fibrosis progresses, the liver tissue becomes stiffer, less elastic; thus, liver stiffness (LS) is considered to be an indicator of liver fibrosis severity [1, 4, 5]. Elastographic techniques can be ultrasound-based or based on magnetic resonance imaging.

According to the latest guidelines [4–9], ultrasound-based elastographic techniques are divided into strain elastography (which measures longitudinal displacement) and shear-wave elastography (SWE—which measures the speed of the shear waves generated into the tissue when an external force is applied). Based on the type of impulse that generates the shear waves, SWE is subdivided into transient elastography (TE—where a mechanical stimulus is applied to the tissue) and acoustic radiation force impulse (ARFI) techniques (where the stimulus deforming the tissue is an acoustic "push pulse" generated by the transducer). Subsequently, ARFI elastography is subdivided into point SWE (in which LS is measured in a region of interest (ROI)) and multidimensional SWE (2D-SWE and 3D-SWE—in which a color-coded elastogram is obtained and shear-wave speed is also measured in a region of interest).

In the following pages, we will present point shear-wave elastography techniques.

## 2. Point shear-wave elastography: basic principles

pSWE is a type of SWE in which tissue stimulation is performed at a certain depth by an acoustic radiation force impulse generated by the transducer (ARFI technology), which generates shear waves that propagate into the tissue, perpendicularly on the axis of the initial pulse. Shear-wave velocity (SWV), expressed in meters/second (m/s), is measured in a predefined ROI chosen by the operator while performing B-mode ultrasonography. The average propagation speed of the shear waves, from a point placed on the lateral margin of the ROI to an opposite point on the ROI, can be measured by detecting its time of arrival at that point, relative to the acoustic "push" pulse [5]. The stiffer the tissue, the higher the shear-wave velocity [4–9].

Most systems performing pSWE allow the choice to express measurement results either in m/s or in kilopascals (kPa). Kilopascal is the unit of the elastic modulus, obtained by converting the SWV to an elastic modulus, using an equation that assumes that the tissue density is always the same and also that the elastic modulus is not influenced by the magnitude, frequency, and direction of the applied force [5]. Thus, even if kPa is the unit to which users are the most familiar (since it was used for Transient Elastography), the most correct one is m/s [5–7].

Two types of pSWE have been more thoroughly evaluated, the ones developed by Siemens (Virtual Touch Quantification) and by Philips (ElastPQ). Currently other manufacturers also offer pSWE on their systems: Esaote, Hitachi, and Samsung [5].

## 3. Point shear-wave elastography (pSWE): examination technique

First of all, before performing SWE the ***operator should be trained*** [5, 6, 8, 9]. If for TE training means performing more than 100 examinations under supervision [10], what training means is less precise for pSWE. A study published by Boursier concluded that there is no training effect on the accuracy of LS measurements by VTQ (ARFI) [11]. Concerning ElastPQ, a published study concluded that after a 1-year learning curve, or 130 examinations, the accuracy of ElastPQ matches that

of TE [12]. Considering that adequate B-mode image is a must for reliable pSWE measurements [5, 9], it is sensible to consider that training not only in elastographic measurements but also in ultrasonography is needed.

According to the guidelines, the ***recommended technique*** of pSWE measurements is with the patient in supine position with the right arm in maximal extension, through an intercostal approach, during breath hold, avoiding deep inspiration or expiration [5, 6, 8]. The transducer should be perpendicular on the liver capsule, and the ROI should be placed in the right liver lobe, as to avoid large blood vessels and masses, at a depth of minimum 1 cm below the liver capsule, best at 4–5 cm from the transducer [5, 6, 8, 9] (**Figures 1** and **2**).

A study published by our group demonstrated that the best correlation of VTQ measurements with histology was obtained for SWV measurements made 1–2 and 2–3 cm beneath the liver capsule but with a lower feasibility for deeper measurements [13]. Several studies observed higher SWV by VTQ in the left liver lobe vs. the right liver lobe [14–16]. Regarding ElastPQ, measurements made in liver segment V had the lowest coefficient of variation, and SWVs at the end-expiration were significantly higher than that at the end-inspiration [17].

For an appropriate estimation of fibrosis, the guidelines recommend to perform ten pSWE measurements and to calculate the median (M) value [5, 6, 8, 9]. When VTQ was launched, the manufacturer did not recommend ***quality criteria***, but several studies demonstrated that there is a better correlation between histologic fibrosis and pSWE measurements if quality criteria such as interquartile range (IQR) and success rate (SR) are met. Regarding VTQ, an IQR/M $\geq$ 30% was associated with a discordance of at least two stages of fibrosis between SWV and histologic fibrosis [18]. In another study from our group, a very strong correlation of VTQ measurements with histologic fibrosis was observed when quality parameters (IQR < 30% and SR $\geq$ 60%) were met ($r = 0.722$, $p < 0.0001$); if not, there was no significant correlation ($r = 0.268$, $p = 0.07$) [19]. Also, standard deviation (SD) of the mean of ten valid SWV measurements by VTQ was evaluated as a quality criterion. Exclusion of patients in whom the SD was higher than 30% lead to an improved accuracy of VTQ [20]. Regarding ElastPQ®, IQR/M $\leq$ 30% is also the most important quality criterion [21, 22]. European guidelines recommend as quality criterion for pSWE an IQR/M $\leq$ 30% [5, 8], while the WFUMB guidelines

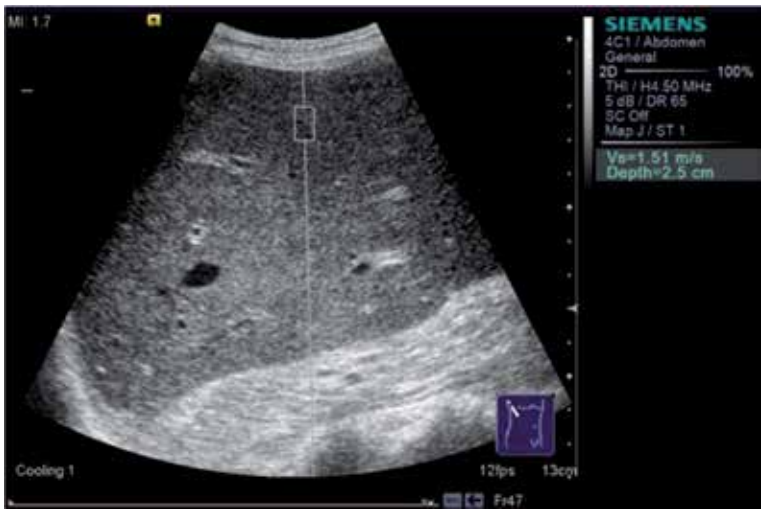


**Figure 1.**
*VTQ measurement.*

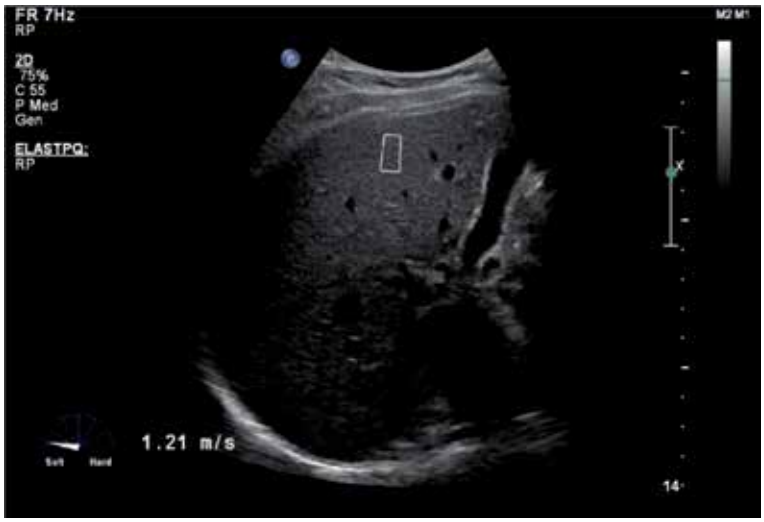


**Figure 2.**
*ElastPQ measurement.*

recommend an even smaller IQR/M, of less than 15%, if results are expressed in m/s [9]. A new multicenter study with ElastPQ® showed that the median value of five measurements with an IQR/M ≤ 30% is accurate enough for daily practice [22].

## 4. Point shear-wave elastography (pSWE): feasibility and reproducibility

As opposed to TE, pSWE is *feasible* in patients with ascites [5, 6, 8, 9]. Furthermore, in published studies, the feasibility is better as compared to TE, being higher than 92%, both in VTQ [11, 23–25] and in ElastPQ [26, 27]. In a multicenter study on VTQ, older age, higher BMI, and male gender were associated with failed and unreliable measurements [25].

Regarding *reproducibility* of VTQ, several studies demonstrated very good inter- and intraobserver reproducibility, with intraclass correlation coefficients (ICC) higher than 0.81 [10, 28, 29]. A study that evaluated factors that influenced reproducibility found out that intraoperator reproducibility was better than the inter-operator one (ICC of 0.90 vs. 0.81) [28]. Both intra- and inter-operator reproducibilities were better in men than in women, in patients with lower BMI, and in patients with no ascites and in cirrhotic than in non-cirrhotic patients [28].

ElastPQ was also proved to be a reproducible method, reported ICC ranging from 0.798 [30] to 0.96 [31]. In a study published by Fraquelli, the reproducibility was influenced by training, but not by age, gender, BMI, liver enzymes, and liver etiology [12].

## 5. Point shear-wave elastography (pSWE): confounding factors

One of the first confounding factors that should be taken into consideration is examination in *non-fasting* conditions. In a study published by our group, it was demonstrated that food intake can lead to a significant increase in SWVs measured by VTQ in healthy volunteers 1 hour post meal, the values decreasing to baseline 3 hours after the meal [32]. Even if no data was published regarding ElastPQ, the

observation in VTQ was similar to what happens with TE measurements in non-fasting patients, and thus the guidelines recommendation that pSWE measurements should be performed in fasting patients [5, 6, 8, 9].

Another factor that can lead to a falsely increased SWV measured by VTQ is *physical exercise* [33]. Thus, the EFSUMB guidelines recommend that SWE should be performed after a minimum 10 minutes of rest [5].

An important confounding factor for SWE is liver necroinflammation, objectified by *elevated aminotransferase levels*. Several studies demonstrated that elevated aminotransferase levels are associated with higher SWVs by VTQ for the same severity of liver fibrosis, as compared to those observed in patients with normal or only slightly elevated aminotransferases [34, 35]. Also, a significant decrease in SWVs was observed in a case report of acute liver failure, in parallel to the normalization of liver function tests [36].

The influence of necroinflammation on SWVs measured by ElastPQ is controversial. In a study by Ma et al., the grade of necroinflammatory activity was independently associated with higher ElastPQ values [30], while in the study of Ferraioli et al., it had no influence [31].

Similar to TE, other confounding factors, which falsely increase SWVs by pSWE are *right heart failure* [37] and the *presence of extrahepatic cholestasis* [38].

Considering all the studies mentioned above, EFSUMB and WFUMB guidelines caution about the confounding factors for pSWE and state that liver inflammation (indicated by AST and/or ALT elevation >5 times the normal limits), obstructive cholestasis, liver congestion, acute hepatitis, and infiltrative liver diseases should be excluded before pSWE to avoid overestimation of fibrosis and/or should be considered when interpreting the results [5, 9].

## 6. Point shear-wave elastography (pSWE): normal values in a healthy liver

The SWV by pSWE in healthy livers were evaluated by several authors. Regarding VTQ, normal SWV values ranged between 1.07 and 1.19 m/s [15, 39–42], and they were not influenced by gender and age, but higher values were observed in the left liver lobe than in the right liver lobe [15].

Regarding ElastPQ, normal values are in the same range as for VTQ [17, 31, 43], but a study found higher values in men than in women [17].

Current guidelines state that SWE measurements in the liver in normal range can rule out significant fibrosis if they are in accordance with clinical and biologic data [5, 9].

## 7. Point shear-wave elastography (pSWE) in patients with chronic hepatopathies

### 7.1 Mixed cohorts

Multiple studies have been published regarding the value of VTQ elastography in patients with chronic liver diseases, considering biopsy as the reference. We summarized some of them in **Table 1**.

Four meta-analyses were published regarding the value of VTQ for liver fibrosis assessment. The first one, by Friedrich-Rust et al., included 518 patients with hepatopathies of various etiologies. The summary AUROCs of VTQ for predicting significant fibrosis ($F \geq 2$), severe fibrosis ($F \geq 3$), and cirrhosis were 0.87, 0.91,

| Study | Etiology | F2 | | F4 | |
|---|---|---|---|---|---|
| | | AUROC TE | Cutoff AUROC VTQ | AUROC TE | Cutoff AUROC VTQ |
| Friedrich-Rust et al. [44] | 86 patients HBV + HCV | 0.86 | 1.37 m/s 0.86 | 0.91 | 1.75 m/s 0.91 |
| Sporea et al. [45] | 223 patients Healthy + HBV + HCV | 0.953 | 1.27 m/s 0.890 | 0.985 | 1.7 m/s 0.931 |
| Takahashi et al. [46] | 80 patients Healthy + HBV + HCV | — | 1.34 m/s 0.94 | — | 1.8 m/s 0.96 |
| Goertz et al. [47] | 57 patients HBV + HCV | — | 0.85 | — | 0.87 |
| Ebinuma et al. [48] | 131 patients Mixed | 0.871 | 1.3 m/s 0.891 | 0.817 | 1.88 m/s 0.888 |
| Colombo et al. [49] | 68 Healthy + mixed | 0.897 | 0.922 | 0.815 | 0.934 |
| Cassinotto et al. [50] | 349 Mixed | 0.84 | 0.81 | 0.90 | 0.90 |

**Table 1.**
*Performance of VTQ in the assessment of liver fibrosis in cohorts of patients with mixed etiologies of chronic hepatopathies, considering LB as the reference method.*

and 0.93, respectively. TE performed significantly better than VTQ for F2 and cirrhosis, while for F3 the performances evaluated by AUROC were similar [51].

The second one included 1163 patients with chronic hepatopathies evaluated by LB, TE, and VTQ [52]. The first conclusion was that VTQ had a better feasibility than TE (unreliable measurements in 2.1 vs. 6.6% cases, respectively, $p < 0.001$). The diagnostic odds ratios were similar for VTQ and TE for detection of significant fibrosis and cirrhosis. The mean optimal cutoff value of VTQ for the detection of F2 was 1.30 ± 0.07 m/s, and for cirrhosis, it was 1.80 ± 0.16 m/s.

The third meta-analysis included 3951 patients with liver biopsy as reference method. The AUROCs of VTQ for predicting the presence of F2, F3, and cirrhosis were 0.84, 0.89, and 0.91, respectively [53].

Finally, the fourth meta-analysis including 2691 patients calculated global sensitivity and specificity of VTQ to predict any stage of fibrosis to be 79 and 86%, respectively. The performance of VTQ was higher for more advanced fibrosis: for F ≥ 3 84% Se and 90% Sp (AUROC—0.94), while for F4 86% Se and 84% Sp (AUROC—0.91) [54].

Regarding ***ElastPQ***, few data are available. In a study that compared ElastPQ to TE considered as reference, ElastPQ had a better feasibility than TE: 98.7% vs. 90.7%. The AUROCs calculated for significant fibrosis, severe fibrosis, and cirrhosis were 0.94, 0.97, and 0.97, respectively [27].

### 7.2 Chronic hepatitis C

There is a lot of published data regarding the performance of VTQ elastography for the assessment of liver fibrosis in patients with chronic hepatitis C, as shown in **Table 2**.

To summarize, according to EFSUMB guidelines, VTQ® cutoffs of 1.21–1.34 m/s predict significant fibrosis (F ≥ 2) (AUROC 0.85–0.89), while VTQ® cutoffs between 1.55 and 2 m/s (AUROC 0.89–0.93) predict cirrhosis [5]. Furthermore,

| Study | Reference method | F ≥ 2 | | F ≥ 3 | | F = 4 | |
|---|---|---|---|---|---|---|---|
| | | Cutoff (m/s) | AUROC | Cutoff (m/s) | AUROC | Cutoff (m/s) | AUROC |
| Friedrich-Rust et al. [44] | LB—64 p | 1.35 | 0.86 | 1.55 | 0.93 | 1.75 | 0.95 |
| Lupșor et al. [23] | LB—112 p | 1.34 | 0.851 | 1.61 | 0.869 | 2 | 0.945 |
| Sporea et al. [55] | LB—274 p | 1.21 | 0.893 | 1.58 | 0.908 | 1.82 | 0.937 |
| Sporea et al. [56] | LB—914 p | 1.33 | 0.792 | 1.43 | 0.829 | 1.55 | 0.842 |
| Rizzo et al. [57] | LB—139 p | 1.3 | 0.86 | 1.7 | 0.94 | 2 | 0.89 |
| Chen et al. [58] | LB—127 p | 1.55 | 0.847 | 1.81 | 0.902 | 1.98 | 0.831 |
| Li et al. [59] | LB—128 p | 1.53 | 0.775 | 1.79 | 0.901 | 1.79 | 0.792 |

**Table 2.**
*Performance of VTQ in the assessment of liver fibrosis in patients with chronic hepatitis C.*

according to recommendation 17 of the same guidelines, "pSWE as demonstrated with VTQ® can be used as the first-line assessment for the severity of liver fibrosis in patients with chronic viral hepatitis C. It performs best with regard to the ruling out of cirrhosis."

Data regarding the value of ElastPQ for the assessment of liver fibrosis severity in chronic hepatitis C is scarce. In a pilot study, the AUROCs of VTQ for predicting F2, F3, and F4 were 0.80, 0.88, and 0.95, respectively [31]. Similar results have been obtained in a more recent study [60].

***Following successful antiviral HCV treatment***, a significant decrease of VTQ values was observed in a study performed by Goertz et al. [61].

### 7.3 Chronic hepatitis B

Several studies have been published regarding the value of VTQ for liver fibrosis assessment in chronic hepatitis B, as shown in **Table 3**.

Sub-analysis of data regarding patients with HBV chronic hepatitis from the Nierhoff meta-analysis on VTQ calculated AUROCs of 0.88 for F2 and 0.93 for F4, with cutoffs of 1.35 and 1.87 m/s, respectively [53].

Data regarding ElastPQ and chronic HBV hepatitis is scarce, and validation is needed. In a study that compared ElastPQ to liver biopsy in chronic hepatitis B, the authors calculated an AUROC of 0.94 with a cutoff of 6.99 kPa for F2 and an AUROC of 0.89 with a cutoff of 9.00 kPa for cirrhosis [30].

Regarding HBV chronic hepatitis and pSWE, EFSUMB guidelines state that "pSWE as demonstrated with VTQ is useful in patients with CHB to identify those with cirrhosis" [5].

### 7.4 Nonalcoholic fatty liver disease (NAFLD)

Several studies have been published regarding VTQ in the evaluation of liver fibrosis in NAFLD patients. Data is presented in **Table 4**.

| Study | Reference method | F ≥ 2 | | F ≥ 3 | | F = 4 | |
|---|---|---|---|---|---|---|---|
| | | Cutoff (m/s) | AUROC | Cutoff (m/s) | AUROC | Cutoff (m/s) | AUROC |
| Friedrich Rust et al. [62] | LB—133 p | — | 0.69 | — | 0.83 | — | 0.96 |
| Zhang et al. [63] | LB—180 p | 1.63 | 0.764 | 1.74 | 0.852 | 2 | 0.825 |
| Dong et al. [64] | LB—81 p | 1.29 | 0.762 | 1.54 | 0.882 | 1.83 | 0.732 |

**Table 3.**
*Performance of VTQ in the assessment of liver fibrosis in patients with chronic hepatitis B.*

| Study | Reference method | F ≥ 3 | | F = 4 | |
|---|---|---|---|---|---|
| | | Cutoff (m/s) | AUROC | Cutoff (m/s) | AUROC |
| Yoneda et al. [65] | LB—54 p | 1.77 | 0.973 | 1.9 | 0.976 |
| Friedrich-Rust et al. [66] | LB—61 p | — | 0.71 | — | 0.74 |
| Fierbinteanu et al. [67] | LB—64 p | — | 0.944 | — | 0.984 |

**Table 4.**
*Performance of VTQ in the assessment of liver fibrosis in patients with nonalcoholic fatty liver disease.*

A recently published meta-analysis including 723 patients who evaluated VTQ as a predictor of liver fibrosis in NAFLD patients calculated a summary sensitivity and specificity of VTQ in detecting significant fibrosis of 80.2 and 85.2%, respectively, with a pooled diagnostic odds ratio of 30.13 and with an AUROC of 0.898 [68].

Considering all these data, EFSUMB guidelines conclude that VTQ can be used to exclude cirrhosis in NAFLD patients [5].

## 8. Point shear-wave elastography (pSWE) for the prediction of liver cirrhosis complications

Cirrhosis is the final stage of chronic hepatopathies and can have severe complications such as portal hypertension, hepatocellular carcinoma, decompensation, etc. The measurement of hepatic vein pressure gradient (HVPG) is the most accurate method for portal hypertension assessment, but it is an invasive method. HVPG >10 mm Hg means clinically significant portal hypertension (CSPH), while HVPG >12 mm Hg is predictive for variceal bleeding [69].

### 8.1 Portal hypertension

An initial study found a good correlation (r = 0.709) of VTQ measurements to HVPG measurements in 48 patients, with the AUROC for predicting CSPH being 0.874 [70]. In a Romanian study in 145 patients, the mean value of VTQ measurements in patients with grades 2 and 3 esophageal varices (EV) was significantly higher than the one in patients with no or small EV (3.06 ± 0.67 vs. 2.81 ± 0.80, p = 0.03) [71].

Several studies have evaluated SWVs in the spleen for the prediction of portal hypertension, with conflicting results. In the study by Rifai et al., spleen SWVs performed better than liver SWVs for predicting CSPH [72]. In the study by Vermehren et al., spleen SWV and liver SWV had similar AUROCs for predicting the presence of at least grade 2 EV, but multiple regression analysis showed that spleen measurements performed better [73]. In the study of Takuma et al., spleen VTQ measurements also performed better than in the liver to predict the presence of varices in a cohort of 340 cirrhotic patients [74].

No data is available regarding ElastPQ.

However, according to the EFSUMB guidelines "reliable cut-offs are not available yet and no strong recommendation regarding the cut-offs to be used can be made due to the limited evidence" [5].

### 8.2 Hepatocellular carcinoma (HCC)

Published data showed only poor value of VTQ to predict the occurrence of HCC, with an AUROC of 0.54 [73].

There is no data regarding ElastPQ.

## 9. Point shear-wave elastography (pSWE): perspectives

Even if pSWE is currently implemented in other systems than from Siemens and Philips, published studies are small or missing altogether.

pSWE technique implemented on the Hitachi Ascendus system was evaluated by a study published in 2017 [75]. Reliable SWV measurements (SWM) were obtained in 87.2% of the 445 patients included. Considering TE as the reference method, cutoff values for pSWE from Hitachi had been calculated to rule in and rule out patients with significant fibrosis ($F \geq 2$) and cirrhosis, respectively. SWV were converted to elastic modulus and expressed in kPa. To rule in $F \geq 2$, the SWM cutoff was 6.78 kPa, while to rule it out, it was 5.55 kPa (AUROC—0.92). To rule in cirrhosis, the SWM cutoff was 9.15 kPa, and to rule it out, it was 8.41 kPa (AUROC—0.94).

A very interesting idea is to combine several techniques in order to assess not only fibrosis severity but also steatosis and inflammation using the same ultrasound machine. pSWE was combined with strain elastography on a Hitachi system. A study evaluated 388 patients with this combined technique, considering liver biopsy as reference method [76]. The AUROCs to predict fibrosis stage were 0.87, 0.80, 0.83, and 0.80 for F1, F2, F3, and F4, respectively, while the AUROCs for activity grade were 0.94, 0.74, and 0.76 for A1, A2, and A3, respectively.

## 10. Conclusion

pSWE is an easy to perform elastographic technique, integrated into a standard ultrasound machine, with similar performance to TE to predict fibrosis severity in patients with hepatopathies of various etiologies, the performance increasing with the fibrosis severity.

## Author details

Roxana Șirli*, Alina Popescu and Ioan Sporea
Department of Gastroenterology and Hepatology, "Victor Babeș" University of Medicine and Pharmacy, Timișoara, Romania

*Address all correspondence to: roxanasirli@gmail.com

## References

[1] European Association for Study of Liver, Asociacion Latinoamericana para el Estudio del Higado. EASL-ALEH clinical practice guidelines: Non-invasive tests for evaluation of liver disease severity and prognosis. Journal of Hepatology. 2015;**63**(1):237-264

[2] Piccinino F, Sagnelli E, Pasquale G, Giusti G. Complications following percutaneous liver biopsy. A multicentre retrospective study on 68,276 biopsies. Journal of Hepatology. 1986;**2**(2):165-173

[3] Regev A, Berho M, Jeffers LJ, Milikowski C, Molina EG, Pyrsopoulos NT, et al. Sampling error and intraobserver variation in liver biopsy in patients with chronic HCV infection. The American Journal of Gastroenterology. 2002;**97**(10):2614-2618

[4] Bamber J, Cosgrove D, Dietrich CF, Fromageau J, Bojunga J, Calliada F, et al. EFSUMB guidelines and recommendations on the clinical use of ultrasound elastography. Part 1: Basic principles and technology. Ultraschall in der Medizin. 2013;**34**(2):169-184

[5] Dietrich CF, Bamber J, Berzigotti A, Bota S, Cantisani V, Castera L, et al. EFSUMB guidelines and recommendations on the clinical use of liver ultrasound Elastography, update 2017 (long version). Ultraschall in der Medizin. 2017;**38**(4):e48

[6] Ferraioli G, Filice C, Castera L, Choi BI, Sporea I, Wilson SR, et al. WFUMB guidelines and recommendations for clinical use of ultrasound elastography: Part 3: Liver. Ultrasound in Medicine & Biology. 2015;**41**(5):1161-1179

[7] Shiina T, Nightingale KR, Palmeri ML, Hall TJ, Bamber JC, Barr RG, et al. WFUMB guidelines and recommendations for clinical use of ultrasound elastography: Part 1: Basic principles and terminology. Ultrasound in Medicine & Biology. 2015;**41**(5):1126-1147

[8] Sporea I, Bota S, Saftoiu A, Sirli R, Gradinaru-Tascau O, Popescu A, et al. Romanian national guidelines and practical recommendations on liver elastography. Medical Ultrasonography. 2014;**16**(2):123-138

[9] Ferraioli G, Wong VW, Castera L, Berzigotti A, Sporea I, Dietrich CF, et al. Liver ultrasound Elastography: An update to the world Federation for Ultrasound in medicine and biology guidelines and recommendations. Ultrasound in Medicine & Biology. 2018;**44**(12):2419-2440

[10] Boursier J, Konate A, Gorea G, Reaud S, Quemener E, Oberti F, et al. Reproducibility of liver stiffness measurement by ultrasonographic elastometry. Clinical Gastroenterology and Hepatology. 2008;**6**(11):1263-1269

[11] Boursier J, Isselin G, Fouchard-Hubert I, Oberti F, Dib N, Lebigot J, et al. Acoustic radiation force impulse: A new ultrasonographic technology for the widespread noninvasive diagnosis of liver fibrosis. European Journal of Gastroenterology & Hepatology. 2010;**22**(9):1074-1084

[12] Fraquelli M, Baccarin A, Casazza G, Conti CB, Giunta M, Massironi S, et al. Liver stiffness measurement reliability and main determinants of point shear-wave elastography in patients with chronic liver disease. Alimentary Pharmacology & Therapeutics. 2016;**44**(4):356-365

[13] Sporea I, Sirli RL, Deleanu A, Popescu A, Focsa M, Danila M, et al. Acoustic radiation force impulse elastography as compared to transient elastography and liver biopsy in patients

with chronic hepatopathies. Ultraschall in der Medizin. 2011;**32**(Suppl 1):S46-S52

[14] Piscaglia F, Salvatore V, Di Donato R, D'Onofrio M, Gualandi S, Gallotti A, et al. Accuracy of VirtualTouch acoustic radiation force impulse (ARFI) imaging for the diagnosis of cirrhosis during liver ultrasonography. Ultraschall in der Medizin. 2011;**32**(2):167-175

[15] Karlas T, Pfrepper C, Wiegand J, Wittekind C, Neuschulz M, Mossner J, et al. Acoustic radiation force impulse imaging (ARFI) for non-invasive detection of liver fibrosis: Examination standards and evaluation of interlobe differences in healthy subjects and chronic liver disease. Scandinavian Journal of Gastroenterology. 2011;**46**(12):1458-1467

[16] Toshima T, Shirabe K, Takeishi K, Motomura T, Mano Y, Uchiyama H, et al. New method for assessing liver fibrosis based on acoustic radiation force impulse: A special reference to the difference between right and left liver. Journal of Gastroenterology. 2011;**46**(5):705-711

[17] Ling W, Lu Q, Quan J, Ma L, Luo Y. Assessment of impact factors on shear wave based liver stiffness measurement. European Journal of Radiology. 2013;**82**(2):335-341

[18] Bota S, Sporea I, Sirli R, Popescu A, Jurchis A. Factors which influence the accuracy of acoustic radiation force impulse (ARFI) elastography for the diagnosis of liver fibrosis in patients with chronic hepatitis C. Ultrasound in Medicine & Biology. 2013;**39**(3):407-412

[19] Bota S, Sporea I, Sirli R, Popescu A, Danila M, Sendroiu M. Factors that influence the correlation of acoustic radiation force impulse (ARFI), elastography with liver fibrosis. Medical Ultrasonography. 2011;**13**(2):135-140

[20] Goertz RS, Sturm J, Pfeifer L, Wildner D, Wachter DL, Neurath MF, et al. ARFI cut-off values and significance of standard deviation for liver fibrosis staging in patients with chronic liver disease. Annals of Hepatology. 2013;**12**(6):935-941

[21] Ferraioli G, Maiocchi L, Lissandrin R, Tinelli C, De Silvestri A, Filice C, et al. Accuracy of the ElastPQ technique for the assessment of liver fibrosis in patients with chronic hepatitis C: A "real life" single center study. Journal of Gastrointestinal and Liver Diseases. 2016;**25**(3):331-335

[22] Ferraioli G, De Silvestri A, Reiberger T, Taylor-Robinson SD, de Knegt RJ, Maiocchi L, et al. Adherence to quality criteria improves concordance between transient elastography and ElastPQ for liver stiffness assessment—A multicenter retrospective study. Digestive and Liver Disease. 2018;**50**(10):1056-1061

[23] Lupsor M, Badea R, Stefanescu H, Sparchez Z, Branda H, Serban A, et al. Performance of a new elastographic method (ARFI technology) compared to unidimensional transient elastography in the noninvasive assessment of chronic hepatitis C. preliminary results. Journal of Gastrointestinal and Liver Diseases. 2009;**18**(3):303-310

[24] Fierbinteanu-Braticevici C, Andronescu D, Usvat R, Cretoiu D, Baicus C, Marinoschi G. Acoustic radiation force imaging sonoelastography for noninvasive staging of liver fibrosis. World Journal of Gastroenterology. 2009;**15**(44):5525-5532

[25] Bota S, Sporea I, Sirli R, Popescu A, Danila M, Jurchis A, et al. Factors associated with the impossibility to obtain reliable liver stiffness measurements by means of acoustic radiation force impulse (ARFI) elastography—analysis of a cohort of 1,031 subjects. European Journal of Radiology. 2014;**83**(2):268-272

[26] Sporea I, Mare R, Lupusoru R, Popescu A, Danila M, Bende F, et al. Comparative study between four ultrasound shear waves Elastographic methods for liver fibrosis assessment. Medical Ultrasonography. 2018;**20**(3):265-271

[27] Mare R, Sporea I, Lupusoru R, Sirli R, Popescu A, Danila M, et al. The value of ElastPQ for the evaluation of liver stiffness in patients with B and C chronic hepatopathies. Ultrasonics. 2017;**77**:144-151

[28] Bota S, Sporea I, Sirli R, Popescu A, Danila M, Costachescu D. Intra- and interoperator reproducibility of acoustic radiation force impulse (ARFI) elastography—Preliminary results. Ultrasound in Medicine & Biology. 2012;**38**(7):1103-1108

[29] Guzman-Aroca F, Reus M, Berna-Serna JD, Serrano L, Serrano C, Gilabert A, et al. Reproducibility of shear wave velocity measurements by acoustic radiation force impulse imaging of the liver: A study in healthy volunteers. Journal of Ultrasound in Medicine. 2011;**30**(7):975-979

[30] Ma JJ, Ding H, Mao F, Sun HC, Xu C, Wang WP. Assessment of liver fibrosis with elastography point quantification technique in chronic hepatitis B virus patients: A comparison with liver pathological results. Journal of Gastroenterology and Hepatology. 2014;**29**(4):814-819

[31] Ferraioli G, Tinelli C, Lissandrin R, Zicchetti M, Dal Bello B, Filice G, et al. Point shear wave elastography method for assessing liver stiffness. World Journal of Gastroenterology. 2014;**20**(16):4787-4796

[32] Popescu A, Bota S, Sporea I, Sirli R, Danila M, Racean S, et al. The influence of food intake on liver stiffness values assessed by acoustic radiation force impulse elastography-preliminary results. Ultrasound in Medicine & Biology. 2013;**39**(4):579-584

[33] Gersak MM, Sorantin E, Windhaber J, Dudea SM, Riccabona M. The influence of acute physical effort on liver stiffness estimation using virtual touch quantification (VTQ). Preliminary results. Medical Ultrasonography. 2016;**18**(2):151-156

[34] Bota S, Sporea I, Peck-Radosavljevic M, Sirli R, Tanaka H, Iijima H, et al. The influence of aminotransferase levels on liver stiffness assessed by acoustic radiation force impulse Elastography: A retrospective multicentre study. Digestive and Liver Disease. 2013;**45**(9):762-768

[35] Yoon KT, Lim SM, Park JY, Kim DY, Ahn SH, Han KH, et al. Liver stiffness measurement using acoustic radiation force impulse (ARFI) elastography and effect of necroinflammation. Digestive Diseases and Sciences. 2012;**57**(6):1682-1691

[36] Kuroda H, Takikawa Y, Onodera M, Kakisaka K, Yoshida Y, Kataoka K, et al. Serial changes of liver stiffness measured by acoustic radiation force impulse imaging in acute liver failure: A case report. Journal of Clinical Ultrasound. 2012;**40**(2):99-104

[37] Goertz RS, Egger C, Neurath MF, Strobel D. Impact of food intake, ultrasound transducer, breathing maneuvers and body position on acoustic radiation force impulse (ARFI) elastometry of the liver. Ultraschall in der Medizin. 2012;**33**(4):380-385

[38] Attia D, Pischke S, Negm AA, Rifai K, Manns MP, Gebel MJ, et al. Changes in liver stiffness using acoustic radiation force impulse imaging in patients with obstructive cholestasis and cholangitis. Digestive and Liver Disease. 2014;**46**(7):625-631

[39] Popescu A, Sporea I, Sirli R, Bota S, Focsa M, Danila M, et al. The mean values of liver stiffness assessed by acoustic radiation force impulse elastography in normal subjects. Medical Ultrasonography. 2011;**13**(1):33-37

[40] Son CY, Kim SU, Han WK, Choi GH, Park H, Yang SC, et al. Normal liver elasticity values using acoustic radiation force impulse imaging: A prospective study in healthy living liver and kidney donors. Journal of Gastroenterology and Hepatology. 2012;**27**(1):130-136

[41] Goertz RS, Amann K, Heide R, Bernatik T, Neurath MF, Strobel D. An abdominal and thyroid status with acoustic radiation force impulse Elastometry—A feasibility study: Acoustic Radiation Force Impulse Elastometry of human organs. European Journal of Radiology. 2011;**80**(3):e226-e230

[42] Madhok R, Tapasvi C, Prasad U, Gupta AK, Aggarwal A. Acoustic radiation force impulse imaging of the liver: Measurement of the normal mean values of the shearing wave velocity in a healthy liver. Journal of Clinical and Diagnostic Research. 2013;**7**(1):39-42

[43] Sporea I, Bota S, Gradinaru-Tascau O, Sirli R, Popescu A. Comparative study between two point shear wave Elastographic techniques: Acoustic radiation force impulse (ARFI) elastography and ElastPQ. Medical Ultrasonography. 2014;**16**(4):309-314

[44] Friedrich-Rust M, Wunder K, Kriener S, Sotoudeh F, Richter S, Bojunga J, et al. Liver fibrosis in viral hepatitis: Noninvasive assessment with acoustic radiation force impulse imaging versus transient elastography. Radiology. 2009;**252**(2):595-604

[45] Sporea I, Badea R, Sirli R, Lupsor M, Popescu A, Danila M, et al. How efficient is acoustic radiation force impulse elastography for the evaluation of liver stiffness? Hepatitis Monthly. 2011;**11**(7):532-538

[46] Takahashi H, Ono N, Eguchi Y, Eguchi T, Kitajima Y, Kawaguchi Y, et al. Evaluation of acoustic radiation force impulse elastography for fibrosis staging of chronic liver disease: A pilot study. Liver International. 2010;**30**(4):538-545

[47] Goertz RS, Zopf Y, Jugl V, Heide R, Janson C, Strobel D, et al. Measurement of liver elasticity with acoustic radiation force impulse (ARFI) technology: An alternative noninvasive method for staging liver fibrosis in viral hepatitis. Ultraschall in der Medizin. 2010;**31**(2):151-155

[48] Ebinuma H, Saito H, Komuta M, Ojiro K, Wakabayashi K, Usui S, et al. Evaluation of liver fibrosis by transient elastography using acoustic radiation force impulse: Comparison with Fibroscan ((R)). Journal of Gastroenterology. 2011;**46**(10):1238-1248

[49] Colombo S, Buonocore M, Del Poggio A, Jamoletti C, Elia S, Mattiello M, et al. Head-to-head comparison of transient elastography (TE), real-time tissue elastography (RTE), and acoustic radiation force impulse (ARFI) imaging in the diagnosis of liver fibrosis. Journal of Gastroenterology. 2012;**47**(4):461-469

[50] Cassinotto C, Lapuyade B, Mouries A, Hiriart JB, Vergniol J, Gaye D, et al. Non-invasive assessment of liver fibrosis with impulse elastography: Comparison of supersonic shear imaging with ARFI and FibroScan(R). Journal of Hepatology. 2014;**61**(3):550-557

[51] Friedrich-Rust M, Nierhoff J, Lupsor M, Sporea I, Fierbinteanu-Braticevici C, Strobel D, et al. Performance of acoustic radiation force impulse imaging for the staging of liver fibrosis: A pooled

meta-analysis. Journal of Viral Hepatitis. 2012;**19**(2):e212-e219

[52] Bota S, Herkner H, Sporea I, Salzl P, Sirli R, Neghina AM, et al. Meta-analysis: ARFI elastography versus transient elastography for the evaluation of liver fibrosis. Liver International. 2013;**33**(8):1138-1147

[53] Nierhoff J, Chavez Ortiz AA, Herrmann E, Zeuzem S, Friedrich-Rust M. The efficiency of acoustic radiation force impulse imaging for the staging of liver fibrosis: A meta-analysis. European Radiology. 2013;**23**(11):3040-3053

[54] Hu X, Qiu L, Liu D, Qian L. Acoustic radiation force impulse (ARFI) Elastography for noninvasive evaluation of hepatic fibrosis in chronic hepatitis B and C patients: A systematic review and meta-analysis. Medical Ultrasonography. 2017;**19**(1):23-31

[55] Sporea I, Sirli R, Bota S, Fierbinteanu-Braticevici C, Petrisor A, Badea R, et al. Is ARFI elastography reliable for predicting fibrosis severity in chronic HCV hepatitis? World Journal of Radiology. 2011;**3**(7):188-193

[56] Sporea I, Bota S, Peck-Radosavljevic M, Sirli R, Tanaka H, Iijima H, et al. Acoustic radiation force impulse elastography for fibrosis evaluation in patients with chronic hepatitis C: An international multicenter study. European Journal of Radiology. 2012;**81**(12):4112-4118

[57] Rizzo L, Calvaruso V, Cacopardo B, Alessi N, Attanasio M, Petta S, et al. Comparison of transient elastography and acoustic radiation force impulse for non-invasive staging of liver fibrosis in patients with chronic hepatitis C. The American Journal of Gastroenterology. 2011;**106**(12):2112-2120

[58] Chen SH, Li YF, Lai HC, Kao JT, Peng CY, Chuang PH, et al. Effects of patient factors on noninvasive liver stiffness measurement using acoustic radiation force impulse elastography in patients with chronic hepatitis C. BMC Gastroenterology. 2012;**12**:105

[59] Li SM, Li GX, Fu DM, Wang Y, Dang LQ. Liver fibrosis evaluation by ARFI and APRI in chronic hepatitis C. World Journal of Gastroenterology. 2014;**20**(28):9528-9533

[60] Conti F, Serra C, Vukotic R, Fiorini E, Felicani C, Mazzotta E, et al. Accuracy of elastography point quantification and steatosis influence on assessing liver fibrosis in patients with chronic hepatitis C. Liver International. 2017;**37**(2):187-195

[61] Goertz RS, Sturm J, Zopf S, Wildner D, Neurath MF, Strobel D. Outcome analysis of liver stiffness by ARFI (acoustic radiation force impulse) elastometry in patients with chronic viral hepatitis B and C. Clinical Radiology. 2014;**69**(3):275-279

[62] Friedrich-Rust M, Buggisch P, de Knegt RJ, Dries V, Shi Y, Matschenz K, et al. Acoustic radiation force impulse imaging for non-invasive assessment of liver fibrosis in chronic hepatitis B. Journal of Viral Hepatitis. 2013;**20**(4):240-247

[63] Zhang D, Chen M, Wang R, Liu Y, Zhang D, Liu L, et al. Comparison of acoustic radiation force impulse imaging and transient elastography for non-invasive assessment of liver fibrosis in patients with chronic hepatitis B. Ultrasound in Medicine & Biology. 2015;**41**(1):7-14

[64] Dong DR, Hao MN, Li C, Peng Z, Liu X, Wang GP, et al. Acoustic radiation force impulse elastography, FibroScan(R), Forns' index and their combination in the assessment of liver fibrosis in patients with chronic hepatitis B, and the impact of inflammatory activity and steatosis on

these diagnostic methods. Molecular Medicine Reports. 2015;**11**(6):4174-4182

[65] Yoneda M, Suzuki K, Kato S, Fujita K, Nozaki Y, Hosono K, et al. Nonalcoholic fatty liver disease: US-based acoustic radiation force impulse elastography. Radiology. 2010;**256**(2):640-647

[66] Friedrich-Rust M, Romen D, Vermehren J, Kriener S, Sadet D, Herrmann E, et al. Acoustic radiation force impulse-imaging and transient elastography for non-invasive assessment of liver fibrosis and steatosis in NAFLD. European Journal of Radiology. 2012;**81**(3):e325-e331

[67] Fierbinteanu Braticevici C, Sporea I, Panaitescu E, Tribus L. Value of acoustic radiation force impulse imaging elastography for non-invasive evaluation of patients with nonalcoholic fatty liver disease. Ultrasound in Medicine & Biology. 2013;**39**(11):1942-1950

[68] Liu H, Fu J, Hong R, Liu L, Li F. Acoustic radiation force impulse Elastography for the non-invasive evaluation of hepatic fibrosis in non-alcoholic fatty liver disease patients: A Systematic Review & Meta-Analysis. PLoS One. 2015;**10**(7):e0127782

[69] Bosch J, Garcia-Pagan JC, Berzigotti A, Abraldes JG. Measurement of portal pressure and its role in the management of chronic liver disease. Seminars in Liver Disease. 2006;**26**(4):348-362

[70] Salzl P, Reiberger T, Ferlitsch M, Payer BA, Schwengerer B, Trauner M, et al. Evaluation of portal hypertension and varices by acoustic radiation force impulse imaging of the liver compared to transient elastography and AST to platelet ratio index. Ultraschall in der Medizin. 2014;**35**(6):528-533

[71] Bota S, Sporea I, Sirli R, Focsa M, Popescu A, Danila M, et al. Can ARFI elastography predict the presence of significant esophageal varices in newly diagnosed cirrhotic patients? Annals of Hepatology. 2012;**11**(4):519-525

[72] Rifai K, Cornberg J, Bahr M, Mederacke I, Potthoff A, Wedemeyer H, et al. ARFI elastography of the spleen is inferior to liver elastography for the detection of portal hypertension. Ultraschall in der Medizin. 2011;**32**(Suppl 2):E24-E30

[73] Vermehren J, Polta A, Zimmermann O, Herrmann E, Poynard T, Hofmann WP, et al. Comparison of acoustic radiation force impulse imaging with transient elastography for the detection of complications in patients with cirrhosis. Liver International. 2012;**32**(5):852-858

[74] Takuma Y, Nouso K, Morimoto Y, Tomokuni J, Sahara A, Toshikuni N, et al. Measurement of spleen stiffness by acoustic radiation force impulse imaging identifies cirrhotic patients with esophageal varices. Gastroenterology. 2013;**144**(1):92-101 e2

[75] Ferraioli G, Maiocchi L, Lissandrin R, Tinelli C, De Silvestri A, Filice C. Ruling-in and ruling-out significant fibrosis and cirrhosis in patients with chronic hepatitis C using a shear wave measurement method. Journal of Gastrointestinal and Liver Diseases. 2017;**26**(2):139-143

[76] Yada N, Tamaki N, Koizumi Y, Hirooka M, Nakashima O, Hiasa Y, et al. Diagnosis of fibrosis and activity by a combined use of strain and shear wave imaging in patients with liver disease. Digestive Diseases. 2017;**35**(6):515-520

Chapter 3

# 2D Shear Wave Elastography for Liver Fibrosis Evaluation

*Alina Popescu, Roxana Şirli and Ioan Sporea*

## Abstract

2D shear wave elastography is a technique embedded in ultrasound machines which allows the interrogation of the tissue by acoustic radiation force impulses induced into the tissues by focused ultrasonic beams and captures the propagation of resulting shear waves in real time. Elasticity is displayed using a color-coded image superimposed on a B-mode image, and at the same time, a quantitative estimation of liver stiffness (LS) can be performed in a certain region of interest (ROI). The published data showed a real value of this method for liver stiffness estimation in patients with chronic hepatitis. It has the following advantages: it is integrated into standard ultrasound systems; it is a real-time elastographic method; and it is also feasible in patients with ascites and with large and adjustable size of the ROI that will be evaluated.

**Keywords:** 2D shear wave elastography, liver stiffness, liver fibrosis, chronic liver diseases, liver cirrhosis

## 1. Introduction

Chronic liver diseases of different etiologies are still an important health problem, staging fibrosis being one of the issues that relate to prognosis and treatment decision. Liver biopsy, the gold standard method for liver fibrosis assessment, is an invasive procedure, with possible complications and lower compliance as compared to noninvasive techniques.

Ultrasound-based liver elastography was developed as a noninvasive, easy to perform, and well-accepted tool for liver fibrosis assessment and proved to be a very dynamic research field in the last years, this being demonstrated also by the large number of publications and guidelines published in this field [1–3].

2D shear wave elastography is one of the new developed ultrasound-based techniques [1], embedded in ultrasound machines, that allow the interrogation of the tissue by dynamic acoustic radiation force impulses induced into the tissues by focused ultrasonic beams and capture the propagation of resulting shear waves in real time. The technique has the advantage that the elasticity is displayed using a color-coded image superimposed on a B-mode image, and at the same time, a quantitative estimation of liver stiffness (LS) can be performed in a certain region of interest (ROI), the results being expressed in kPa or m/s.

The measurements are performed, similar to other elastography techniques, with the patient lying in supine position with the right arm in maximal abduction, in the right liver lobe, by placing the probe in between the ribs, in the seventh to ninth intercostal space, perpendicular on the liver surface [1]. The examiner should apply sufficient pressure on the probe to make good contact with the tissue,


**Figure 1.**
*2D SWE.SSI.*

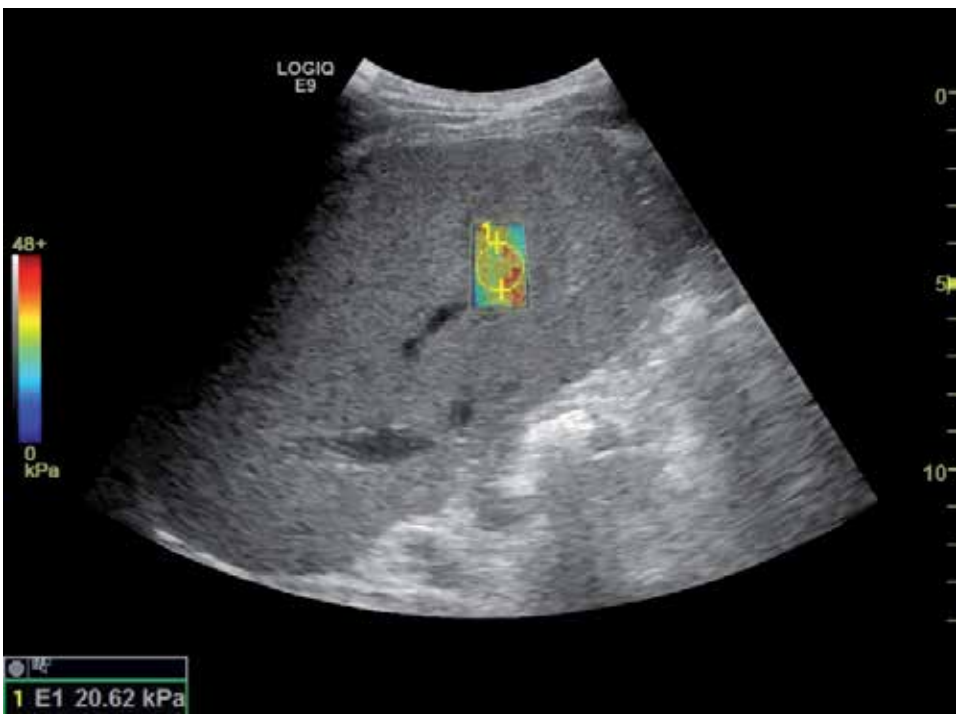


**Figure 2.**
*2D SWE.GE.*

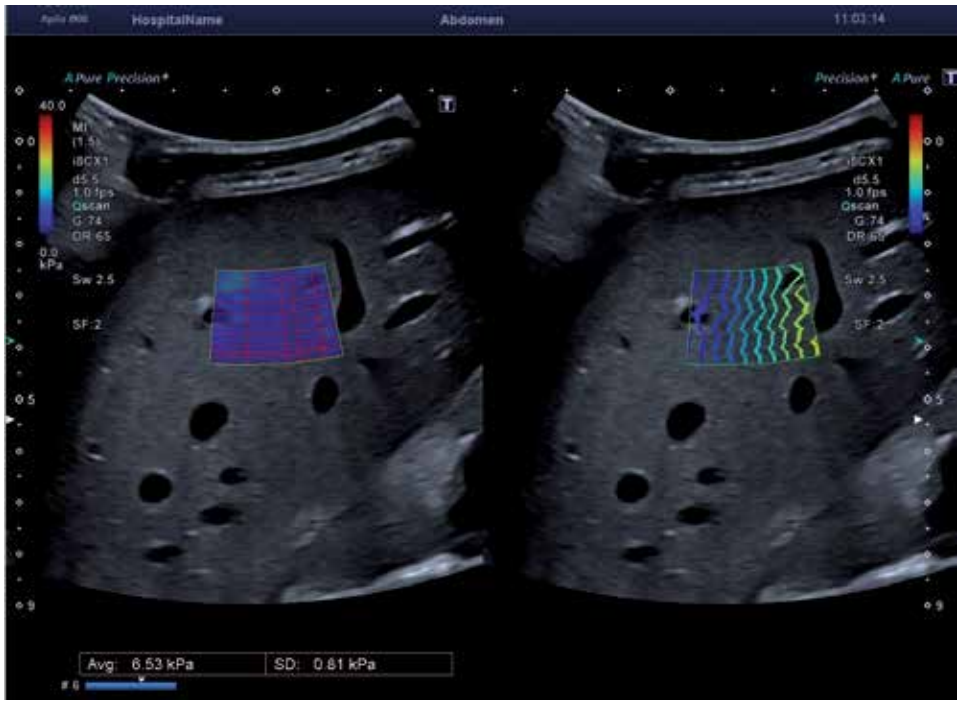


**Figure 3.**
*2D SWE with a propagation map (Canon).*

should stabilize the hand and the probe while performing the measurement, and should ask the patient to stop breathing and avoid deep inspiration. The ROI should be placed in an area free of vessels, at least 1–2 cm and at maximum of 6 cm under the liver capsule [1].

The technique has the advantage that can be performed also in patients with ascites, but an adequate B-mode ultrasound live image is necessary for reliable results. On the other hand, published data showed that for a high feasibility of the method, ultrasound experience is needed, especially in difficult cases, for example, obese patients or narrow intercostal spaces [1, 4, 5].

First 2D SWE technique was developed by Supersonic Imagine (France) (2D SWE.SSI) and embedded in Aixplorer® system (**Figure 1**). Other companies followed with similar techniques, for example, General Electric (2D SWE.GE) (**Figure 2**), 2D SWE technique with a propagation map Canon-Toshiba (**Figure 3**), Philips (ElastQ), Samsung, etc.

## 2. 2D SWE.SSI

Published data showed that 2D SWE.SSI is a feasible and reproducible method [6]. The manufacturer recommends a minimum of three valid measurements to be obtained and rejects any measurement that achieves less than 90% stability index (SI), as a reliability criterion. Other authors [7] used standard deviation/median liver stiffness of ≤0.10 and measurement depth of <5.6 cm as quality parameters for reliable measurements. Most published data showed that reliable LS measurements can be obtained in 90–98.9% of cases [5–10] with a good intra- and interobserver reproducibility [9, 11, 12].

### 2.1 Healthy volunteers

The values of LS evaluated by 2D SWE.SSI in healthy volunteers varied from 2.6 to 6.2 kPa [13–15], with higher values in male vs. female patients (6.6 ± 1.5 vs. 5.7 ± 1.3 kPa, p = 0.01.) [14].

### 2.2 Confounding factors

Similar to other ultrasound-based elastographic methods, the liver stiffness results obtained by 2D SWE.SSI may be influenced by food intake; some authors suggest that the values increase significantly in the first hour after food intake and decrease after 60 min after meal [16, 17], while in other studies, these results were not reproduced [18], suggesting that maybe this method is less influenced by food intake. Nevertheless, while more studies are necessary to clarify this issue, the measurements should be performed in fasting condition to avoid any errors.

Other studies are also needed to evaluate the effect of cytolysis, cholestasis, or congestive heart failure on the liver stiffness values obtained through 2D SWE.

### 2.3 2D SWE.SSI for predicting liver fibrosis in chronic liver diseases of various etiologies

Several studies showed good accuracy for 2D SWE.SSI for predicting significant fibrosis and liver cirrhosis in chronic liver diseases of different etiologies (**Table 1**). Overall, the method has good accuracy for evaluating both significant and severe fibrosis, slightly better for liver cirrhosis, but with very different cutoff values between etiologies and between different studies.

| Ref. | Year | Etiology | Patients (*n*) | Fibrosis stage | AUROC | Cutoffs (kPa) | Se (%) | Sp (%) | PPV (%) | NPV (%) |
|---|---|---|---|---|---|---|---|---|---|---|
| Jeong et al. [20] | 2014 | Mixt | 70 | F ≥ 2 | 0.915 | 8.60 | 78.2 | 93.3 | 97.7 | 53.8 |
| | | | | F = 4 | 0.878 | 14.00 | 77.3 | 85.4 | 70.8 | 89.2 |
| Deffieux et al. [21] | 2015 | Mixt | 120 | F ≥ 2 | 0.890 | 8.90 | 77.0 | 79.0 | 77.0 | 79.0 |
| | | | | F = 4 | 0.890 | 10.20 | 83.0 | 76.0 | 38.0 | 96.0 |
| Sporea et al. [22] | 2014 | Mixt | 383 | F ≥ 2 | 0.859 | 7.8 | 76.8 | 82.6 | 77.9 | 81.5 |
| | | | | F = 4 | 0.914 | 11.5 | 80.6 | 92.7 | 60.9 | 97.1 |
| Sporea et al. [23] | 2018 | Mixt | 82 | F ≥ 2 | 0.853 | 7.1 | 96.8 | 78 | 73.8 | 97.5 |
| | | | | F = 4 | 0.94 | 13 | 78.9 | 97.7 | 88.2 | 95.5 |
| Bavu et al. [24] | 2011 | HCV | 113 | F ≥ 2 | 0.950 | 9.12 | 81.0 | 72.0 | | |
| | | | | F = 4 | 0.970 | 13.30 | 80.0 | 87.0 | | |
| Ferraioli et al. [5] | 2012 | HCV | 121 | F ≥ 2 | 0.920 | 7.10 | 90.0 | 87.5 | 91.3 | 85.7 |
| | | | | F = 4 | 0.980 | 10.40 | 87.5 | 96.8 | 87.5 | 96.8 |
| Tada et al. [25] | 2013 | HCV | 55 | F ≥ 2 | 0.940 | 8.80 | 88.9 | 91.9 | 84.2 | 94.4 |
| Leung et al. [8] | 2013 | HBV | 226 | F ≥ 2 | 0.880 | 7.100 | 84.70 | 92.10 | 85.3 | 91.7 |

| Ref. | Year | Etiology | Patients (*n*) | Fibrosis stage | AUROC | Cutoffs (kPa) | Se (%) | Sp (%) | PPV (%) | NPV (%) |
|---|---|---|---|---|---|---|---|---|---|---|
| | | | | F = 4 | 0.980 | 10.100 | 97.40 | 93.00 | 60.1 | 99.6 |
| Zeng et al. [26] | 2014 | HBV | 206 | F ≥ 2 | 0.917 | 7.200 | 86.36 | 86.96 | 88.8 | 84.2 |
| | | | | F = 4 | 0.945 | 11.700 | 91.89 | 89.70 | 66.7 | 98.0 |
| Wu et al. [27] | 2016 | HBV | 437 | F ≥ 2 | 0.903 | 8.200 | 78.16 | 85.28 | 82.6 | 81.4 |
| | | | | F = 4 | 0.926 | 11.256 | 91.80 | 84.31 | 48.7 | 98.4 |
| Zhuang et al. [28] | 2017 | HBV | 304 | F ≥ 2 | 0.970 | 7.600 | 92.00 | 90.00 | 98.4 | 64.3 |
| | | | | F = 4 | 0.980 | 10.400 | 94.60 | 94.90 | 95.7 | 93.5 |
| Zeng et al. [29] | 2017 | HBV | 257 | F ≥ 2 | 0.882 | 7.100 | 88.89 | 76.38 | 76.2 | 89.0 |
| | | | | F = 4 | 0.926 | 11.300 | 93.55 | 87.25 | 52.7 | 98.9 |
| Cassinotto et al. [30] | 2016 | NAFLD | 291 | F ≥ 2 | 0.860 | 8.90 | 68.0 | 94.0 | | |
| | | | | F = 4 | 0.880 | 10.00 | 95.0 | 69.0 | | |
| Takeuchi et al. [31] | 2018 | NAFLD | 71 | F ≥ 2 | 0.750 | 11.57 | 52.0 | 44.0 | | |
| | | | | F = 4 | 0.900 | 15.73 | 100.0 | 82.0 | | |
| Thiele et al. [32] | 2016 | Alcohol | 199 | F ≥ 2 | 0.940 | 10.20 | 82.0 | 93.0 | 90.0 | 88.0 |
| | | | | F = 4 | 0.950 | 16.40 | 94.0 | 91.0 | 71.0 | 99.0 |
| Zeng et al. [33] | 2017 | Autoimmune | 114 | F ≥ 2 | 0.850 | 9.70 | 81.7 | 81.3 | 91.8 | 63.4 |
| | | | | F = 4 | 0.860 | 16.30 | 87.0 | 80.2 | 52.6 | 96.1 |
| Li et al. [34] | 2018 | Autoimmune | 51 | F ≥ 2 | 0.781 | 9.15 | 83.3 | 72.7 | | |

**Table 1.**
*Diagnostic performance of 2D SWE.SSI for significant fibrosis (F ≥ 2) and cirrhosis (F = 4) in different chronic liver diseases—adapted after Jeong JY et al. [19].*

Two comparative studies between transient elastography, point SWE (VTQ) and 2D SWE.SSI, were proposed by Cassinotto et al. in chronic liver diseases [35] and NAFLD patients [30]. The first study enrolled 349 consecutive patients with chronic liver diseases who underwent liver biopsy. For each patient, LS was assessed by 2D SWE.SSI, pSWE (VTQ), and transient elastography (FibroScan, M and XL probes). 2D SWE.SSI, transient elastography and VTQ, correlated significantly with histological fibrosis score ($r = 0.79$, $p < .00001$; $r = 0.70$, $p < .00001$; $r = 0.64$, $p < .00001$, respectively) with no significant differences between methods for the diagnosis of mild fibrosis and cirrhosis.

The second study [30] included 291 NAFLD patients in whom liver stiffness was assessed by 2D SWE.SSI, transient elastography (M probe), and VTQ within 2 weeks prior to liver biopsy. The AUROC for 2D SWE.SSI, transient elastography, and VTQ were 0.86, 0.82, and 0.77 for diagnoses of ≥F2; 0.89, 0.86, and 0.84 for ≥F3; and 0.88, 0.87, and 0.84 for F4, respectively. The cutoff values for 2D SWE.SSI and transient elastography for predicting fibrosis with a sensitivity ≥90% were very close: 6.3/6.2 kPa for ≥F2, 8.3/8.2 kPa for ≥F3, and 10.5/9.5 kPa for F4.

In an individual patient data based on meta-analysis [36] that included 1340 patients and compared 2D SWE.SSI with liver biopsy as reference method, 2D SWE.SSI showed a good to excellent performance in LS assessment in patients with HCV, HBV, and NAFLD, with AUROCs of 86.3, 91.6, and 85.9% for diagnosing significant fibrosis ($F \geq 2$) and 96.1, 97.1, and 95.5% for diagnosing cirrhosis ($F = 4$), respectively. The optimal cutoff for diagnosing significant fibrosis in all patients was 7.1 kPa, while for diagnosing liver cirrhosis was 13.5 kPa in HCV and NAFLD and 11.5 kPa in HBV patients.

Other three meta-analyses published that included more than 900 patients each [37–39] confirmed these results, with pooled sensitivities between 0.84 and 0.85, pooled specificities between 0.81 and 0.83 and AUROC between 0.85 and 0.87 for significant fibrosis and with pooled sensitivities between 0.87 and 0.89, and pooled specificities between 0.86 and 0.88 and AUROC between 0.93 and 0.94 for liver cirrhosis.

### 2.4 2D SWE.SSI for predicting liver cirrhosis complications

The method was studied also as a predictor for the presence of clinically significant portal hypertension. Thus, while Kim et al. showed that for a cutoff value of 15.2 kPa, the sensitivity and specificity of 2D SWE.SSI for predicting clinically significant portal hypertension were 85.7 and 80%, respectively, (AUROC 0.819) (HVPG >10 mmHg) [40], Procopet et al. [7], by using standard deviation/median liver stiffness ≤0.10 and measurement depth < 5.6 cm as quality criteria, had better results for the optimal cutoff value of 15.4 kPa (AUROC =0.948, with sensitivity and specificity both higher than 90%).

Another study that included 79 patients with liver cirrhosis [41] evaluated LS and spleen stiffness (SS) by 2D SWE.SSI, TE, and HVPG measurements; 2D SWE.SSI LS of more than 24.6 kPa had a sensitivity, specificity, and accuracy for clinically significant portal hypertension of 81, 88, and 82%, respectively, with better performance than SS (AUROC of 0.87 vs. 0.64, $P = 0.003$).

In a larger study that enrolled 401 consecutive cirrhotic patients [42], the LS cutoff values for a NPV ≥90% for high-risk esophageal varices, history of ascites, Child-Pugh B/C, variceal bleeding, and clinical decompensation were 12.8, 19, 21.4, 30.5, and 39.4 kPa, respectively, with AUROC of 0.77 for detection of esophageal varices.

Jeong et al. [43] looked on the role of 2D SWE in predicting the development of hepatocellular carcinoma, showing that patients with LS ≥10 kPa by 2D SWE had a fourfold higher risk of presenting hepatocellular carcinoma than those with LS <10 kPa.

More studies are needed to address these issues and conclude for the clinical practice.

### 2.5 2D SWE.SSI in pediatric population

The field of elastography, as noninvasive evaluation tool, became of interest also in pediatric population [44]. Thus a study that enrolled 54 consecutive children and adolescents with different chronic liver diseases that were examined by means of TE, ARFI, and 2D SWE.SSI showed a sensitivity of 2D SWE.SSI for detecting F1, F2, F3, and liver cirrhosis of 92.85, 83.33, 87.5, and 85.71%, respectively [45], better than a point SWE technique.

## 3. 2D SWE.GE

Another system that implemented the 2D SWE technique comes from General Electrics, embedded first in **LOGIQ E9/LOGIQ E10** ultrasound systems.

This new technique showed also good intra- and interobserver reproducibility. In a study that included 60 patients evaluated by 2D SWE.GE by three examiners with different levels of experience in ultrasound-based elastography and ultrasound, the overall agreement between examiners was excellent: 0.915 (95% confidence interval [CI]: 0.870-0.946). The intra-observer reproducibility for each of the examiners was excellent; however, the inter-class correlation coefficients were higher for the examiners more experienced in elastography: 0.936 (95% CI: 0.896-0.963) vs. 0.966 (95% CI: 0.943-0.980) vs. 0.984 (95% CI: 0. 973-0.991) [46].

The method showed also very good feasibility and reproducibility also in pediatric population. In a study that enrolled 243 healthy participants aged 4–17 years, valid measurements were obtained in 242 of 243 (99.6%) subjects for 2D SWE. GE, with an intraclass correlation coefficients between observers of 0.84 [47].

The mean LS measurement by 2D SWE.GE in healthy subjects was 5.1 ± 1.3 kPa, significantly higher than the LS measurement assessed by transient elastography (4.3 ± 0.9 kPa, $p < 0.0001$) and significantly higher for male vs. female, 5.9 ± 1.2 vs. 4.7 ± 1.2 kPa ($p = 0.0005$) [48].

There are few data available in the literature regarding the performance of this method in evaluating liver fibrosis in chronic liver diseases, but the results are promising.

Thus in a study that enrolled 331 consecutive subjects with or without chronic hepatopathies [49] in whom LS was evaluated in the same session by means of two elastographic techniques, transient elastography and 2D SWE.GE, reliable LS measurements were obtained in 95.8% subjects by 2D SWE.GE and 94.2% by TE ($p = 0.44$), with a strong correlation between the LS values obtained by the two methods: $r = 0.83$, $p < 0.0001$. The best cutoff value for $F \geq 2$, $F \geq 3$, and for $F = 4$ were 6.7, 8.2, and 9.3 kPa.

Similar results were obtained in an Italian study [50] that enrolled 54 healthy subjects and 174 patients with chronic liver diseases and compared 2D SWE.GE with liver biopsy as reference method and obtained reliable LS measurements in all subjects, with a strong correlation the LS measurements and liver fibrosis ($r = 0.628$). The AUROC values were better also for severe fibrosis: for $F \geq 2$: 0.857, for $F \geq 3$: 0.946, and for $F = 4$: 0.935.

## 4. 2D SWE with propagation map

**2D SWE with propagation map** (**Figure 3**), technique developed by Canon-Toshiba, is a more recent technology that appeared on the market but also with good perspectives in the field of liver elastography. Thus, in a study [51] on 115 consecutive patients that underwent 2D SWE by two different operators and transient elastography by sonographers during the same day, the correlation coefficient of the intraclass correlation test between an experienced radiologist and a third-year radiology resident was 0.878, and there was a moderate correlation between 2D SWE and transient elastography ($r = 0.511$) in the diagnosis of liver fibrosis. The best cutoff values for predicting significant fibrosis and liver cirrhosis by 2D SWE were > 1.78 (AUROC = 0.777) and > 2.24 m/s (AUROC = 0.935), respectively.

## 5. Conclusion

Even if 2D SWE techniques are quite newer on the market, they proved to be reliable methods for liver fibrosis evaluation, and several advantages can be

highlighted: they are integrated into standard ultrasound systems, are real-time elastographic methods, and are feasible also in patients with ascites and with large and adjustable size of the ROI that will be evaluated. These techniques have better accuracy for predicting liver cirrhosis, with accuracy more than 95%, and they also have good accuracy (more than 85%) for predicting significant fibrosis (F2).

## Author details

Alina Popescu*, Roxana Şirli and Ioan Sporea
Department of Gastroenterology and Hepatology, "Victor Babeș" University of Medicine and Pharmacy Timișoara, Romania

*Address all correspondence to: alinamircea.popescu@gmail.com

## References

[1] Dietrich CF, Bamber J, Berzigotti A, et al. EFSUMB guidelines and recommendations on the clinical use of liver ultrasound Elastography, update 2017 (short version). Ultraschall in der Medizin. 2017;**38**(4):377-394

[2] Ferraioli G, Filice C, Castera L, et al. WFUMB guidelines and recommendations for clinical use of ultrasound elastography: Part 3: Liver. Ultrasound in Medicine & Biology. 2015;**41**(5):1161-1179

[3] Sporea I, Bota S, Săftoiu A, et al. Romanian Society of Ultrasound in medicine and biology. Romanian national guidelines and practical recommendations on liver elastography. Medical Ultrasonography. 2014;**16**(2):123-138

[4] Grădinaru-Taşcău O, Sporea I, Bota S, et al. Does experience play a role in the ability to perform liver stiffness measurements by means of supersonic shear imaging (SSI)? Medical Ultrasonography. 2013;**15**:180-183

[5] Ferraioli G, Tinelli C, Dal Bello B, et al. Accuracy of real-time shear wave elastography for assessing liver fibrosis in chronic hepatitis C: A pilot study. Hepatology. 2012;**56**:2125-2133

[6] Lupșor-Platon M, Badea R, Gersak M, et al. Noninvasive assessment of liver diseases using 2D shear wave Elastography. Journal of Gastrointestinal and Liver Diseases. 2016;**25**(4):525-532

[7] Procopet B, Berzigotti A, Abraldes JG, et al. Real-time shear-wave elastography: Applicability, reliability and accuracy for clinically significant portal hypertension. Journal of Hepatology. 2015;**62**:1068-1075

[8] Leung VY, Shen J, Wong VW, et al. Quantitative elastography of liver fibrosis and spleen stiffness in chronic hepatitis B carriers: Comparison of shear-wave elastography and transient elastography with liver biopsy correlation. Radiology. 2013;**269**:910-918

[9] Hudson JM, Milot L, Parry C, et al. Inter- and intra-operator reliability and repeatability of shear wave elastography in the liver: A study in healthy volunteers. Ultrasound in Medicine & Biology. 2013;**39**:950-955

[10] Poynard T, Munteanu M, Luckina E, et al. Liver fibrosis evaluation using real-time shear wave elastography: Applicability and diagnostic performance using methods without a gold standard. Journal of Hepatology. 2013;**58**:928-935

[11] Ferraioli G, Tinelli C, Zicchetti M, et al. Reproducibility of real-time shear wave elastography in the evaluation of liver elasticity. European Journal of Radiology. 2012;**81**:3102-3106

[12] Zoumpoulis PS, Theotokas I, Mastorakou E, et al. Technical and software adjustments for a reliable shear wave Elastography estimation of fibrosis in chronic liver disease. Ultrasound in Medicine & Biology. 2011;**8S**:S58

[13] Zoumpoulis PS, Mastorakou E, Theotokas I, et al. Shear wave Elastography for the evaluation of diffuse liver disease: Determining Normal and pathological values in kPa. Ultrasound in Medicine & Biology. 2011;**8S**:S58

[14] Șirli R, Bota S, Sporea I, et al. Liver stiffness measurements by means of supersonic shear imaging in patients without known liver pathology. Ultrasound in Medicine & Biology. 2013;**39**:1362-1367

[15] Suh CH, Kim SY, Kim KW, et al. Determination of normal hepatic

elasticity by using real-time shear-wave elastography. Radiology. 2014;**271**(3):895-900

[16] Vonghia L, Werlinden W, Pelckmans P, Michielsen P, Francque S. Liver stiffness by shear wave elastography is influenced by meal and meal related haemodynamic modifications. Ultraschall in der Medizin. 2013;**34**:WS_SL24_09. DOI: 10.1055/s-0033-1354961

[17] Gersak MM, Badea R, Lenghel LM, Vasilescu D, Botar-Jid C, Dudea SM. Influence of food intake on 2-D shear wave Elastography assessment of liver stiffness in healthy subjects. Ultrasound in Medicine & Biology. 2016;**42**:1295-1302

[18] Popescu A, Lupusoru R, Bende F, et al. The influence of food intake on liver stiffness measurements obtained by two 2D-SWE methods. Ultraschall in der Medizin. 2016;**37**:S1-S78. DOI: 10.1055/s-0036-1587862

[19] Jeong JY, Cho YS, Sohn JH. Role of two-dimensional shear wave elastography in chronic liver diseases: A narrative review. World Journal of Gastroenterology. 2018;**24**(34):3849-3860

[20] Jeong JY, Kim TY, Sohn JH, et al. Real time shear wave elastography in chronic liver diseases: Accuracy for predicting liver fibrosis, in comparison with serum markers. World Journal of Gastroenterology. 2014;**20**:13920-13929

[21] Deffieux T, Gennisson JL, Bousquet L, et al. Investigating liver stiffness and viscosity for fibrosis, steatosis and activity staging using shear wave elastography. Journal of Hepatology. 2015;**62**:317-324

[22] Sporea I, Bota S, Grădinaru-Taşcău O, et al. Which are the cut-off values of 2D-shear wave Elastography (2D-SWE) liver stiffness measurements predicting different stages of liver fibrosis, considering transient Elastography (TE) as the reference method? European Journal of Radiology. 2014;**83**:e118-e122

[23] Sporea I, Mare R, Lupusoru R, et al. Comparative study between four ultrasound shear waves Elastographic methods for liver fibrosis assessment. Medical Ultrasonography. 2018;**20**(3):265-271

[24] Bavu E, Gennisson JL, Couade M, et al. Noninvasive in vivo liver fibrosis evaluation using supersonic shear imaging: A clinical study on 113 hepatitis C virus patients. Ultrasound in Medicine & Biology. 2011;**37**:1361-1373

[25] Tada T, Kumada T, Toyoda H, et al. Utility of real-time shear wave elastography for assessing liver fibrosis in patients with chronic hepatitis C infection without cirrhosis: Comparison of liver fibrosis indices. Hepatology Research. 2015;**45**:E122-E129

[26] Zeng J, Liu GJ, Huang ZP, et al. Diagnostic accuracy of two-dimensional shear wave elastography for the non-invasive staging of hepatic fibrosis in chronic hepatitis B: A cohort study with internal validation. European Radiology. 2014;**24**:2572-2581

[27] Wu T, Wang P, Zhang T, et al. Comparison of two-dimensional shear wave Elastography and real-time tissue Elastography for assessing liver fibrosis in chronic hepatitis B. Digestive Diseases. 2016;**34**:640-649

[28] Zhuang Y, Ding H, Zhang Y, et al. Two-dimensional shear-wave Elastography performance in the noninvasive evaluation of liver fibrosis in patients with chronic hepatitis B: Comparison with serum fibrosis indexes. Radiology. 2017;**283**:873-882

[29] Zeng J, Zheng J, Huang Z, et al. Comparison of 2-D shear wave Elastography and transient Elastography

for assessing liver fibrosis in chronic hepatitis B. Ultrasound in Medicine & Biology. 2017;**43**:1563-1570

[30] Cassinotto C, Boursier J, de Lédinghen V, et al. Liver stiffness in nonalcoholic fatty liver disease: A comparison of supersonic shear imaging, FibroScan, and ARFI with liver biopsy. Hepatology. 2016;**63**:1817-1827

[31] Takeuchi H, Sugimoto K, Oshiro H, et al. Liver fibrosis: Noninvasive assessment using supersonic shear imaging and FIB4 index in patients with non-alcoholic fatty liver disease. Journal of Medical Ultrasonics. 2018;**45**:243-249

[32] Thiele M, Detlefsen S, Sevelsted Møller L, et al. Transient and 2-dimensional shear-wave Elastography provide comparable assessment of alcoholic liver fibrosis and cirrhosis. Gastroenterology. 2016;**150**:123-133

[33] Zeng J, Huang ZP, Zheng J, et al. Non-invasive assessment of liver fibrosis using two-dimensional shear wave elastography in patients with autoimmune liver diseases. World Journal of Gastroenterology. 2017;**23**:4839-4846

[34] Li C, Dhyani M, Bhan AK, et al. Diagnostic performance of shear wave Elastography in patients with autoimmune liver disease. Journal of Ultrasound in Medicine. 2019 Jan;**38**(1):103-111

[35] Cassinotto C, Lapuyade B, Mouries A, et al. Noninvasive assessment of liver fibrosis with impulse elastography: Comparison of supersonic shear imaging with ARFI and Fibroscan. Journal of Hepatology. 2014;**61**(3):550-557

[36] Herrmann E, de Lédinghen V, Cassinotto C, et al. Assessment of biopsy-proven liver fibrosis by two-dimensional shear wave elastography: An individual patient data-based meta-analysis. Hepatology. 2018;**67**:260-272

[37] Li C, Zhang C, Li J, et al. Diagnostic accuracy of real-time shear wave Elastography for staging of liver fibrosis: A meta-analysis. Medical Science Monitor. 2016;**22**:1349-1359

[38] Jiang T, Tian G, Zhao Q, et al. Diagnostic accuracy of 2D-shear wave Elastography for liver fibrosis severity: A meta-analysis. PLoS One. 2016;**11**(6):e0157219

[39] Feng JC, Li J, Wu XW, et al. Diagnostic accuracy of SuperSonic shear imaging for staging of liver fibrosis: A meta-analysis. Journal of Ultrasound in Medicine. 2016;**35**(2):329-339

[40] Kim TY, Jeong WK, Sohn JH, et al. Evaluation of portal hypertension by real-time shear wave elastography in cirrhotic patients. Liver International. 2015;**35**:2416-2424

[41] Elkrief L, Rautou PE, Ronot M, et al. Prospective comparison of spleen and liver stiffness by using shear-wave and transient Elastography for detection of portal hypertension in cirrhosis. Radiology. 2015;**275**(2):589-598

[42] Cassinotto C, Charrie A, Mouries A, et al. Liver and spleen elastography using supersonic shear imaging for the non-invasive diagnosis of cirrhosis severity and oesophageal varices. Digestive and Liver Disease. 2015;**47**(8):695-701

[43] Jeong JY, Sohn JH, Sohn W, Park CH, Kim TY, Jun DW, et al. Role of shear wave Elastography in evaluating the risk of hepatocellular carcinoma in patients with chronic hepatitis B. Gut and Liver. 2017;**11**:852-859

[44] Dietrich CF, Sirli R, Ferraioli G, et al. Current knowledge in ultrasound-based liver Elastography of Pediatric patients. Applied Sciences. 2018;**8**(6):944

[45] Belei O, Sporea I, Gradinaru-Tascau O, et al. Comparison of three ultrasound based elastographic techniques in children and adolescents with chronic diffuse liver diseases. Medical Ultrasonography. 2016;**18**(2):145-150

[46] Moga TV, Stepan AM, Pienar C, et al. Intra- and inter-observer reproducibility of a 2-D shear wave Elastography technique and the impact of ultrasound experience in achieving reliable data. Ultrasound in Medicine & Biology. 2018;**44**(8):1627-1637

[47] Mjelle AB, Mulabecirovic A, Havre RF, et al. Normal liver stiffness values in children: A comparison of three different Elastography methods. Journal of Pediatric Gastroenterology and Nutrition. 2019;**68**(5):706-712

[48] Bende F, Mulabecirovic A, Sporea I, et al. Assessing liver stiffness by 2-D shear wave Elastography in a healthy cohort. Ultrasound in Medicine & Biology. 2018;**44**(2):332-341

[49] Bende F, Sporea I, Șirli R, et al. Performance of 2D-SWE.GE for predicting different stages of liver fibrosis, using transient Elastography as the reference method. Medical Ultrasound. 2017;**19**(2):143-149

[50] Serra C, Grasso V, Conti F, et al. A new two-dimensional shear wave Elastography for noninvasive assessment of liver fibrosis in healthy subjects and in patients with chronic liver disease. Ultraschall in der Medizin. 2018;**39**:432-439

[51] Lee ES, Lee JB, Park HR, et al. Shear wave liver Elastography with a propagation map: Diagnostic performance and inter-observer correlation for hepatic fibrosis in chronic hepatitis. Ultrasound in Medicine & Biology. 2017;**43**(7):1355-1363

Chapter 4

# Quantification of Liver Steatosis

*Ioan Sporea, Roxana Șirli and Alina Popescu*

## Abstract

The prevalence of non-alcoholic fatty liver disease (NAFLD) and non-alcoholic steatohepatitis (NASH) is increasing in the modern world. Fatty infiltration of the liver can be assessed by standard ultrasound, by controlled attenuation parameter (CAP) using the FibroScan device or, more recently, by ultrasound systems that evaluate the attenuation in the liver. Standard ultrasound (US) for steatosis evaluation was used for a long time as a semi-quantitative method for steatosis assessment in the liver. A "bright liver" with "posterior attenuation" is the typical US sign of liver steatosis. Considering the attenuation severity, steatosis is subjectively graded as mild, moderate or severe. Using the kidney/liver ratio, a more accurate evaluation can be made. Controlled attenuation parameter (CAP) was developed by EchoSens, France, and implemented into the FibroScan device. CAP manages an objective assessment of steatosis severity with rather good accuracy. More recently, ultrasound companies such as Hitachi, General Electric and Canon, implemented in their system algorithms which allow an objective assessment of liver steatosis, using the attenuation of the ultrasound beams.

**Keywords:** non-alcoholic fatty liver disease, non-alcoholic steatohepatitis, liver steatosis, standard ultrasound, controlled attenuation parameter

## 1. Introduction

In the last years, the field of hepatology changed regarding the etiology of predominant liver diseases. New treatments with direct acting agents (DAA) for HCV chronic infection, or modern analogues for HBV infection, decreased the importance of the very precise evaluation of liver fibrosis severity in these two diseases. Furthermore, the increasing number of patients with obesity, type 2 diabetes or hypertriglyceridemia in the developed world, increased the prevalence of non-alcoholic fatty liver disease (NAFLD) and non-alcoholic steatohepatitis (NASH), changing the focus of hepatologists on these diseases.

Speaking about the risk factors for NAFLD, overweight and obesity play a central role. Worldwide estimations show that approximately 1.9 billion people are overweight and approximately 650 million are obese [1]. In such patients, fatty infiltration of the liver is quite common, going from simple steatosis to NASH. On the other hand, in adult population (and especially in aging population), the prevalence of type 2 diabetes mellitus can be as high as 1/11 individuals [2]. Thus, in this huge cohort of patients, it became essential to make a confident and non-invasive evaluation of liver disease severity. This assessment must reveal the severity of steatosis, the severity of fibrosis and inflammation.

In this chapter, we will cover only the quantification of liver steatosis using ultrasound methods. They are quite simple, inexpensive, and can be performed as point of care methods, by clinicians or by radiologists.

Fatty infiltration of the liver can be assessed by standard ultrasound, by controlled attenuation parameter (CAP) using the FibroScan device (EchoSens, Paris), or, more recently, by ultrasound systems that evaluate the attenuation in the liver.

## 2. Standard ultrasound (US) for steatosis evaluation

Standard ultrasound (US) for steatosis evaluation was used for a long time as a semi-quantitative method for steatosis assessment in the liver. A "bright liver" with "posterior attenuation" is the typical US sign of liver steatosis (**Figure 1**). Considering the attenuation severity, steatosis is subjectively graded as mild, moderate or severe. Using the kidney/liver ratio, a more accurate evaluation can be made (knowing that in normal conditions, the liver and right kidney have similar ultrasound appearance) (**Figure 2**).

Some studies were published regarding the value of transabdominal ultrasound for the quantification of steatosis, considering liver biopsy as the "gold standard". In a study performed by Palmentieri et al. [3] the ultrasound "bright liver" echo pattern was compared to liver biopsy in a cohort of 235 patients. "Bright liver" was found in 67% of patients with steatosis of any degree and in 89% of patients with histologic steatosis ≥30%. The sensitivity (Se), specificity (Sp), positive predictive value (PPV) and negative predictive value (NPV) of "bright liver" echo pattern and "posterior attenuation" for the presence of any steatosis were 64, 97, 96 and 65%,

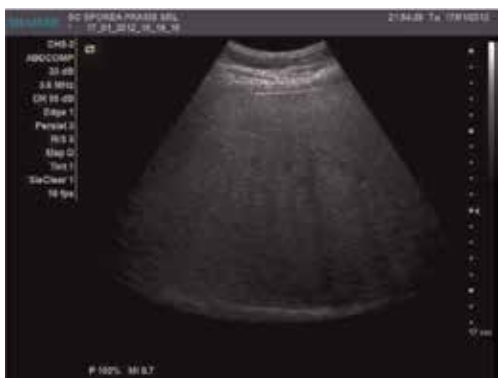

**Figure 1.**
*Moderate steatosis-posterior attenuation.*

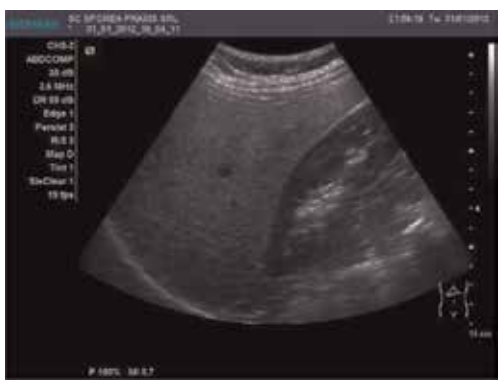

**Figure 2.**
*Increased hepato-renal index.*

respectively. However, when only severe steatosis was taken into consideration (a subgroup of patients who had steatosis of ≥30%) the Se, Sp, PPV and NPV were 91, 93, 89 and 94%, respectively.

In another study performed by Mathiesen et al. [4] liver ultrasound was compared with hepatic histology for steatosis assessment in a series of 165 patients. The steatosis was graded as none, mild, moderate or severe. In patients with increased echogenicity, 86.7% had liver steatosis at least moderate. This study revealed that for the detection of steatosis, standard US had 90% Se, 82% Sp, 87% PPV and 87% NPV.

Some studies tried to use Computer Assisted Diagnosis (CAD) to increase the accuracy of US for the detection and evaluation of steatosis severity [5]. In a study performed in 120 subjects, CAD was able to make a correct classification of steatosis severity with 82.2% accuracy [6].

Similar results were obtained by the group of Xia [7] in a study on 127 subjects. In this study, CAD was used to compare liver attenuation and liver/kidney index by US to magnetic resonance spectroscopy considered as the "gold standard". A very good correlation of US findings with MRI steatosis quantification ($r = 0.884$) was observed.

Ultrasound hepatic/renal ratio in connection with hepatic attenuation can increase the accuracy of liver fat quantification [8]. In a study performed by Zhang, in a cohort of 170 subjects, where ultrasound was compared with magnetic resonance spectroscopy, an equation of quantitative model for fatty liver prediction was assessed, using ultrasound hepatic/renal ratio and hepatic echo-intensity attenuation rate. In this quantitative ultrasound model, sensitivity and specificity for fatty liver were 94.7 and 100%.

In review paper by Castera et al. [9] it was concluded that liver US has 60–94% sensitivity and 84–95% specificity for detecting hepatic steatosis and that the sensitivity increases with the severity of fatty infiltration.

Probably the most relevant study concerning the performance of US in diagnosing liver steatosis is a large meta-analysis that included 49 studies and 4720 subjects [10]. In this study, the sensitivity of US for moderate and severe steatosis was 84.8%, with 93.6% specificity as compared to liver biopsy, with the area under the summary receiving operating characteristics curve of 0.93. Considering this study as reference, we can say that standard transabdominal US can be used in clinical practice to perform a semi-quantitative evaluation of steatosis, with quite good accuracy. However, if we intend to follow-up these kind of patients, maybe a more objective method is needed, with results expressed as numeric values. On the other hand, the operator's experience in ultrasound is important for steatosis quantification, and, maybe, the quality of the ultrasound machine should be taken into consideration.

## 3. Controlled attenuation parameter (CAP)

Controlled attenuation parameter (CAP) was developed by EchoSens, France, and implemented into the FibroScan device. Initially the CAP algorithm was available only on the M probe (for non-obese patients), but more recently it is also available on the XL probe (for obese) (**Figure 3**).

Many studies were published showing the value of CAP for liver steatosis assessment, most of them using liver biopsy as the reference method. CAP measures the total ultrasound attenuation, using vibration controlled Transient Elastography (TE). The measurement results are expressed in dB/m, with values ranging between 100 and 400 dB/m. The first evaluation of CAP was performed in a cohort of 115 patients with liver histology [11]. CAP was very well correlated with steatosis (Spearman $\rho = 0.81$, $p < 0.00001$) and the AUROCs for the detection of >10


**Figure 3.**
*FibroScan with CAP, with M and XL probes. Steatosis values are displayed in light blue and liver stiffness values in yellow.*

and >33% steatosis were 91 and 95% respectively. CAP was evaluated also with the XL probe by the same author in a cohort of 59 patients [12]. In this study, the AUROCs for the detection of >2 and >16% liver fat were 83/84% and 92/91% for the M/XL probes, respectively.

Another study performed on 440 patients who had liver biopsy as reference method showed that the AUROCs of CAP for the diagnosis of steatosis >10, >33 and >66% were 79, 84, and 84%, respectively [13]. On multivariate analysis, factors significantly associated with elevated CAP were BMI 25–30 kg/m$^2$, BMI > 30 kg/m$^2$, metabolic syndrome, alcohol intake more than 14 drinks/week and liver stiffness >6 kPa.

In a study on 201 patients who also had undergone liver biopsy, histologic steatosis was the only factor that independently influenced CAP values [14]. For moderate and severe steatosis, CAP cut-off values of 285 and 294 dB/m had 82.0 and 81.5% accuracy, respectively. However, for mild steatosis, the accuracy was only 76.1% at a cut-off 260 dB/m. These last two studies showed maybe a more realistic value of CAP for liver steatosis assessment, the accuracy being around 80–85% (less for mild steatosis).

In another study in a cohort of 101 NAFLD patients with liver biopsy, CAP was associated in a multivariate analysis with steatosis grade (odds ratio [OR] = 29.16, $p < 0.001$), serum triglycerides (OR = 13.59, $p = 0.037$) and body mass index (BMI; OR = 4.34, $p < 0.001$) [15]. In this study, the optimal CAP cut-offs for estimation of steatosis grades S1 (5–33% of hepatocytes), S2 (>33–66% of hepatocytes), and S3 (>66% of the hepatocytes) were 263 dB/m, 281 dB/m, and 283 dB/m, respectively, and the AUROC's for S1, S2, and S3 were 0.97, 0.86, and 0.75, respectively.

In a very recent multicenter study [16], where FibroScan was compared to liver biopsy in patients with NAFLD, from 450 consecutive patients, 404 patients had valid measurements using M and XL probes. AUROC of CAP for steatosis evaluation was 0.87 for S ≥ S1, 0.77 for S ≥ S2, and 0.70 for S3. In the same study, the cut-off values for S ≥ S1, S ≥ S2, and S = S3 were 302 dB/m, 331 dB/m, and 337 dB/m,

respectively. Two important information came from this study: the AUROCs of CAP are decreasing with the severity of steatosis, and the cut-off values of CAP are higher than in other published studies, for all degrees of steatosis.

In different studies, different cut-off values were proposed for different degrees of steatosis, the first being proposed by the manufacturer: 230 dB/m for mild steatosis, 275 dB/m for moderate steatosis and 300 dB/m for severe steatosis. Other studies obtained different values, but they were correlated with the cohort of patients, with the severity of steatosis, the presence of diabetes and others.

The first meta-analysis evaluating the accuracy of CAP for steatosis quantification showed that the optimal CAP cut-off values for mild, moderate and severe steatosis were 232.5, 255 and 290 dB/m respectively [17]. In this study, the summarized sensitivity and specificity values were 78 and 79% for mild, 85 and 79% for moderate, and 83 and 79% for severe steatosis. However, this meta-analysis calculated a rather low specificity for CAP, being approx. 80%.

Another meta-analysis, comparing CAP with liver biopsy, was performed by Karlas in a cohort of 2735 patients: 37% with chronic hepatitis B, 36% with chronic hepatitis C, 20% with NAFLD/NASH, 7% with other chronic hepatitis. Histologic steatosis distribution was as follows: 51/27/16/6% for S0/S1/S2/S3. In this meta-analysis, the calculated optimal cut-offs were 248 dB/m for S0 vs. S1–S3, 268 dB/m for S0–S1 vs. S2–S3 and 280 dB/m for S0–S2 vs. S3, with AUROCs of 0.82, 0.86 and 0.88 respectively [18].

Other studies compared CAP to MRI quantification of steatosis. Proton density fat fraction (PDFF) by MRI was lately proposed as a sensitive modality of liver fat evaluation. In a cohort of 104 consecutive patients, all with liver biopsy, MRI-PDFF was compared with CAP for diagnosis of steatosis (grades 1–3 vs. 0) [19]. In this study, MRI-PDFF detected any steatosis with an AUROC of 0.99, significantly higher than that of CAP (AUROC 0.85). In the same time, MRI-PDFF identified S2 or S3 with AUROC values of 0.90 and 0.92, while CAP identified S2 or S3 with AUROC values of 0.70 and 0.73.

In another comparative study between CAP and PDFF, performed in Japan in a cohort of 142 patients with NAFLD and liver biopsy, CAP measurements identified patients with $S \geq 2$ with an AUROC of 0.73 and PDFF methods identified them with an AUROC of 0.90 [20].

A comparative study between CAP and PDFF was performed in 119 adults with liver biopsy, evaluating the performance to diagnose 5 and 10% fatty infiltration in PDFF [21]. In this study, using CAP with M or XL probes, AUROC of CAP for the detection of MRI-PDFF $\geq 5\%$ was 0.80 (at the cut-point of 288 dB/m) and of MRI-PDFF $\geq 10\%$ was 0.87 (at the cut-point of 306 dB/m). When the authors considered the IQR (interquartile range) as a qualitative parameter, it was shown that CAP measurements with an IQR (inter quartile range) below 30 dB/m had a more robust AUROC as compared to those with an IQR higher than this (0.92 versus 0.70, $p = 0.0117$).

In the study performed by Wong et al. [22] in a prospective multicenter study, including 754 patients, they found that the IQR of CAP was associated with the accuracy of this method and that the AUROC of CAP was 0.90 in patients with IQR $<40$ (and 0.77 if $\geq 40$ dB/m, respectively, $p = 0.004$). Finally they proposed like a qualitative criteria for CAP to use IQR $< 40$ dB/m.

These comparative studies clearly showed a better performance of MRI-PDFF vs. CAP to diagnose steatosis, but we must have in mind that CAP can be a point of care method and that the price of such investigation is much lower than the price of MRI-PDFF. Most published papers concerning the accuracy of CAP for fat quantification calculated accuracies ranging from 0.75 to 0.85, increasing with the severity of steatosis.

## 4. Ultrasound systems evaluating the attenuation

For a long time the posterior attenuation of ultrasound beams in standard liver evaluation was used as a subjective parameter for steatosis assessment. More recently, ultrasound companies such as Hitachi, General Electric and Canon, implemented in their system algorithms which allows an objective assessment of liver steatosis, using the attenuation of the ultrasound beams.

### 4.1 Attenuation coefficient (ATT)

*Attenuation coefficient (ATT) from Hitachi* was evaluated in a prospective multicenter cohort of 351 patients [23], where liver biopsy and ATT measurement were performed in the same day. In this study, the median values of ATT for steatosis grades S0, S1, S2, and S3 were 0.55, 0.63, 0.69 and 0.85 dB/cm/MHz, respectively, increasing with the severity of steatosis ($p < 0.001$). In the same time, the AUROCs for $S \geq 1$, $S \geq 2$, and $S \geq 3$ were 0.79, 0.87, and 0.96, respectively.

The Combi-Elasto algorithm from Hitachi quantifies steatosis (ATT), but in the same time the shear-waves speed is used for estimation of the stiffness or elasticity (E) of the liver expressed in kPa and also to produce some indexes, such as Liver Fibrosis Index (LFI) and Activity Index (AI) (**Figures 4–5**).

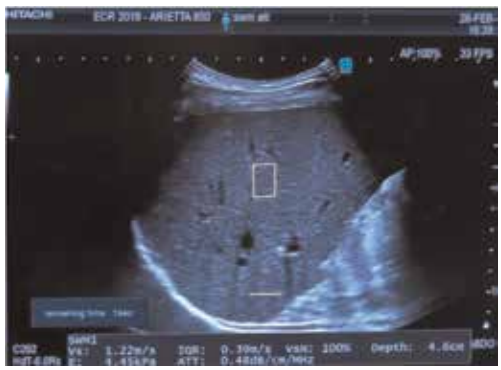

**Figure 4.**
*Attenuation coefficient (ATT).*

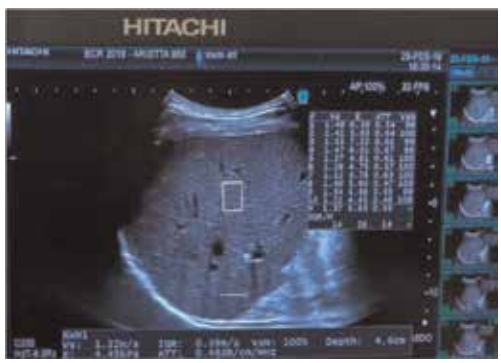


**Figure 5.**
*ATT coefficient with ten measurement values.*

### 4.2 Ultrasound-guided attenuation parameter (UGAP)

*Ultrasound-guided attenuation parameter (UGAP) from General Electric* was recently proposed for steatosis quantification. In a paper published by a Japanese group, UGAP was compared with liver biopsy and CAP in a cohort of 163 patients [24]. In this study, the median value of UGAP in patients with S0, S1, S2 and S3 grade steatosis were 0.485, 0.560, 0.660 and 0.720 respectively (increasing with the severity of steatosis), and in the same time, the AUROCs of UGAP for identifying >S1, >S2 and S3 were 0.900, 0.953 and 0.959, respectively, significantly better than the results obtained with CAP.

### 4.3 Attenuation image (ATI)

*Attenuation image (ATI) from Canon* was introduced for liver steatosis quantification. This method permit a simple quantification of liver steatosis, by using a region of interest applied on the standard ultrasound image, where the attenuation is evaluated. Values of this parameter are expressed in dB/cm/MHz and it also has a parameter of the quality of acquisition, that must be higher than $R^2 > 0.90$ (**Figure 6a**).

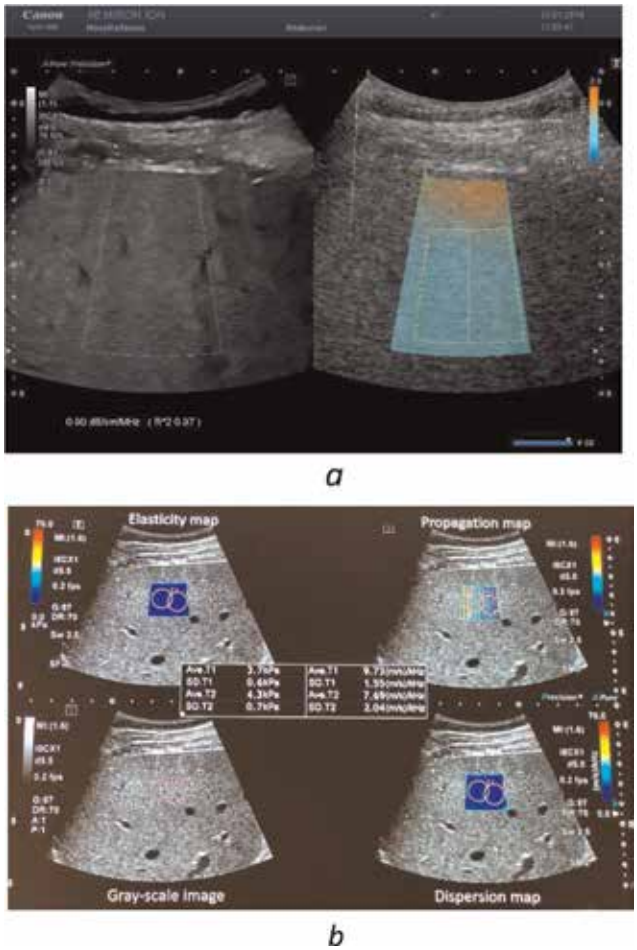


**Figure 6.**
*(a) Attenuation image from Canon and (b) evaluation of dispersion with Canon system.*

In a preliminary study in which ATI was compared with CAP (FibroScan, EchoSens), in a cohort of 113 consecutive subjects [25], a strong positive correlation was found between the attenuation coefficients of steatosis obtained by the 2 methods, r = 0.81, p < 0.001. Using CAP as reference, the AUROCs of ATI for ≥S1, ≥S2 and ≥S3 were excellent (0.89, 0.88, respectively 0.95, p < 0.001) and the proposed cut-off values for were: S1 = 0.64 dB/cm/mHz, S2 = 0.79 dB/cm/mHz and S3 = 0.86 dB/cm/mHz.

The Canon system can also evaluate dispersion, considering the viscoelastic properties of liver tissue (**Figure 6b**).

### 4.4 Attenuation parameter

*Attenuation parameter from Aixplorer* evaluates attenuation of ultrasound, concomitantly with the display of speed of sound (SoS), used for fatty infiltration estimation. Similar to other modern ultrasound machines, the new system is able to quantify the tissue viscosity, expressed in Pa s (**Figure 7a** and **b**).

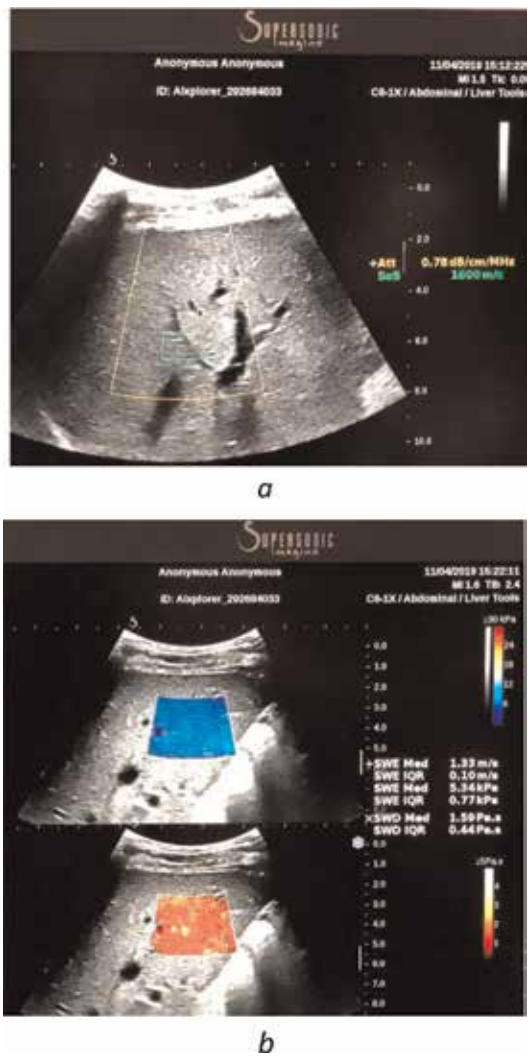


**Figure 7**
*(a) Attenuation quantification and (b) viscosity imaging.*

Many of the new ultrasound systems are able to estimate with the same machine steatosis severity, liver stiffness and, more recently, inflammation. This is the next step toward a multiparametric approach of liver diseases, using ultrasound machines.

In conclusion, quantification of liver steatosis using ultrasound is a good method for daily practice. The low cost, easy feasibility and accessibility make these methods useful for the large number of potential patients with fatty liver.

## Author details

Ioan Sporea, Roxana Șirli* and Alina Popescu
Department of Gastroenterology and Hepatology, "Victor Babeș" University of Medicine and Pharmacy, Timișoara, Romania

*Address all correspondence to: roxanasirli@gmail.com

IntechOpen

## References

[1] Loomba R, Sanyal AJ. The global NAFLD epidemic. Nature Reviews. Gastroenterology & Hepatology. 2013; **10**:686-690

[2] International Diabetes Federation. Diabetes: Facts and Figures. 2019. Available online: http://www.idf.org/ [Accessed: 30 June 2019]

[3] Palmentieri B, de Sio I, La Mura V, et al. The role of bright liver echo pattern on ultrasound B-mode examination in the diagnosis of liver steatosis. Digestive and Liver Disease. 2006;**38**:485-489

[4] Mathiesen UL, Franzen LE, Aselius H, et al. Increased liver echogenicity at ultrasound examination reflects degree of steatosis but not of fibrosis in asymptomatic patients with mild/ moderate abnormalities of liver transaminases. Digestive and Liver Disease. 2002;**34**:516-522

[5] Gaitini D, Baruch Y, Ghersin E, et al. Feasibility study of ultrasonic fatty liver biopsy: Texture vs. attenuation and backscatter. Ultrasound in Medicine & Biology. 2004;**30**:1321-1327

[6] Mihăilescu DM, Gui V, Toma CI, et al. Computer aided diagnosis method for steatosis rating in ultrasound images using random forests. Medical Ultrasonography. 2013;**15**:184-190

[7] Xia MF, Yan HM, He WY, et al. Standardized ultrasound hepatic/renal ratio and hepatic attenuation rate to quantify liver fat content: An improvement method. Obesity. 2012;**20**: 444-452

[8] Zhang B, Ding F, Chen T, et al. Ultrasound hepatic/renal ratio and hepatic attenuation rate for quantifying liver fat content. World Journal of Gastroenterology. 2014;**20**:17985-17992

[9] Castera L, Vilgrain V, Angulo P. Noninvasive evaluation of NAFLD. Nature Reviews. Gastroenterology & Hepatology. 2013;**10**:666-675

[10] Hernaez R, Lazo M, Bonekamp S, et al. Diagnostic accuracy and reliability of ultrasonography for the detection of fatty liver: A meta-analysis. Hepatology. 2011;**54**:1082-1090

[11] Sasso M, Beaugrand M, de Ledinghen V, et al. Controlled attenuation parameter (CAP): A novel VCTE™ guided ultrasonic attenuation measurement for the evaluation of hepatic steatosis: Preliminary study and validation in a cohort of patients with chronic liver disease from various causes. Ultrasound in Medicine & Biology. 2010;**36**:1825-1835

[12] Sasso M, Audière S, Kemgang A, et al. Liver steatosis assessed by controlled attenuation parameter (CAP) measured with the XL probe of the FibroScan: A pilot study assessing diagnostic accuracy. Ultrasound in Medicine & Biology. 2016;**42**:92-103

[13] de Lédinghen V, Vergniol J, Capdepont M, et al. Controlled attenuation parameter (CAP) for the diagnosis of steatosis: A prospective study of 5323 examinations. Journal of Hepatology. 2014;**60**:1026-1031

[14] Lupșor-Platon M, Feier D, Stefănescu H, et al. Diagnostic accuracy of controlled attenuation parameter measured by transient elastography for the non-invasive assessment of liver steatosis: A prospective study. Journal of Gastrointestinal and Liver Diseases. 2015;**24**:35-42

[15] Chan WK, Nik Mustapha NR, Mahadeva S. Controlled attenuation parameter for the detection and quantification of hepatic steatosis in

nonalcoholic fatty liver disease. Journal of Gastroenterology and Hepatology. 2014;**29**:1470-1476

[16] Eddowes PJ, Sasso M, Allison M, et al. Accuracy of FibroScan controlled attenuation parameter and liver stiffness measurement in assessing steatosis and fibrosis in patients with nonalcoholic fatty liver disease. Gastroenterology. 2019;**156**:1717-1730

[17] Shi KQ, Tang JZ, Zhu XL, et al. Controlled attenuation parameter for the detection of steatosis severity in chronic liver disease: A meta-analysis of diagnostic accuracy. Journal of Gastroenterology and Hepatology. 2014; **29**:1149-1158

[18] Karlas T, Petroff D, Sasso M, et al. Individual patient data meta-analysis of controlled attenuation parameter (CAP) technology for assessing steatosis. Journal of Hepatology. 2017;**66**: 1022-1030

[19] Park CC, Nguyen P, Hernandez C. Magnetic resonance elastography vs transient elastography in detection of fibrosis and noninvasive measurement of steatosis in patients with biopsy-proven nonalcoholic fatty liver disease. Gastroenterology. 2017;**152**:598-607

[20] Imajo K, Kessoku T, Honda Y, et al. Magnetic resonance imaging more accurately classifies steatosis and fibrosis in patients with nonalcoholic fatty liver disease than transient elastography. Gastroenterology. 2016; **150**:626-637

[21] Caussy C, Alquiraish MH, Nguyen P, et al. Optimal threshold of controlled attenuation parameter with MRI-PDFF as the gold standard for the detection of hepatic steatosis. Hepatology. 2018;**67**: 1348-1359

[22] Wong VWS, Petta S, Hiriart JB, et al. Validity criteria for the diagnosis of fatty liver by M probe-based controlled attenuation parameter. Journal of Hepatology. 2017;**67**:577-584

[23] Tamaki N, Koizumi Y, Hirooka M, et al. Novel quantitative assessment system of liver steatosis using a newly developed attenuation measurement method. Hepatology Research. 2018;**48**: 821-828

[24] Fujiwara Y, Kuroda H, Abe T, et al. The B-mode image-guided US attenuation parameter accurately detect hepatic steatosis in chronic liver disease. Ultrasound in Medicine and Biology. 2018;**44**(11):2223-2232

[25] Sporea I, Bâldea V, Lupușoru R, et al. Value of Viscosity, Viscoelasticity and Attenuation Measurement Using Shear Wave Ultrasound Elastography. Oral Presentation. Granada, Spain: Euroson; 2019

Chapter 5

# Elastography in Chronic Liver Diseases

*Samuel N. Gitau and Issa K. Menge*

## Abstract

Elastography is useful for diagnosing and grading hepatic fibrosis in patients with chronic liver diseases (CLD). In addition, it may be used as a noninvasive tool for surveillance and prognostication of patients with complications related to CLD. Elastography uses real-time ultrasound to assess for tissue elasticity and is a fast, simple, reproducible, and reliable method for noninvasive liver fibrosis evaluation. Management of chronic liver disease is dependent on the grade of liver fibrosis to ascertain the urgency and choice of treatment and advice on further screening for cirrhosis and hepatocellular carcinoma. This chapter will highlight the role of elastography in the evaluation of chronic liver disease including hepatitis B and C and HIV-related liver disease and nonalcoholic fatty liver disease (NAFLD).

**Keywords:** diffuse liver disease, hepatitis B, hepatitis C, nonalcoholic fatty liver disease

## 1. Introduction

Chronic liver diseases are a major cause of morbidity and mortality worldwide with around 800,000 deaths per year attributable to liver cirrhosis [1]. There are a myriad of causes of chronic liver disease including viral infections, alcohol abuse, nonalcoholic fatty liver disease, biliary disease, autoimmune disease, genetic causes, and metabolic disorders [2]. Liver fibrosis results from chronic injury induced by a variety of causes with infection being the leading one. Most patients with chronic liver disease are often asymptomatic with symptoms only setting in when complications of the disease such as portal hypertension, cirrhosis, and hepatocellular carcinoma develop.

Management of chronic liver disease is dependent on the grade of liver fibrosis to ascertain the urgency and choice of treatment and advice on further screening for cirrhosis and hepatocellular carcinoma. Though liver biopsy has traditionally been the gold standard for diagnosis and staging of liver fibrosis, the procedure has paramount shortfalls as a medical screening test. It lacks the safety profile, accuracy, and accessibility of a standard medical screening test. It is an invasive technique with rates of morbidity of 3 in 100 and mortality of 3 in 10,000 reported [3]. In addition, sampling errors may arise because only 1/50,000 of the liver is sampled during the procedure. Inter- and intra-observer variability of between 10 and 20% in interpretation and staging of hepatic fibrosis have been reported which may lead to under-staging or over-staging of fibrosis [4]. A study by Maharaj et al. [5], where three percutaneous liver biopsies were performed in the same patients using the same entry points, found a concordance rate for cirrhosis in all three

biopsy specimens of only 50%. Taking into consideration all these shortfalls, the "gold standard" for the true liver disease status would be the histological analysis of nearly the entire liver which is not feasible. Effectively, liver biopsy is an "imperfect gold standard," and the definitive diagnosis of liver fibrosis in routine clinical practice is practically impossible [6].

Elastography uses real-time ultrasound to assess for tissue elasticity and is a fast, simple, reproducible, and reliable method for noninvasive liver fibrosis evaluation.

Elastography as a tool for evaluation of disease relates to one of the first physical exam skills every physician learns, i.e., palpation. This is based on the premise that diseased organs feel harder than the normal surrounding tissue. Using elastography, tissue stiffness (or hardness) can be measured and converted into an image. Young's modulus is used to quantify the elasticity or stiffness of a tissue and is calculated from the ratio between a uniform compression (stress, s) applied to the tissue and the resulting induced tissue deformation (strain, e) as shown in the equation below [7].

$$\text{Young"s modulus (elasticity)} = \text{Stress/Strain or } E = s/e \quad (1)$$

Using a reference amount of force applied to the tissue, its elasticity can be determined. Elasticity is measured in pressure units, pascal, or kilopascals (kPa).

The stiffness (elasticity) of normal, healthy liver is very low (of the order of 2 kPa, comparable to a soft gelatin gel) [8]. In response to inflammation, liver cells die and are replaced by scar tissue. As fibrosis progresses, the scar tissue becomes progressively rigid, and as a result the stiffness of the tissue increases. The stiffness of fibrotic liver is a reflection of the severity of the disease. Using elastography, an image of the shear stiffness of a tissue can be created [9]. It can therefore be used to monitor the extent of liver damage. Elastography is a painless and rapid procedure and does not require any preparation.

There are two main ways of performing elastography. The maiden method which has been widely used is transient elastography (TE) popularly known as FibroScan. The other relatively new methods are real-time elastography (RTE) using shear waves and acoustic radiation force impulse imaging (ARFI) [10–12].

Transient elastography uses both ultrasound (around 5 MHz) and low-frequency (50 Hz) mechanically generated shear waves to determine tissue elasticity. The propagation velocity of the shear waves is directly related to elasticity with the speed greater in stiff (fibrosed) tissue than in a softer tissue. The shear wave is generated by an external low-frequency vibrator which strikes the patient's skin and produces the shear wave whose propagation in the tissue of interest is measured and provided as an average elasticity [10]. In evaluation of liver elasticity, the measurements are acquired from the right lobe of the liver through the intercostal space. Ten liver stiffness measurements are obtained and the median considered as the representative value.

The limitations of this technique include the low volume of parenchyma explored, absence of real-time ultrasound guidance, measurement difficulties in cases of obesity and presence of ascites, and lack of specificity for the distinction of significant fibrosis level. The learning curve in correctly performing the examination without imaging guidance also serves to limit its reproducibility [10]. These drawbacks have led to the quest for a better elastographic method the birth of which is real-time elastography (RTE).

RTE does not require an external vibrator to generate the shear wave as is the case with transient elastography. The probe of the ultrasound machine produces a localized radiation force deep in the tissue of interest. This radiation force induces a shear wave, which then propagates through the tissue from a focal point. Several

focal points are then generated in a line perpendicular to the surface of the patient's skin (**Figure 1**).

The transmission of the shear wave is then detected by the rapid acquisition of ultrasound which takes only a few milliseconds, thus the patient or operator movement does not impact the result. The speed at which the shear wave propagates is then estimated from the measurement of the displacement induced by the shear wave and a real-time two-dimensional color map displayed. This color map is color-coded for the different shear wave speeds representing the degrees of stiffness from soft to hard. This color map is accompanied by an anatomic reference gray-scale (or B-mode) image; hence the area of sampling can be identified on the image (**Figure 2**).

Elastographic reference ranges have been developed for distinguishing mild fibrosis from significant fibrosis and cirrhosis following using histology (METAVIR score) as the reference standard [13–15] (see details in **Table 1**).

## 2. Elastography in hepatitis B and C

An estimated 240 and 160 million people in the world have chronic hepatitis B and C virus infections, respectively, according to the Centers for Disease Control and Prevention [16].

Elastography has been validated as a surrogate marker of liver fibrosis in a great number of studies, mainly in patients with chronic hepatitis B and C infections, and has enabled decision on when to start antiviral treatment without the need of performing liver biopsy [17].

The recommended velocity cutoffs for degree of liver fibrosis in patients with hepatitis C using the different elastography techniques are summarized in **Table 1** [18]. These cutoffs have been adapted for all cases of chronic liver disease.

In chronic hepatitis C, elastography has been shown to perform better for diagnosis of significant fibrosis (METAVIR score F ≥ 2) and cirrhosis (METAVIR score F4). The area under the ROC curve (AUROC) for the assessment of significant fibrosis ranged from 0.77 to 0.90 (F ≥ 2) and 0.90 to 0.97 for assessment of cirrhosis [17, 19–21]. Similar findings have been observed in patients with chronic viral

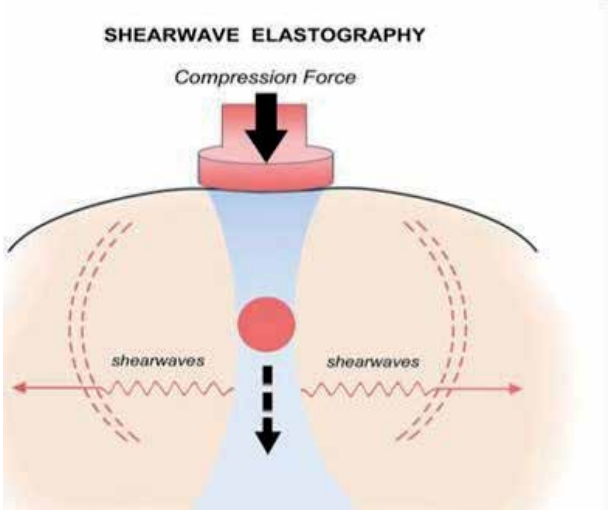


**Figure 1.**
*Image illustrating propagation of shear waves from a focal point.*

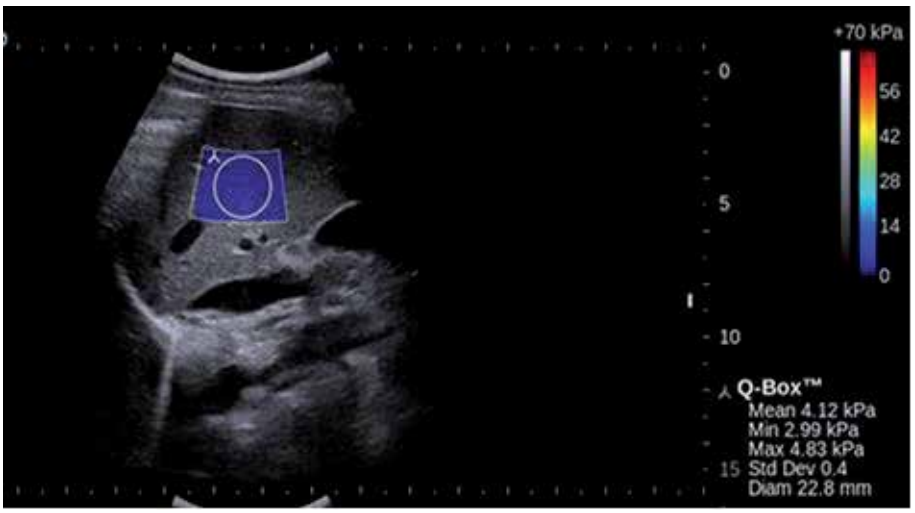


**Figure 2.**
*Gray-scale image showing acquisition of an elastography reading using RTE.*

| | | | Velocity Cutoff | | | | |
|---|---|---|---|---|---|---|---|
| Pathologic Findings | METAVIR Score | Proposed Risk-based Group | Transient Elastography (FibroScan) | Point SWE (Siemens) | Point SWE (Philips) | 2D SWE (Aixplorer) | Point SWE (GE)* |
| No fibrosis | F0 | Low risk (≤F2): unlikely to need follow-up | <7 kPa (<1.5 m/sec) | <5.6 kPa (<1.2 m/sec) | <5.7 kPa (<1.37 m/sec) | <7 kPa (<1.5 m/sec) | <8.29 kPa (<1.65 m/sec) |
| Fibrous portal expansion | F1 | | | | | | |
| Few bridges or septa | F2 | | | | | | |
| Numerous bridges or septa | F3 | High risk (F3 or F4): clinically significant fibrosis | >15 kPa (>2.2 m/sec) | >15 kPa (>2.2 m/sec) | >15 kPa (>2.2 m/sec) | >15 kPa (>2.2 m/sec) | >9.40 kPa (>1.77 m/sec) |
| Cirrhosis | F4 | | | | | | |

**Table 1.**
*Recommended velocity cutoffs for degree of liver fibrosis in patients with hepatitis C using the different elastography techniques. Source: [18].*

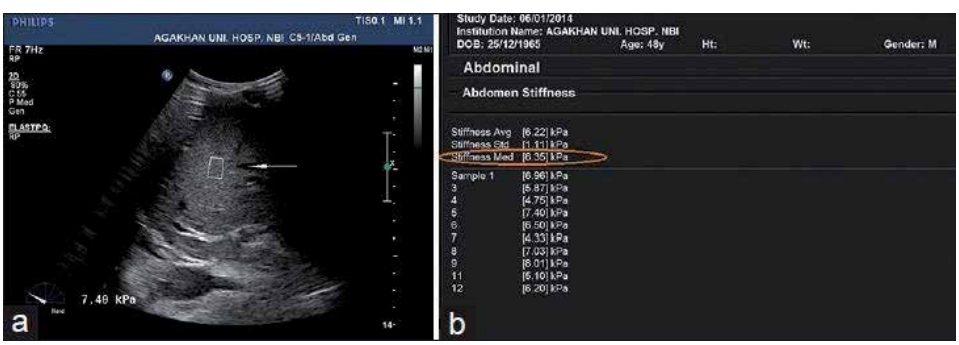


**Figure 3.**
*A 39-year-old male with the human immunodeficiency virus and hepatitis B virus coinfection. (a) Grayscale ultrasound image of the liver shows a shear wave elastography acquisition box (arrow) with a high elastography score of 7.4 kPa. (b) a table showing 10 liver stiffness measurements readings for the same patient with a high median elastography score of 6.35 kPa (encircled). Source: [25].*

hepatitis B where AUROC values ranged from 0.81 to 0.95 for significant fibrosis and from 0.80 to 0.98 for patients with cirrhosis [22, 23]. This shows that elastography forms an important screening tool for identifying patients with significant fibrosis that would warrant treatment.

There has been an increase in the proportion of liver-related deaths due to HCC in patients with HIV (from 15% in 2000 to 25% in 2005) with underlying HIV-HCV coinfection in the majority of the deaths [24]. In a study on liver fibrosis in patients with HIV-HBV coinfection using shear wave elastography, HBV coinfection was associated with 4.5 times increase in the prevalence of significant fibrosis which impacts progress of liver disease with its potential associated morbidity and mortality in patients with HIV [25]. Monitoring of degree of fibrosis in these patients is therefore very important, and elastography provides a noninvasive means of doing this (**Figure 3**).

The World Health Organization recommends the use of elastography (where available) for screening for liver fibrosis in patients with chronic hepatitis B infection [26].

## 3. Nonalcoholic fatty liver disease

Due to the increasing rates of sedentary lifestyle and obesity, nonalcoholic fatty liver disease (NAFLD) is now the most common cause of abnormal liver function tests (LFTs) in the Western world [27]. NAFLD is defined as the presence of more than 5% of steatotic hepatocytes in patients who do not consume excessive alcohol (less than 30 g/day for men and less than 20 g/day for women) [28, 29]. It is a spectrum of disease starting from simple steatosis progressing to nonalcoholic steatohepatitis (NASH), through advanced fibrosis and cirrhosis. Up to 80% of patients with central obesity and type 2 diabetes have evidence of NAFLD on imaging [28].

In most patients, NAFLD coexists with other liver pathologies including hepatitis C, hemochromatosis, and alcoholic liver disease. The presence of NAFLD on a background of these diseases causes more rapid disease progression. Treatment with steatogenic drugs including steroids, tamoxifen, and amiodarone can also cause fatty liver infiltration [30].

Most patients with NAFLD have simple steatosis, which has good clinical outcome and no overall increase in mortality. However, up to a third of these patients have NASH which is the progressive form of NAFLD. Up to 40% of patients with NASH develop progressive liver fibrosis with 20–30% culminating in cirrhosis. Patients with cirrhosis secondary to NASH are at an increased risk of developing hepatocellular carcinoma (2.6% per year) [31–36].

NAFLD can be diagnosed by the demonstration of hepatic steatosis on imaging or histology where other etiologies of liver disease or steatosis have been excluded. Although most clinicians rely on deranged liver function tests to identify patients with NAFLD, this can be inaccurate as majority of the patients will remain within normal-range ALT levels. Furthermore, even for those patients identified to have elevated ALT, the ALT typically falls (and AST may rise) as fibrosis progresses to cirrhosis. Importantly ALT values do not demonstrate positive correlation with histological findings. Therefore, isolated measurement of ALT is of little value in both the diagnosis of NAFLD and determination of its severity [37–39].

When fatty liver disease is suspected clinically, this should be confirmed with imaging. Ultrasound is usually the first-line investigation for patients suspected to have hepatic steatosis. It provides a qualitative assessment of fatty infiltration of the liver where gray-scale findings are used. The echogenicity of the liver parenchyma is compared to that of the kidney and other internal liver structures such the vascular

walls to diagnose and grade hepatosteatosis. Normal liver is hypoechoic relative to the renal cortex and becomes relatively hyperechoic with the presence of fatty infiltration. Ultrasound is effective in diagnosing steatosis if the percentage of involved hepatocytes is >33%; its diagnostic performance is however low with lesser degrees of fatty liver infiltration. Consequently, a normal liver ultrasound finding does not invariably rule out the presence of mild liver steatosis. Additionally, conventional ultrasound cannot assess the degree of fibrosis [40].

Liver elastography technique can measure steatosis simultaneously with the assessment of liver stiffness. It is paramount to stage the degree of fibrosis in patients with NAFLD as this will help identify patients with advanced fibrosis and resultant increased risk of liver-related complications such as liver failure and hepatocellular carcinoma [41].

It has been shown that there is a positive correlation between shear wave velocity and increasing hepatic fibrosis. In a study of 246 subjects with NAFLD, the AUROCs for the detection of $F \geq 2$ and $F \geq 3$ were 0.84 and 0.93, respectively. The sensitivity and specificity for advanced fibrosis ($F \geq 3$) were 91% and 75% with an elastography score cutoff of 7.9 kPa [42].

Inflammation is also known to increase shear wave velocity since the presence of edema results in reduced elasticity. It is therefore important to exclude active inflammation as this can confound the staging of liver fibrosis in the setting of NASH [43].

In summary, elastography plays a critical role in the evaluation of patients with NAFLD since early diagnosis of severe liver fibrosis allows for the institution of appropriate therapy as well as prognostication.

## Author details

Samuel N. Gitau* and Issa K. Menge
Department of Radiology, Aga Khan University Hospital, Nairobi, Kenya

*Address all correspondence to: samuelnguku12@gmail.com

## References

[1] WHO. Mortality database 2006. 2006 (updated 2006; cited 2009 Dec 1). Available from: http://www.who.int/healthinfo/morttables/en/index.html

[2] Sebastiani G, Castera L, Halfon P, et al. The impact of liver disease aetiology and the stages of hepatic fibrosis on the performance of non-invasive fibrosis biomarkers: An international study of 2411 cases. Alimentary Pharmacology & Therapeutics. 2011;**34**(10):1202-1216

[3] Montalto G, Soresi M, Carroccio A, Bascone F, Tripi S, Aragona F, et al. Percutaneous liver biopsy: A safe outpatient procedure? Digestion. 2001;**63**(1):55-60

[4] Cadranel JF, Rufat P, Degos F. Practices of liver biopsy in France: Results of a prospective nationwide survey. For the Group of Epidemiology of the French Association for the Study of the liver (AFEF). Hepatology. 2000;**32**(3):477-481

[5] Maharaj B, Maharaj RJ, Leary WP, Cooppan RM, Naran AD, Pirie D, et al. Sampling variability and its influence on the diagnostic yield of percutaneous needle biopsy of the liver. Lancet. 1986;**1**(8480):523-525

[6] Poynard T, Munteanu M, Imbert-Bismut F, Charlotte F, Thabut D, Le Calvez S, et al. Prospective analysis of discordant results between biochemical markers and biopsy in patients with chronic hepatitis C. Clinical Chemistry. 2004;**50**(8):1344-1355

[7] Garra BS. Imaging and estimation of tissue elasticity by ultrasound. Ultrasound Quarterly. 2007;**23**(4):255-268

[8] Catheline S, Gennisson JL, Delon G, Fink M, Sinkus R, Abouelkaram S, et al. Measuring of viscoelastic properties of homogeneous soft solid using transient elastography: An inverse problem approach. The Journal of the Acoustical Society of America. 2004;**116**(6):3734-3741

[9] Carstensen EL, Parker KJ, Lerner RM. Elastography in the management of liver disease. Ultrasound in Medicine & Biology. 2008;**34**(10):1535-1546

[10] Sandrin L, Fourquet B, Hasquenoph JM, Yon S, Fournier C, Mal F, et al. Transient elastography: A new noninvasive method for assessment of hepatic fibrosis. Ultrasound in Medicine & Biology. 2003;**29**(12):1705-1713

[11] Srinivasa Babu A, Wells ML, Teytelboym OM, et al. Elastography in chronic liver disease: Modalities, techniques, limitations, and future directions. Radiographics. 2016;**36**(7):1987-2006

[12] Frulio N, Trillaud H. Ultrasound elastography in liver. Diagnostic and Interventional Imaging. 2013;**94**(5):515-534

[13] Ferraioli G, Parekh P, Levitov AB, Filice C. Shear wave elastography for evaluation of liver fibrosis. Journal of Ultrasound in Medicine. 2014;**33**(2):197-203

[14] Leung VY, Shen J, Wong VW, Abrigo J, Wong GL, Chim AM, et al. Quantitative elastography of liver fibrosis and spleen stiffness in chronic hepatitis B carriers: Comparison of shear-wave elastography and transient elastography with liver biopsy correlation. Radiology. 2013;**269**(3):910-918

[15] Kettaneh A, Marcellin P, Douvin C, Poupon R, Ziol M, Beaugrand M, et al. Features associated with success

rate and performance of FibroScan measurements for the diagnosis of cirrhosis in HCV patients: A prospective study of 935 patients. Journal of Hepatology. 2007;**46**(4):628-634

[16] Centers for Disease Control and Prevention. Viral hepatitis. 2014. Centers for Disease Control and Prevention website: http://www.cdc.gov/hepatitis/index.htm

[17] Castera L, Forns X, Alberti A. Non-invasive evaluation of liver fibrosis using transient elastography. Journal of Hepatology. 2008;**48**(5):835-847

[18] General Electric. LOGIQ E9 shear wave elastography white paper (document ID: JB23292GB). GE website

[19] Ziol M, Handra-Luca A, Kettaneh A, Christidis C, Mal F, Kazemi F, et al. Noninvasive assessment of liver fibrosis by measurement of stiffness in patients with chronic hepatitis C. Hepatology. 2005;**41**:48-54

[20] Arena U, Vizzutti F, Abraldes JG, Corti G, Stasi C, Moscarella S, et al. Reliability of transient elastography for the diagnosis of advanced fibrosis in chronic hepatitis C. Gut. 2008;**57**:1288-1293

[21] Kim SU, Jang HW, Cheong JY, Kim JK, Lee MH, Kim DJ, et al. The usefulness of liver stiffness measurement using FibroScan in chronic hepatitis C in South Korea: A multicenter, prospective study. Journal of Gastroenterology and Hepatology. 2011;**26**:171-178

[22] Ogawa E, Furusyo N, Murata M, Ohnishi H, Toyoda K, Taniai H, et al. Longitudinal assessment of liver stiffness by transient elastography for chronic hepatitis B patients treated with nucleoside analog. Hepatology Research. 2011;**41**:1178-1188

[23] Marcellin P, Ziol M, Bedossa P, Douvin C, Poupon R, de Ledinghen V, et al. Non-invasive assessment of liver fibrosis by stiffness measurement in patients with chronic hepatitis B. Liver International. 2009;**29**:242-247

[24] Salmon-Ceron D, Lewden C, Morlat P, Bevilacqua S, Jougla E, Bonnet F, et al. Liver disease as a major cause of death among HIV infected patients: Role of hepatitis C and B viruses and alcohol. Journal of Hepatology. 2005;**42**(6):799-805

[25] Gitau SN, Vinayak S, Silaba M, Adam R, Shah R. High prevalence of liver fibrosis in patients with human immunodeficiency virus monoinfection and human immunodeficiency virus hepatitis-B Co-infection as assessed by shear wave elastography: Study at a teaching hospital in Kenya. Journal of Clinical Imaging Science. 2016;**6**:22. [Published: 07 June 2016]

[26] WHO Guidelines for the prevention, care and treatment of persons with chronic hepatitis b infection. March 2015

[27] Armstrong MJ. Presence and severity of non-alcoholic fatty liver disease in a large prospective primary care cohort. Journal of Hepatology. 2012;**56**:234-240

[28] Williams CD, Stengel J, Asike MI, et al. Prevalence of nonalcoholic fatty liver disease and nonalcoholic steatohepatitis among a largely middle-aged population utilizing ultrasound and liver biopsy: A prospective study. Gastroenterology. 2011;**140**:124-131

[29] Argo CK, Caldwell SH. Epidemiology and natural history of non-alcoholic steatohepatitis. Clinics in Liver Disease. 2009;**13**:511-531

[30] Powell EE, Jonsson JR, Clouston AD. Steatosis: Co-factor in other liver diseases. Hepatology. 2005;**42**(1):5-13

[31] Matteoni CA, Younossi ZM, Gramlich T, et al. Non alcoholic fatty liver disease: A spectrum of clinical and pathological severity. Gastroenterology. 1999;**116**:1413-1419

[32] Dam-Larsen S. Long term prognosis of fatty liver: Risk of chronic liver disease and death. Gut. 2004;**53**:750-755

[33] Ekstedt M, Franzen LE, Mathiesen UL, et al. Long-term follow-up of patients with NAFLD and elevated liver enzymes. Hepatology. 2006;**44**:865-873

[34] Wong VW, Wong GL, Choi PC, et al. Disease progression of non-alcoholic fatty liver disease: A prospective study with paired liver biopsies at 3 years. Gut. 2010;**59**:969-974

[35] Fassio E, Alvarez E, Dominguez N, et al. Natural history of non alcoholic steatohepatitis: A longitudinal study of repeat liver biopsies. Hepatology. 2004;**40**:820-826

[36] Ascha MS, Hanouneh IA, Lopez R, et al. The incidence and risk factors of hepatocellular carcinoma in patients with nonalcoholic steatohepatitis. Hepatology. 2010;**51**:1972-1978

[37] Chalasani N, Younossi Z, Lavine JE, et al. The diagnosis and management of non-alcoholic fatty liver disease: Practice guideline by the American Gastroenterological Association, American Association for the Study of Liver Diseases, and American College of Gastroenterology. Gastroenterology. 2012;**142**:1592-1609

[38] Mofrad P, Contos MJ, Haque M, et al. Clinical and histologic spectrum of nonalcoholic fatty liver disease associated with normal ALT values. Hepatology. 2003;**37**:1286-1292

[39] McPherson S, Stewart SF, Henderson E, et al. Simple non-invasive fibrosis scoring systems can reliably exclude advanced fibrosis in patients with non-alcoholic fatty liver disease. Gut. 2010;**59**:1265-1269

[40] Saadeh S, Younossi ZM, Remer EM, et al. The utility of radiological imaging in nonalcoholic fatty liver disease. Gastroenterology. 2002;**123**:745-750

[41] Sasso M, Tengher-Barna I, Ziol M, et al. Novel controlled attenuation parameter for noninvasive assessment of steatosis using Fibroscan((R)): Validation in chronic hepatitis C. Journal of Viral Hepatitis. 2012;**19**:244-253

[42] Dyson JK, McPherson S, Anstee QM. Republished: Non-alcoholic fatty liver disease: Non-invasive investigation and risk stratification. Postgraduate Medical Journal. 2014;**90**:254-266

[43] Deffieux T, Gennisson JL, Bousquet L, Corouge M, Cosconea S, Amroun D, et al. Investigating liver stiffness and viscosity for fibrosis, steatosis and activity staging using shear wave elastography. Journal of Hepatology. 2015;**62**:317-324

Chapter 6

# Elastometry Indices of Unchanged Liver in Healthy Children

*Mikhail Pykov, Natalia Kuzmina, Nikolay Rostovtsev and Alexander Kinzersky*

## Abstract

Two hundred healthy children aged 3–18 years were included in the study to determine liver stiffness indices by means of shear wave elastometry. The difference is significant when we compared shear wave velocity in children aged 3–6 years, on the one hand, and in children aged 7–18 years, on the other ($p = 0.001$). Liver stiffness indices in boys and girls were not different. As a result, liver stiffness indices in children in various age groups have been obtained, which can be recommended as normal ones for pediatric patients.

**Keywords:** ultrasound diagnostics, shear wave elastography, fibrosis, liver, children

## 1. Relevance

Chronic diffuse liver diseases are an urgent issue in present children gastroenterology. Interest to this group of liver diseases is due to their increasing incidence, frequent severe course, tendency to progression, and unfavorable outcomes. This problem requires great attention as chronic liver diseases are often polyetiological and their course is insufficiently symptomatic because of the great compensatory capacities of the organ. Clinical manifestations and patient presentation often take place when severe morphological changes have already occurred and adaptation and compensatory mechanisms have been wasted. [1]. Regardless of the etiology, cirrhosis is the cause of fatal outcome in patients due to the development of complications, i.e., hemorrhage from the esophageal varices, ascites, encephalopathy, hemorrhagic syndrome, and transformation to hepatocellular carcinoma [2]. In children chronic liver diseases develop as a result of influence of various etiologic factors such as viruses, autoantibodies, cholestasis, metabolic disorders, toxic agents, etc. on the liver parenchyma for a long time. Most often the process evolves due to bile duct disorders (75.6%), alpha-1 antitrypsin insufficiency (63.6%), autoimmune hepatitis (56.9%), chronic hepatitis D (57.4%), and Wilson-Konovalov disease (45.6%) [3].

Diagnostics of early fibrosis changes in the liver is prognostically important in the evaluation of the disease course. Presently, "the gold standard" of diagnostic method in diffuse liver disease is considered transcutaneous puncture biopsy with histologic investigation of tissue sampling, which enables to confirm, specify, and even alter the clinical diagnosis. However, the method is invasive and may cause a number of complications; moreover, in children their number is greater coming up to 4%. There are objective reasons limiting the use of biopsy method, i.e., a small

size of the tissue sampling. As liver fibrosis may have irregular distribution, different locations may show different stages of liver fibrosis and histologic activity [4, 5]. Thus, in pediatric medical practice, specialists are encouraged to search for noninvasive methods enabling not only to reveal liver changes but also to dynamically follow up the fibrosis process.

Ultrasound elastography is a great breakthrough in the evolution of noninvasive methods of visualization of liver conditions in general and ultrasound diagnostics in particular. There are only a few publications describing indices of liver stiffness in children obtained by one-dimensional and two-dimensional shear wave elastography (SWE). While studying stiffness indices in kPa (kilopascal) and m/s, the scientists pay attention to the data on liver stiffness obtained by different ultrasound and elastography techniques which cannot be compared. Normal indices for various age and gender groups are not clearly defined in the literature. Taking all these into account, the purpose of our study is to determine gender-age indices of liver "stiffness" in healthy children.

## 2. Material and methods

Two hundred healthy children aged 3–18 years were included in the study. Written informed consent was obtained from the legal representatives of all children. The study was approved by the ethics committee of FGBOU DPO, Moscow. All patients were allocated to three age groups according to age periodization of Mazurin and Vorantsov [6]. The first group consisted of 103 children, the second one consisted of 52, and the third one consisted of 45. According to this periodization, extrauterine period (besides the neonatal, infancy, and early childhood periods) includes preschool period (from 3 to 6 years), junior school period (from 7 to 11 years), and senior school period (from 12 to 18 years). There were 103 girls and 97 boys among them. The following criteria were considered allocating children to the control group: height and weight of each child within the interval from 5th to 95th percentile of age norm [7]; absence of liver diseases and (or) congestive heart failure in the anamnesis: absence of inflammatory alterations according to general and biochemical blood analysis (signs of cholestasis, cytolysis); absence of pathology of the liver, bile ducts, pancreas, and spleen according to ultrasound study in the grayscale and Doppler study (chromatic Doppler mapping, impulse-wave Doppler) modes; and a quiet behavior of a child during examination. The examination was performed on Aixplorer device (SuperSonic Imagine, France) by broadband convex sensor acting within frequency range of 1–6 MHz. The study was done when a patient was fasting after standard ultrasound examination of abdominal organs and retroperitoneal space. Finishing the grayscale mode and Doppler ultrasound, elastography shear wave (SWE ) mode was started. Tissue stiffness was demonstrated on the screen as a chromatic coded map (qualitative characteristics), and quantitative value of stiffness was evaluated in kilopascal (kPa).

After SWE mode activation, there appeared two images on the screen: the first one, displayed in the real-time mode a scanned area in the B-mode, and the second one, the same image with elastogram (**Figure 1**).

The mapping color depended on the chosen type of chromatic map. The chosen type of chromatic map colored stiffer tissues in red, while softer tissues in blue. The tissues of "mean" stiffness were colored in intermediate colors from light blue and green to yellow.

Elastometry was performed in elder children during breath-holding for not more than 10 s or during shallow breathing in. The patients were in a supine or pronation position. To visualize the liver, subcostal, intercostal, longitudinal, and

**Figure 1.**
*ESB mode study. Bellow a scanned area in the B-mode, above the same image with elastogram.*

transversal epigastric accesses were used. The sensor was placed perpendicularly to the body surface. Measurements were taken in different segments of the right and left hepatic lobes and in the areas free from the vascular structures, fixing the zone of scanning at the depth of 3–5 cm from the capsule. The area of interest (a light window) was chosen with subsequent expectation of image stabilization to get a homogeneous coloring of the light window. The measurement was considered successful when region of interest (ROI) was filled with color by more than 90%. Not <10 measurements were made, which enabled to calculate the mean value of liver stiffness.

## 3. Statistical analysis of data

Statistical analysis of data was performed by IBM SPSS Statistics 19. If the parameters were normal, Kolmogorov-Smirnov criterion with Liljefors significance adjustment was used. As the distribution of characteristic in one of the groups deviated from normal, Kruskal-Wallis criterion was used with subsequent pairwise comparison by means of nonparametric Mann-Whitney test. All quantitative values were presented as $M$ (mean value), $m$ (standard error of the mean value), $\sigma$ (standard deviation), median (50th percentile), and 25th–75th percentiles of both minimal and maximal values. Comparison of quantitative parameters was performed using Mann–Whitney test, and qualitative ones were compared by Fisher criterion of accuracy. Differences ($p < 0.05$) were considered significant.

## 4. Results

Elastography image of the unchanged liver in all patients in the comparison group was characterized by parenchyma coloring of both lobes in homogeneous blue without areas of local stiffness increase (**Figure 2**).

Median of $E_{mean}$ value in the comparison group was 5.00 kPa, $E_{max}$—6.3 kPa. The obtained data are presented in **Table 1**.

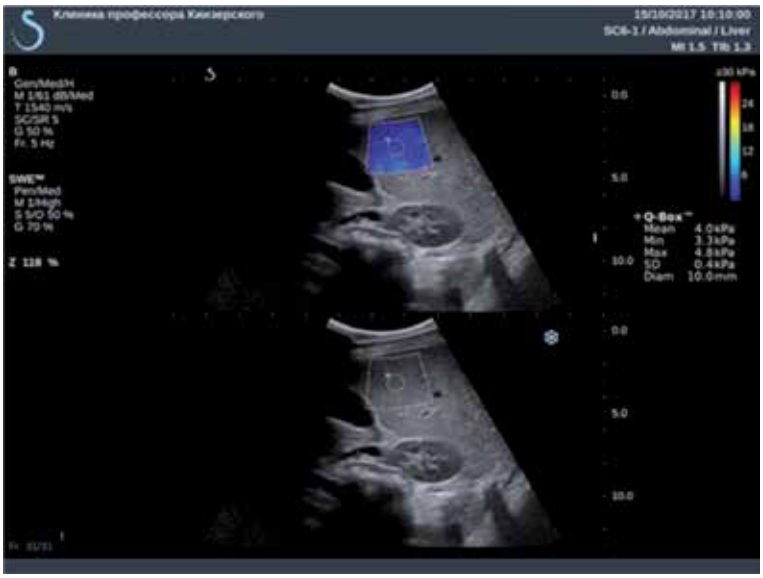


**Figure 2.**
*An example of liver stiffness evaluation in a healthy child aged 5 years: B-mode (below) and two-dimensional shear wave elastography mode (above). These are the results of one of 10 measurements. $E_{mean}$ = 4.0 kPa. Homogeneous coloring without areas of local stiffness increase.*

| Group $N$ = 200 | Young modulus, kPa | | | | |
|---|---|---|---|---|---|
| | $M \pm m$ | Median | Maximal-minimal values | 25th–75th percentile | σ |
| 3–18 years | 5.01 ± 0.03 | 5.00 | 3.00–6.30 | 4.70–5.38 | 0.49 |

**Table 1.**
*Young modulus value ($E_{mean}$, kPa) of the unchanged liver parenchyma in the study group of healthy children.*

| Age groups $N$ = 200 | Young modulus, kPa | | | | |
|---|---|---|---|---|---|
| | $M \pm m$ | Median | Maximal-minimal values | 25th–75th percentile | σ |
| 3–6 years ($n$ = 103) | 4.89 ± 0.04 | 4.90 | 3.48–6.18 | 4.56–5.22 | 0.45 |
| 7–11 years ($n$ = 52) | 5.09 ± 0.07 | 5.03 | 3.00–6.00 | 4.98–5.41 | 0.48 |
| 12–18 years ($n$ = 45) | 5.18 ± 0.08 | 5.24 | 4.05–6.20 | 4.77–5.54 | 0.51 |

**Table 2.**
*Young modulus value ($E_{mean}$, kPa) of parenchyma of unchanged liver in different age groups.*

Median in the age group 3–6 years ($n$ = 103) was 4.90 kPa, $E_{max}$—6.18 kPa. Median in the age group 7–11 years ($n$ = 52) was 5.03 kPa, $E_{max}$—6.00 kPa. Median in the age group 12–18 years ($n$ = 45) was 5.24 kPa, $E_{max}$——6.20 kPa. The obtained data on unchanged liver parenchyma values in different age groups are presented in **Table 2**.

To adjust gender differences in the values of unchanged liver parenchyma, Young modulus analysis in girls ($n$ = 103) and in boys ($n$ = 97) was performed. $E_{mean}$ median in boys is 5.08 kPa and in girls is 4.99 kPa ($p$ = 0.345). The analysis results are presented in **Table 3**.

| Group | Young modulus, kPa | | | | |
|---|---|---|---|---|---|
| | ***M* ± *m*** | **Median** | **Maximal-minimal values** | **25th–75th percentile** | **σ** |
| Boys (*n* = 97) | 5.07 ± 0.07 | 5.08 | 4.06–6.00 | 4.82–5.50 | 0.48 |
| Girls (*n* = 103) | 5.03 ± 0.05 | 4.99 | 4.26–5.70 | 4.78–5.33 | 0.36 |

**Table 3.**
*Young modulus value ($E_{mean}$, kPa) of parenchyma of unchanged liver in different gender groups of healthy children (aged 3–18 years).*

Thus, normal elastography picture of the liver is characterized by homogeneous coloring of parenchyma in the color window without areas of local stiffness increase. Mean value of Young modulus is 5.01 ± 0.03 kPa, and median of $E_{mean}$ value in the comparison group was—5.00 kPa (4.70–5.38). Significant increase of liver stiffness in children older than 6 years was established. Significant gender differences in stiffness were not found.

According to the results of other research groups, the values of the shear wave velocity in the liver parenchyma of the right and left lobes do not have statistically significant differences. Point shear wave elastography (ARFI elastography) was performed by Feoktistova et al. [8] in 100 children aged from 6 months up to 16 years. There were no any significant differences of shear wave speed between the right and left lobes [8]. The authors believed it is possible to measure the stiffness of both the right and left lobes of the liver due to the relatively lesser force of the aortic pulsation, as well as the small thickness of the anterior abdominal wall with a small degree of subcutaneous and preperitoneal fat tissue in the epigastrium. To determine the standard shear wave velocity values [9], 103 children aged from 2 weeks to 17 years were examined. The authors indicate that during statistical processing of data, no significant differences were found in the lobes of the liver [9].

Taking into account literature data testifying the absence of significant differences between the right and left lobe stiffness, measurements were made in both of them. The findings were combined to further analyze the quantitative data. Mean liver stiffness value was calculated in 10 measurements in two lobes of each child.

Interestingly, the mean value of stiffness in the control group (5.01 ± 0.03) kPa coincided more with the study of researchers Huang et al. (509 healthy adult volunteers) [10] and Shin et al. (76 healthy children [11], which were 5.10 ± 1.02 and 5.5 ± 1.3 kPa, respectively) (two-dimensional elastometry). The mean value of stiffness in the study of Engelmann et al. (TE) was 4.7 kPa [12]. The results differed from the findings of Franchi-Abella et al. [13] and Tutar et al. [14] where the mean value of stiffness obtained by convex sensor was higher: 6.94 ± 1.42 and 7.41 kPa, respectively. But one should take into consideration that both studies were performed on control groups consisting of 50 healthy children, which may reduce their statistical power.

To adjust age-specific features of unchanged parenchyma stiffness, all study patients were allocated to three groups according to Mazurin and Vorontsov age periodization. Subgroup 1 consisted of 103 children aged 3–6 years. Subgroup 2 consisted of 52 children aged 7–11 years. Subgroup 3 consisted of 45 children aged 12–18 years. Median in the age group 3–6 years ($n$ = 103) was 4.90 kPa, in the age group 7–11 years ($n$ = 52) was 5.03 kPa, and in the age group 12–18 years ($n$ = 45) was 5.24 kPa (**Table 2**). Significant differences of stiffness were obtained comparing the values in age groups 3–6 and 7–11 years ($p$ = 0.001) and 3–6 and 12–18 years ($p$ = 0.001). Statistically significant differences between subgroups 2 and 3 were not established ($p$ > 0.001). Thus, liver stiffness values in children older than 6 years

are significantly higher. Probably, in a larger sampling, there will appear a tendency to stiffness increase as patients get older.

The same results of stiffness increase with age were established by Engelmann et al. and Sagir et al. [15] who studied normal indices of stiffness by transient elastography method in groups of 240 and 198 children. Engelmann et al. [12] established the values of stiffness median for age group 0–5 years, 4.40 kPa; for age group 6–11 years, 4.73 kPa; and for age group 11–18 years, 5.10 kPa ($p$ = 0.001). Sagir et al. [15] also observed age and stiffness dependence: 4.8 ± 1.4 kPa (0–5 years), 5.6 ± 1.3 kPa (6–11 years), and 5.7 ± 1.7 kPa (12–18 years). Stiffness values in these age groups coincided with the results obtained in our study.

As a result of the study, there were no established statistically significant differences in gender stiffness values: $E_{mean}$ median in boys is 5.08 kPa and in girls is 4.99 kPa ($p$ = 0.345). Comparing the two groups, statistically significant differences were considered ($p$ > 0.001).

Gender characteristics of parenchyma stiffness were analyzed in the work of Franchi-Abella et al. where any differences in stiffness depending on the gender were also not established [13].

## 5. Conclusion

Young modulus values obtained from healthy children may be recommended as a standard investigation. The use of shear wave elastometry within a complex ultrasound evaluation will contribute to better early diagnostics of the changed parenchyma. Prospectively, a widespread use of ultrasound elastography will result in decreasing the number of biopsies.

## Author details

Mikhail Pykov[1*], Natalia Kuzmina[2], Nikolay Rostovtsev[3] and Alexander Kinzersky[4]

1 Division of Pediatric Radiology, Russian Medical Academy of Postgraduate Education, Moscow, Russia

2 Ultrasound Diagnostics Department, Chelyabinsk Regional Children Clinical Hospital, Chelyabinsk, Russia

3 Department of Pediatric Surgery, Federal State Budgetary Institution of Higher Education "South Ural State Medical University", Chelyabinsk, Russia

4 Professor Kinzersky Clinic, Chelyabinsk, Russia

*Address all correspondence to: pykov@yandex.ru

## References

[1] Orlovsky DV, Oshmyanskaya NY, Nedzvetskaya NV. Place of puncture biopsy in diagnosis of chronic diffuse liver diseases. Gastroenterology. 2013;**48**(2):47-52

[2] Gotje SV. Liver transplantation: The current state of the problem. Almanac of the Vishnevsky Institute of surgery. 2008;**3**(30):9-17

[3] Gotje SV, Kaganov BS, Zaynutdinov ZM, Tsirulnikova OM. Criteria of diagnostics and clinical course of liver cirrhosis in children. Infectious Diseases. 2008;**6**(3):14-21

[4] Minuk GY, Sutherland LR, Wiseman DA, MacDonald FR, Ding DL. Prospective study of the incidence of ultrasound-detected intrahepatic and subcapsular hematomas in patients randomized to 6 or 24 hours of bed rest after percutaneous liver biopsy. Gastroenterology. 1987;**92**(2):290-293

[5] Dezsőfi A, Baumann U, Dhawan A, Durmaz O, Fischler B, Hadzic N, et al. Liver biopsy in children: Position paper of the ESPGHAN hepatology committee. Journal of Pediatric Gastroenterology and Nutrition. 2015;**60**(3):408-420

[6] Mazurin AV, Vorontsov IM. Propaedeutics of Children Diseases. Moscow: Medicine; 1985. p. 432

[7] Baranov AA, editor. Pediatrics. National Guidelines. GEOTAR-Media: Moscow; 2009. p. 1024

[8] Feoktistova EV, Pykov MI, Amosova AA, Tarasov MA, Dubrovin MM. Application of ARFI—Elastography for liver stiffness evaluation of children of different age groups. Ultrasound and Functional Diagnostics. 2013;**6**:46-55

[9] Hanquinet S, Courvoisier D, Kanavaki A, et al. Acoustic radiation force impulse imaging—Normal values of liver stiffness in healthy children. Pediatric Radiology. 2013;**43**(5):539-544

[10] Huang Z, Zheng J, Zeng J, Wang X, Wu T, Zheng R. Normal liver stiffness in healthy adults assessed by real-time shear wave elastography and factors that influence this method. Ultrasound in Medicine and Biology. 2014;**40**(11):2549-2555

[11] Shin HJ, Kim M-J, Kim HY, Roh YH, Lee M-J. Optimal acquisition number for hepatic shear wave velocity measurements in children. PLoS One. 2016;**11**(12). DOI: 10.1371/journal.pone.0168758. [Accessed: 21 December 2016]

[12] Engelmann G, Gebhardt C, Wenning D, Wühl E, Hoffmann GF, Selmi B, et al. Feasibility study and control values of transient elastography in healthy children. European Journal of Pediatrics. 2012;**171**(2):353-360

[13] Franchi-Abella S, Corno L, Gonzales E, Antoni G, Fabre M, Ducot B, et al. Feasibility and diagnostic accuracy of supersonic shear-wave elastography for the assessment of liver stiffness and liver fibrosis in children: A pilot study of 96 patients. Radiology. 2016;**278**(2):554-562

[14] Tutar O, Beşer ÖF, Adaletli I, Tunc N, Gulcu D, Kantarci F, et al. Shear wave elastography in the evaluation of liver fibrosis in children. Journal of Pediatric Gastroenterology and Nutrition. 2014;**58**(6):750-755

[15] Sagir A, Ney D, Oh J, Pandey S, Kircheis G, Mayatepek E, et al. Evaluation of acoustic radiation force impulse imaging (ARFI) for the determination of liver stiffness using transient elastography as a reference in children. Ultrasound International Open. 2015;**1**(1):E2-E7. DOI: 10.1055/s-0035-1554659

Section 2

# Breast Elastography

Chapter 7

# Strain Elastography in Invasive Lobular Carcinoma

*Angelica Rita Chiorean, Roxana Pintican, Diana Feier, Dan Eniu and Maria Magdalena Duma*

## Abstract

Breast cancer remains the second cause of mortality in women, even if the mortality rates linked to it have drastically dropped at the present time. Invasive lobular carcinoma (ILC) accounts for 5–15% of the breast cancers and it is the second most encountered type among invasive carcinomas. There has been reported a high rate for bilateral lesions (6–47%), multifocality/multicentricity (21%), all affecting ILC overall survival. Due to its nonspecific symptoms and to the fact that it does not invoke a vigorous desmoplastic response and has a low likelihood of producing calcifications, the ILC tends to be insidious on mammography. Contrast enhanced MRI has the lowest false negative rate in detecting ILC and it is the most accurate method of determining the lesion extension, though it is expensive and not widely available. Therefore, the ultrasound (US) plays a significant role in the diagnosis of ILC. US elastography imaging (EI) individualizes malignant breast lesions with high sensitivity and specificity. Recent studies suggested that US elastography can even diagnose lobular cancers that have benign findings on conventional imaging. Goal: present various US aspects and exemplify the added diagnostic value of strain elastography—how it may change the BIRADS category and further therapeutic management?

**Keywords:** breast cancer, invasive lobular carcinoma, elastography, ultrasound, BI-RADS

## 1. Introduction

Breast cancer remains the second cause of mortality in women, even if the mortality rates linked to it have drastically dropped at the present time. Based on the origin of the cancer cells, there are two types of breast cancer subtypes: ductal and lobular. Both include an "in situ" and an "invasive" form, depending on their extension to the neighboring tissues. We will further address invasive lobular cancer (ILC), which accounts for 5–15% of the breast cancers and is the second most encountered type among invasive carcinomas.

## 2. Epidemiology

ILC has an estimated incidence of 2.7 per 100.000 people, with a mean diagnostic age higher than for invasive ductal carcinoma. About two-thirds of women are 55 or older at the time of the diagnosis, ILC tending to occur even later in life [1].

## 3. Pathology and ILC subtypes

The tumor develops at the terminal ductal-lobular unit (TDLU), and it is composed of cancer cells that are individually dispersed or arranged in a single-file pattern. Often, the cells form a target-like configuration around normal breast ducts. Two main histology findings are characteristic for invasive lobular cancer: the noncohesive cell pattern and the minimal desmoplastic response. The first is an effect of the E-cadherin (CDH1) germline mutation encountered in about 85% of the tumors, which results in the loss of adhesion proteins and a discohesive morphologic pattern [2]. The second is due to the fact that malignant cells grow in the mammary stroma and adipose tissue and induce less desmoplastic reaction than ductal carcinoma, which has important repercussions on the imaging aspects [3].

As it regards the ILC subtypes, occasionally the classic single-file formation is absent, and there is a different pattern encountered: solid (large sheets with little stroma), alveolar (groups of 20 cells), or tubular-lobular (tubelike structures together with single-file pattern) [2, 3].

The classic ILC presents with tumor cells that are usually small, uniform, and round with minimal pleomorphism. Otherwise, a less often subtype cell might be reported: pleomorphic or signet-ring cells.

The majority of ILC are positive for estrogen and progesterone receptors and are negative for the HER2 amplification (consistent with a luminal A category).

## 4. Signs and symptoms

The invasive lobular carcinoma may be asymptomatic. Due to the typical spread pattern, some of the patients may present with the first sign of ILC as a skin thickening or hardening of the breast rather than a distinct lump. Basically there are no ILC-specific signs or symptoms; the patients' physical examination may reveal general breast cancer-related changes such as a swelling area, skin irritation or dimpling, breast or nipple pain, nipple discharge (other than breast milk), and even an axillary lump [4].

Due to the lack and nonspecific symptoms, up to 10% of the patients present with metastatic disease at the time of diagnosis [1].

## 5. Diagnosis of ILC

Breast cancer in general might be diagnosed using different complementary methods or techniques, starting with a physical breast examination; whether we are using screening or diagnostic mammography (Mx), ultrasound, or magnetic resonance (MRI), it is well known that imaging often underestimates this disease's extension. The tissue analysis remains the gold standard for tumor diagnostic, regardless if the tumor tissue originates from a biopsy or a surgical excision.

Regarding the tumor appearance, a high rate for bilateral lesions (6–47%) has been reported, multifocality/multicentricity (21%), all affecting the ILC overall survival (**Figure 1**) [1].

### 5.1 Mammography

The sensitivity of mammography is reported to be lower for ILC than for invasive ductal carcinoma, ranging from 34–72%, and it is frequently seen in only one view (often on cranio-caudal compared to mediolateral oblique) [5]. Most commonly, the tumor presents as a spiculated mass lesion without calcifications.

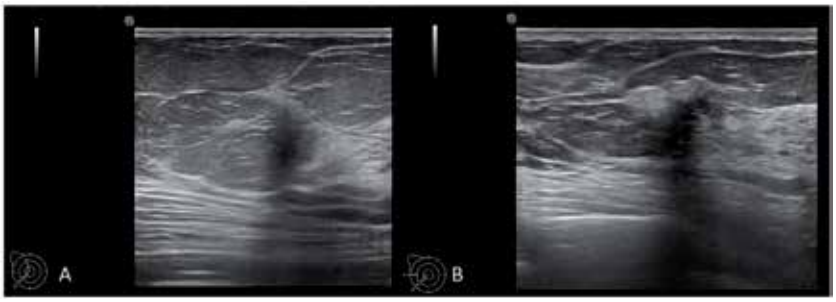


**Figure 1.**
*Multifocal ILC. Ultrasound suspect lesions located in the right breast, first at 11 o'clock (A) and second at 9 o'clock (B).*

In some cases, architectural distortions or asymmetrical densities are observed; moreover, up to 16% of ILC remains mammographically occult or are attributed to benign lesions (**Figure 2**).

### 5.2 Ultrasound

The studies reported a sensibility of 98% in the ultrasound diagnostic of ILC [6]. The tumor usually presents as a hypoechoic mass, with ill-defined margins and posterior acoustic shadowing (58%), occasionally without shadowing (27%) [6]. Contrary to ductal carcinoma, which commonly presents as a lesion perpendicular to the surface, ILC may exhibit a so-called "wider than tall" shape, a tumor that is parallel to the skin. In some cases, the mass might be heterogeneous with an iso- or hyperechoic halo (**Figure 3**).

#### *5.2.1 B-mode*

Two classic signs of ILC were described using B-mode of ultrasound. First, the Golden Gate sign resulted from 2 to 3 adjacent Cooper's ligaments involved by cancer so that the shadowing area (hypoechoic area) resembles the shape of a suspension bridge seen from the profile. The second one, named the picket fence sign, is observed when more numerous and more closely spaced Cooper's ligaments are involved in cancer and the shadowing area resembles the profile of a picket fence (**Figure 4**).

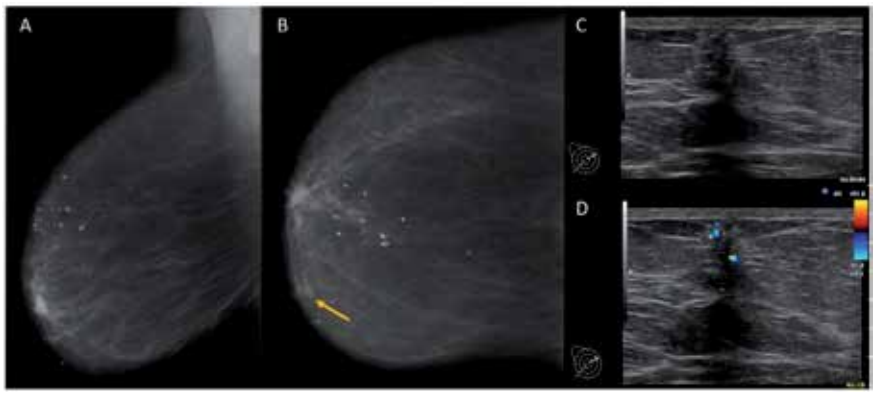


**Figure 2.**
*Subtle ILC mammographic findings: An asymmetry of density is seen on the CC view (B, arrow), without a correspondent on MLO projection (A). Note the same density of the lesion as of the normal tissue breast. The ultrasound (CD) revealed a 5 mm, spiculated, hypoechoic lesion with vascularization on color Doppler.*

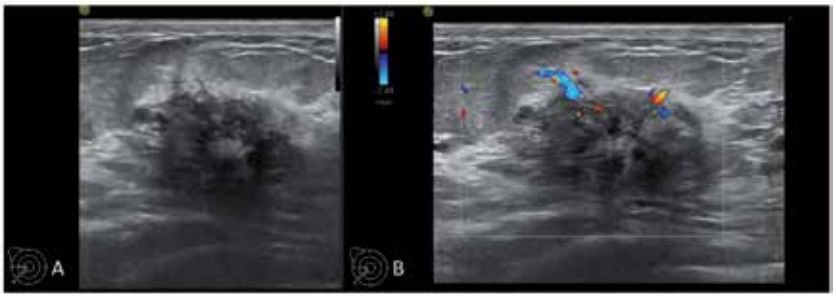


**Figure 3.**
*ILC presented as a heterogeneous mass, with small cystic areas included and ill-defined margins (A), vascularized on color Doppler (B). Note the mass orientation, parallel to the surface, with a "wider than tall" appearance.*

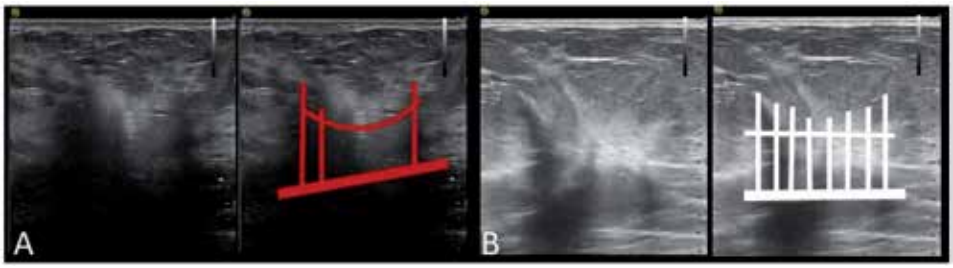


**Figure 4.**
*Classic sign of ILC: Golden Gate bridge (A) and picket fence (B).*

### *5.2.2 Doppler mode*

The Doppler mode highlights the presence of the blood vessels within the tumor, whether it is a mild, moderate, or intensely vascularized tumor mass. The vessel's spreading pattern is not characteristic, usually the tumor presenting with diffusely distributed vascularization. Rarely, a malignant mass may present as an avascular tumor, due to the present-day limitation of the technique (vessels too small to be highlighted).

### *5.2.3 Elastography*

In breast ultrasound, both strain (static) and shear wave (dynamic) elastography are used. Ultrasound elastography of the ILC masses exhibits various patterns, from soft to mosaic and predominantly hard tumors. Tsukuba score (TS) is often used to qualitatively classify the elasticity of the masses, from 1 (soft) to 5 (extensively hard lesions) (**Table 1**).

The elasticity varies between different lobular cancer masses, which may even have an elastography score similar with the normal adjacent breast tissue. An important take-home message lies in the lesion's grayscale aspect: if the B-mode indicates any sign of malignancy, a normal hardness should not delay the following biopsy.

ILC commonly presents as hard masses (Tsukuba 4 or 5 score). Sometimes a mosaic pattern might be obtained, and rarely a blue-green-red (BGR) appearance may be noted.

A topic of interest nowadays is represented by the US prediction regarding the breast cancer tumor grades. The mean elasticity/B-mode ratio was reported as statistically different between ILC and grade III ductal carcinoma, versus mucinous or grade I and II ductal cancers [7].

| | | |
|---|---|---|
| Score 1<br>Complete deformability of lesion | 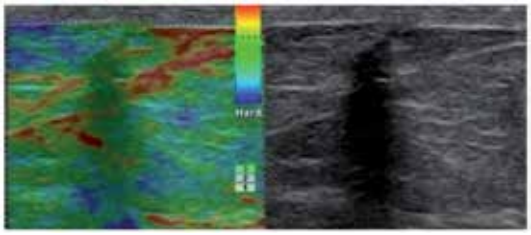 | Benign |
| Score 2<br>Lesion with little stiff areas | 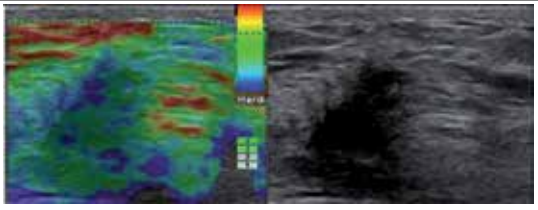 | Benign |
| Score 3<br>Central stiff area with peripheral deformability | 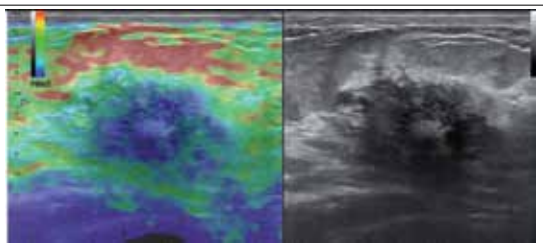 | Probably benign |
| Score 4<br>Completely stiff lesion | 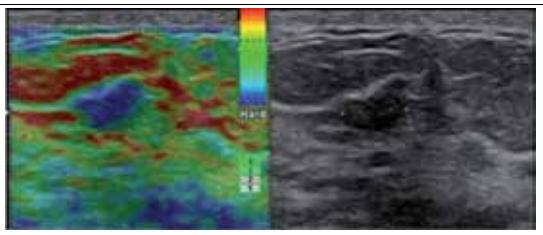 | Malignant |
| Score 5<br>Stiff lesion and surrounding area | 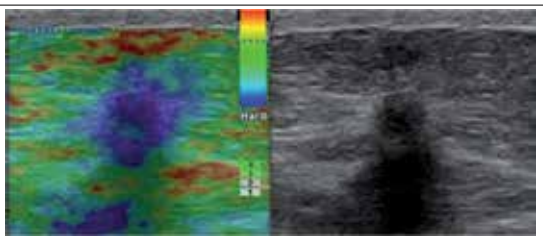 | Malignant |
| BGR sign<br>Blue-green-red pattern | 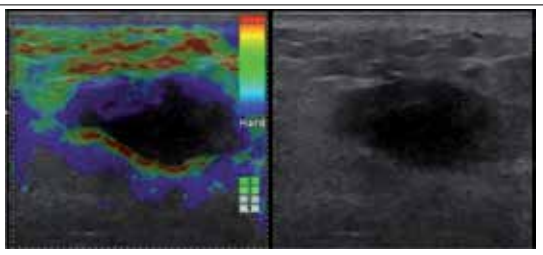 | Benign/cyst/ malignant with necrotic area |

**Table 1.**
*Tsukuba qualitative score. The left column displays the elastography score, the middle column shows the elastography/B-mode appearances, and the right column describes the score meaning. All the abovementioned lesions were proven to be invasive lobular cancers.*

On the topic of shear wave elastography, the method provides a quantitative assessment and tissue stiffness values, represented in kilopascals (kPa). A value higher than 45.7 kPa for the mean elasticity was attributed to malignant breast tumors (**Figure 5**) [8].

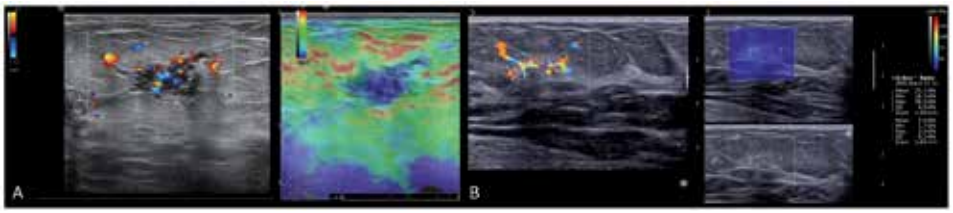


**Figure 5.**
*Breast elastography techniques. (A) Vascularized lesion, hard on strain elastography. (B) Vascularized area, soft on shear wave elastography. Note the difference between stiffness' color coding: Blue in strain EI = hard, blue in share wave EI = soft.*

A comparison of strain and shear wave ultrasound elastography in differentiating benign and malignant breast lesions concluded that strain ultrasound elastography is more specific (93.7%) and less sensitive (81.7%), while shear wave ultrasound elastography is more sensitive (95.8%) and less specific (84.8%) in differentiating benign from malignant breast lesions [9].

There are three additional and important EI key aspects that help in the ILC diagnostic:

1. Highlighting hardly visible lesions—Sometimes a breast lesion might be isoechoic to the surrounding breast tissue, scarcely visible in grayscale; in some cases elastography may help us in identifying those hard lesions with greater confidence (the lesions will appear as isoechoic on B-mode and blue on strain EI).

2. Identifying pseudo-benign lesions—EI may indicate lobular cancers that have benign or normal findings on conventional imaging as suspicious [10].

3. Suggesting a larger lesion—It is known that imaging often underestimates ILC. Even so, EI may sometimes suggest a lesion's extension by highlighting a hard area that exceeds the grayscale lesion (lesions with Tsukuba 5 score).

To conclude, whether or not it is a strain or a shear wave, elastography methods are adding value to the ILC diagnostic and should be definitely used in the assessment of every patient. Moreover, it may change the BI-RADS category from a probable benign lesion (score 3) to a suspicious lesion (score 4). Thereby, elastography has an important impact in the patient's therapeutic management, which translates in certain cases, in switching from a short-time follow-up to biopsy.

By educational purposes, all ultrasound characteristics presented above will be highlighted in the following case-based section. The various ILC imaging appearances were grouped in subcategories, as it follows:

a. Hypoechoic mass with posterior acoustic shadowing (**Figure 6**).

b. Hypoechoic mass without posterior acoustic shadowing (**Figure 7**).

c. Architectural distortion (**Figures 8** and **9**).

d. Iso- or hypoechoic area or non-mass lesion (**Figures 10** and **11**).

e. Hyperechoic lesion. Even if the hyperechoic appearance usually represents a benign entity, up to 5% of the ILC were reported as hyperechoic lesions, out of which 48% were associated with posterior acoustic shadowing (**Figure 12**) [11].

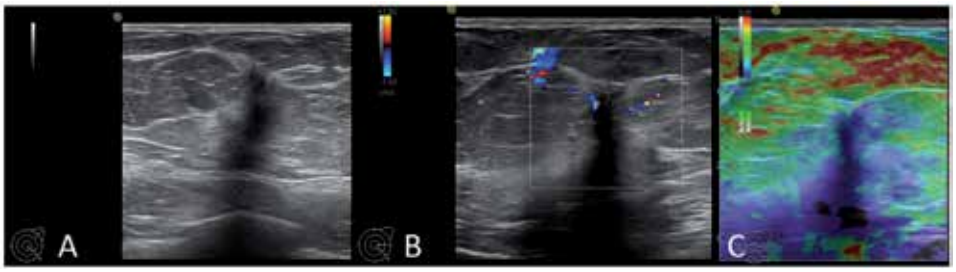


**Figure 6.**
*ILC lesion presents as a hypoechoic mass with intense posterior acoustic shadowing (A), vascularized (B), and hard on elastography (C, TS 5).*

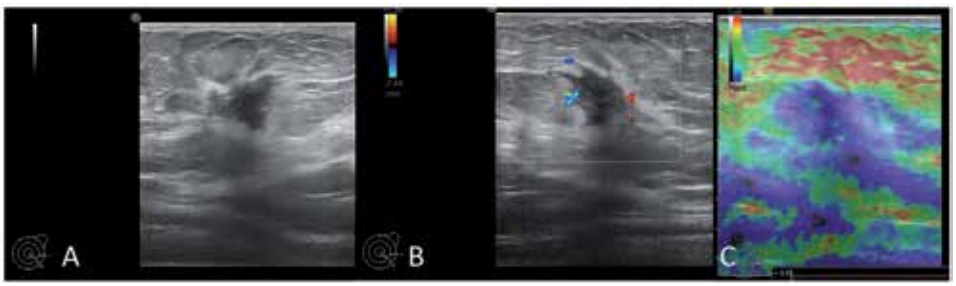


**Figure 7.**
*ILC lesion presents as an ill-defined, hypoechoic mass without posterior acoustic shadowing (A), hypovascular (B), and hard on elastography (C, TS 5).*

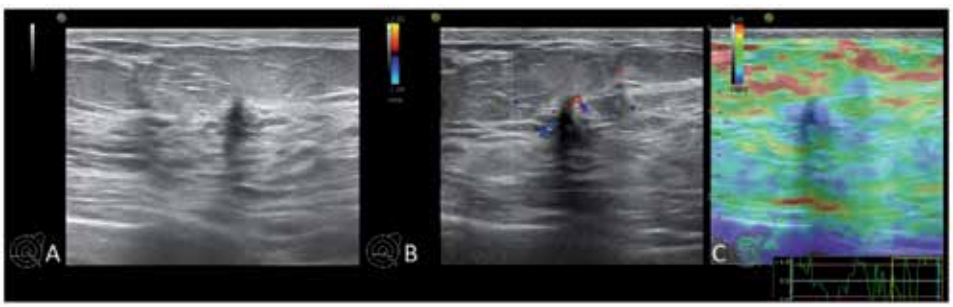


**Figure 8.**
*ILC lesion presents as an architectural distortion with mild posterior acoustic shadowing, hardly visible on grayscale (A). The area is hypovascular (B) and hard on elastography (C, TS 4).*

f. Well-defined nodule. Studies reported up to 2–12% of the ILC cases as a pseudo-benign, well-defined nodule (**Figure 13**) [12].

g. Occult lesion. Not often, ILC may not be highlighted by ultrasound. Authors report up to 10% of the cases missed on US [12]. Sometimes, a lesion might be detected during a second-look US after an MRI depiction (**Figure 14**).

h. Axillary abnormality. Regarding the US sensitivity in the metastasis detection, the technique was reported positive in about 50% of the N1 cases. Furthermore, US is able to exclude 96% of the N2 and N3 axillary metastasis (more than four positive lymph nodes). The fine needle biopsy is less sensitive in ILC than invasive ductal carcinoma (IDC vs. ILC; 98.4% vs. 53.6%; $p < 0.001$) (**Figure 15**) [13].

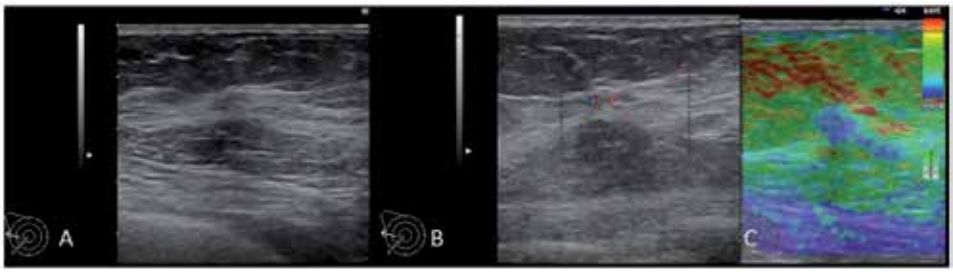


**Figure 9.**
*Hardly visible ILC isoechoic lesion (A) associated with a hypovascular architectural distortion (B). The lesion is easily spotted on elastography, as a hard area (C, TS 4).*

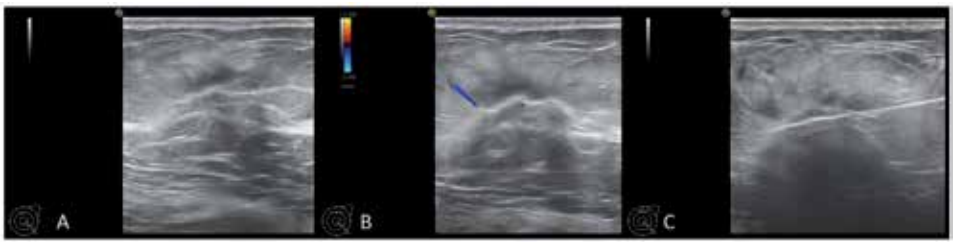


**Figure 10.**
*Hypoechoic area with hyperechoic halo resembling the picket fence sign (A), with minimal vascularization on color Doppler (B). The core needle biopsy (C) revealed an ILC lesion, with positive estrogen and progesterone receptors RE = 100%, RP = 25%, Ki67 = 15%, and HER2 negative.*

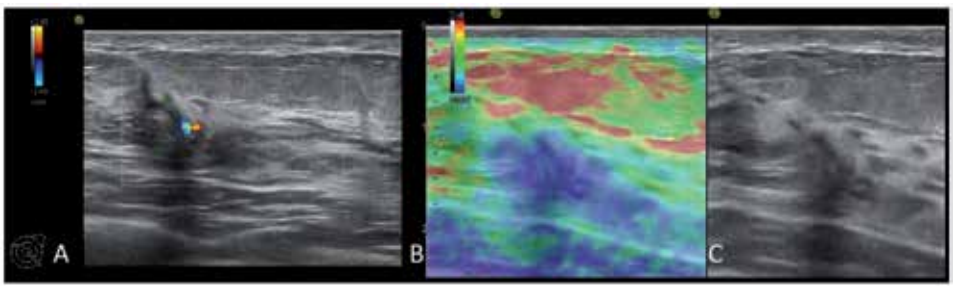


**Figure 11.**
*Hypoechoic, hypovascular area which presents with mild posterior acoustic shadowing (AC). Note that the hard area is larger on elastography than grayscale (B, TS 5).*

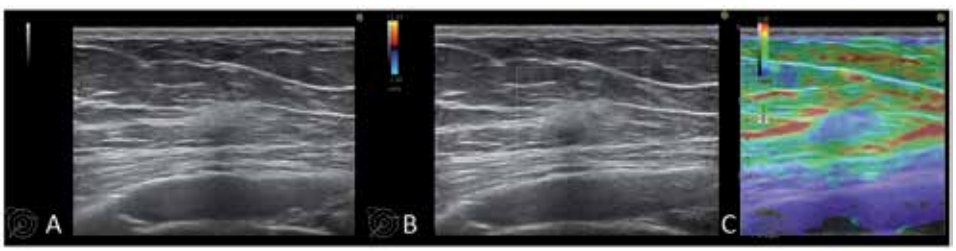


**Figure 12.**
*Hyperechoic, ill-defined lesion (A), apparently avascular (B), but hard on elastography (C, TS 4). At the time of diagnosis, the patient presented peritoneal metastasis.*

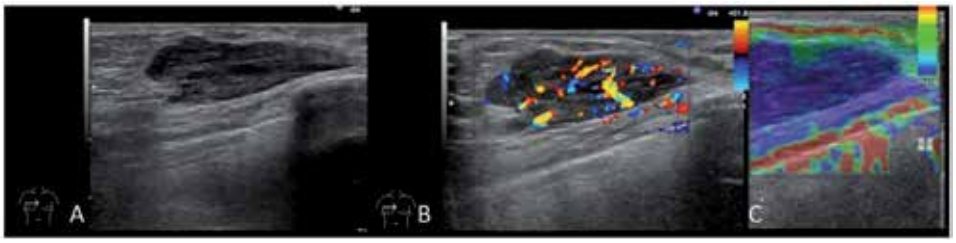


**Figure 13.**
*A patient with a history of ILC treated with mastectomy 24 years ago. The present US revealed a well-defined, hypoechoic nodule in the area of mastectomy (A). The nodule is intensely vascularized (B) and hard on elastography (C, TS 4). Initially considered a BI-RADS 4a lesion, after EI the lesion has been assigned to a higher BI-RADS 4b score. The core needle biopsy showed an ILC relapse.*

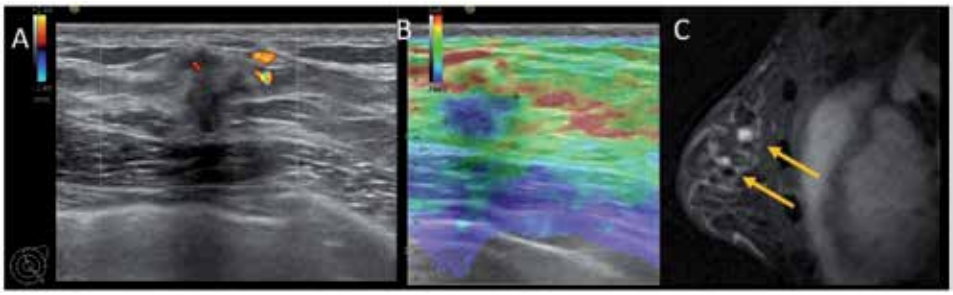


**Figure 14.**
*A breast lesion with suspect features was detected at US and proven to be an ILC (AB). The following staging MRI highlighted not one, but two lesions (C), concluding that one of the lesions was US occult.*

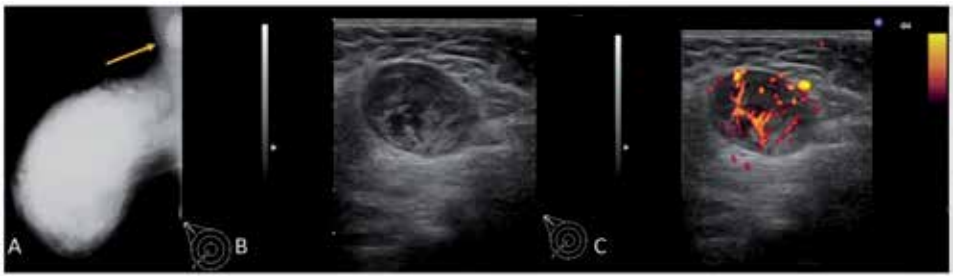


**Figure 15.**
*The mammography shows a highly dense right breast and an abnormal axillary mass (A, arrow). The US revealed an enlarged, rounded lymph node (B), with intense and chaotic vascularization (C). The core needle biopsy concluded an ILC metastasis.*

i. ILC with BGR appearance. Rarely, ILC may display a blue-green-red sign due to a necrotic component. Even if the BGR sign is commonly attributed to cysts, its presence in a solid, suspicious mass may never delay a biopsy (**Figure 16**).

j. ILC lesions in which elastography changed the BI-RADS score. It was previously established that in order to achieve an accurate breast cancer diagnosis, US B-mode should be combined with Color Doppler and elastography. Regarding EI, there was a positive impact in breast cancer diagnosis, especially for small lesions [14]. Moreover, in invasive lobular cancer, EI demonstrated to improve the BI-RADS classification, particularly for lesions smaller than 13 mm (**Figures 17–19**) [15].

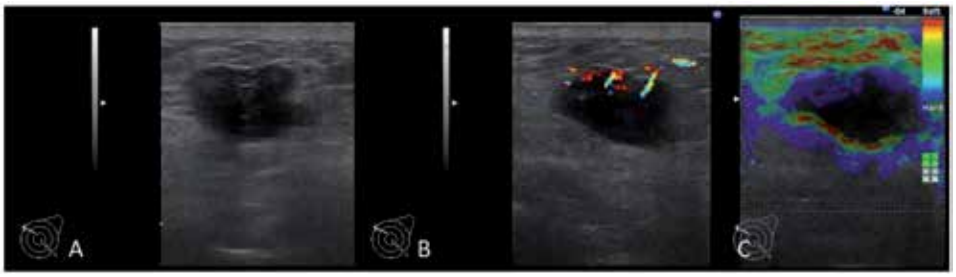


**Figure 16.**
*Intensely hypoechoic nodule with partially well-defined, partially ill-defined margins (A), moderately vascularized on color Doppler examination (B). The elastography displays a blue-green-red appearance (C). Core biopsy revealed an ILC lesion.*

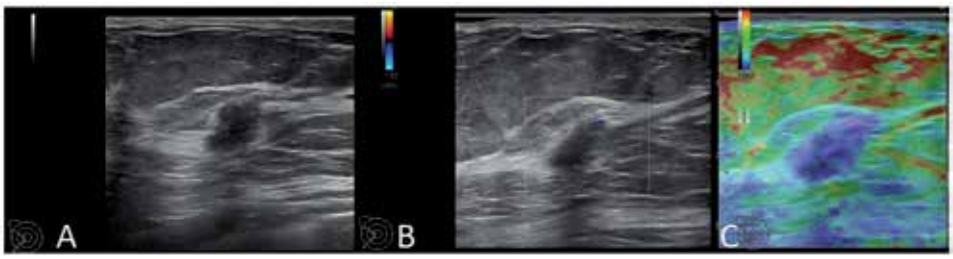


**Figure 17.**
*BI-RADS 3 to BI-RADS 4a. ILC presented as a small hypoechoic lesion with indistinct margins (A), hypovascular (B), and hard aspect on EI (C, TS 4/5). The lesion was upgraded from BI-RADS 3 to BI-RADS 4a after the elastography criterion was added.*

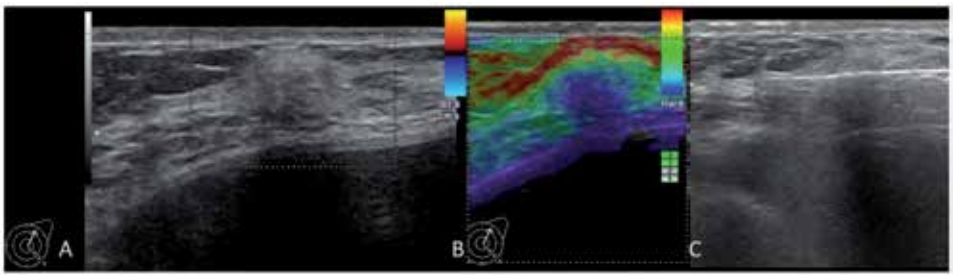


**Figure 18.**
*BI-RADS 4a to BI-RADS 4b. A small, avascular, hyperechoic lesion with indistinct margins (A) and hard on EI (B, TS 4). The core needle biopsy revealed ILC (C). The lesion was upgraded from BI-RADS 4a to BI-RADS 4b after the elastography criterion was added.*

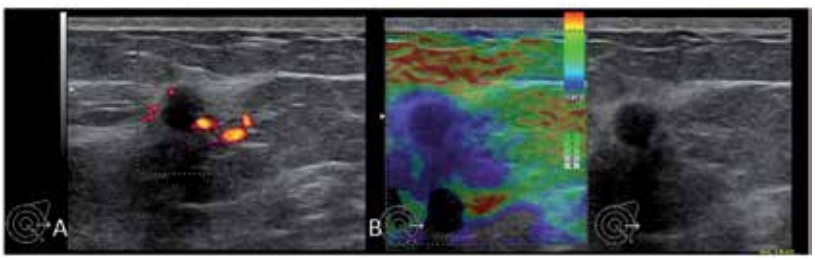


**Figure 19.**
*Doppler US reveals a hypoechoic round lesion with partially angulated margins and peripheral vascularity (A). On strain elastography (B), the entire lesion and its surrounding parenchyma were shaded blue (TS 5). The lesion was upgraded from BI-RADS 4B to BI-RADS 4C after the elastography criterion was added.*

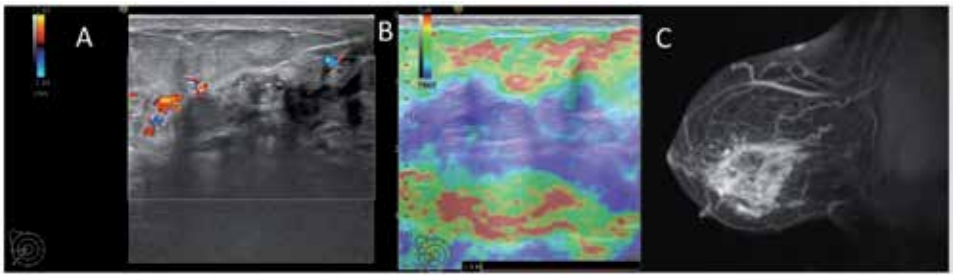


**Figure 20.**
*Heterogeneous US area of ILC, which is moderately vascularized and hard on elastography (AB, TS 5). The MRI (C) shows a non-mass enhancement, with a regional distribution, larger than the area predicted on US.*

### 5.3 MRI

Due to its propensity for bilaterality and multicentricity, breast MRI is usually recommended when histology of a lesion reveals an ILC. MRI easily highlights occult Mx and US lesions and has the lowest false-negative rate in detecting ILC [16]. In addition, MRI has the highest accuracy in measuring ILC sizes, whether it is a mass or non-mass enhancement pattern. ILC kinetic is rarely a type III curve (washout) or type I curve, more often displaying a type II (plateau) curve (**Figure 20**).

## 6. Treatment and prognosis

Depending on the disease's stage, there is a local ILC treatment represented by surgery and radiation therapy and a systemic treatment characterized by chemotherapy, hormonal therapy, or targeted therapies. Due to its diffuse invasive nature, positive resection margins are common.

ILC spreads slowly outside the breast, but when it does, it tends to manifests with atypical metastases, affecting the gastrointestinal tract (as a diffuse spreading process of the colon 26%, stomach, or small bowel), ovaries (21%), peritoneum (as Krukenberg syndrome, 30%), retroperitoneum, leptomeningeal, or bone. It may also cause lymph node, lung, or liver metastasis.

Despite the multifocality, the bilateral lesions, and the atypical metastases, the prognosis for ILC patients with a given size and stage is believed to be slightly higher than for patients with invasive ductal carcinoma.

## 7. Conclusion

The ultrasound plays a significant role in the diagnosis of invasive lobular carcinoma. Ultrasound elastography imaging individualizes malignant breast lesions with high sensitivity and specificity, being sometimes a "problem-solving" method. Moreover, it may change the BI-RADS category and have an important impact on the patient's therapeutic management.

## Acknowledgements

There are no acknowledgments nor funding sources.

## Conflict of interest

All authors declare no conflict of interest.

## Notes/thanks/other declarations

We would like to thank our families for the support and understanding.

## Author details

Angelica Rita Chiorean[1,2*], Roxana Pintican[3], Diana Feier[1,2], Dan Eniu[1,4] and Maria Magdalena Duma[5]

1 "Iuliu Haţieganu" University of Medicine and Pharmacy, Cluj-Napoca, Romania

2 Medimages Breast Center, Cluj-Napoca, Romania

3 Department of Radiology and Medical Imaging, County Hospital, Cluj-Napoca, Romania

4 "Prof. Dr. Ion Chiricuţă" Oncology Institute, Surgery Department, Cluj-Napoca, Romania

5 Micromedica Clinic, Piatra-Neamţ, Romania

*Address all correspondence to: chiorean_angi@yahoo.com

## References

[1] Invasive Lobular Cancer. [Internet]. Available from: http://www.breastcancer.org/symptoms/types/ilc [Accessed: 20 May 2019]

[2] Srivastava S. Breast Malignant, Males, Children [Internet]. 2017. Available from: http://www.pathologyoutlines.com/topic/breastmalignantlcis.html [Accessed: 20 May 2019]

[3] Jones KN, Magut M, Henrichsen TL, et al. Pure lobular carcinoma of the breast presenting as a hyperechoic mass: Incidence and imaging characteristics. AJR. American Journal of Roentgenology. 2013;**201**:W765-W769. DOI: 10.2214/AJR.12.9742

[4] Breast Cancer Signs and Symptoms online. Available at: https://www.cancer.org/cancer/breast-cancer/about/breast-cancer-signs-and-symptoms.html [Accessed: 20 May 2019]

[5] Berg WA, Birdwell RL. Diagnostic Imaging Breast. Salt Lake City: Amyrsis; 2006. pp. 144-147

[6] Selinko VL, Middleton LP, Dempsey PJ. Role of sonography in diagnosing and staging invasive lobular carcinoma. Journal of Clinical Ultrasound. 2004;**32**:323-332. DOI: 10.1002/jcu.20052

[7] Grajo JR, Barr RG. Strain elastography for prediction of breast cancer tumor grades. Journal of Ultrasound in Medicine. 2014;**33**:129-134. DOI: 10.7863/ultra.33.1.129

[8] Olgun DÇ, Korkmazer B, Kılıç F, et al. Use of shear wave elastography to differentiate benign and malignant breast lesions. Diagnostic and Interventional Radiology. 2014;**20**: 239-244. DOI: 10.5152/dir.2014.13306

[9] Chang JM, Won JK, Lee KB, et al. Comparison of shear-wave and strain ultrasound elastography in the differentiation of benign and malignant breast lesions. AJR. American Journal of Roentgenology. 2013;**201**:347-356. DOI: 10.2214/AJR.12.10416

[10] Sim YT, Vinnicombe S, Whelehan P, Thomson K, Evans A. Value of shear-wave elastography in the diagnosis of symptomatic invasive lobular breast cancer. Clinical Radiology. 2015;**70**:604-609. DOI: 10.1016/j.crad.2015.02.004

[11] Jones KN, Magut M, Henrichsen TL, Boughey JC, Reynolds C, Glazebrook KN. Pure lobular carcinoma of the breast presenting as a hyperechoic mass: Incidence and imaging characteristics. AJR. 2013;**201**:W765-W769. DOI: 10.2214/AJR.12.9742

[12] Johnson K, Sarma D, Hwang ES. Lobular breast cancer series: Imaging. Breast Cancer Research. 2015;**17**:94. DOI: 10.1186/s13058-015-0605-0

[13] Topps A, Clay V, Absar M, Howe M, Lim Y, Johnson R, et al. The sensitivity of pre-operative axillary staging in breast cancer: Comparison of invasive lobular and ductal carcinoma. European Journal of Surgical Oncology. 2014;**40**:813-817. DOI: 10.1016/j.ejso.2014.03.026

[14] Botticeli A, Mazzotti E, Di Stefano D, et al. Positive impact of elastography in breast cancer diagnosis: An institutional experience. Journal of Ultrasound. 2015;**18**:321-327. DOI: 10.1007/s40477-015-0177-y

[15] Chiorean A, Szep M, Feier D, et al. Impact of strain Elastography on BI-RADS classification in small invasive lobular carcinoma. Medical Ultrasonography. 2018;**20**:148-153. DOI: 10.11152/mu-1272

[16] Boetes C, Veltman J, van Die L, et al. The role of MRI in invasive lobular carcinoma. Breast Cancer Research and Treatment. 2004;**86**:31-37. DOI: 10.1023/B:BREA.0000032921.10481.dc

Chapter 8

# Shearwave Elastography in Differentiating Benign and Malignant Breast Lesions

*Binafsha Manzoor Syed, Jawaid Naeem Qureshi and Bikha Ram Devrajani*

## Abstract

Shearwave elastography is a new advance technique of the ultrasound with ultrafast shearwave mode which displays evaluation of the elasticity in real time. As the disease process tend to affect stiffness of the tissue thereby distorting its architecture. This architectural change makes the basic principal of the palpation part of the clinical examination. The shearwave elastography uses the principal of palpation. The output of shearwave is displayed in qualitative mode in the form of color change (ranging from blue to red) and quantitative mode as measure of elasticity in kilopascals (ranging from 0 to 300). The soft tissues are penetrated easily giving a homogenous pattern with blue to green color while cancers show color from red to dark red portraying high elasticity. The scoring system for interpretation of the shearwave results suggest that benign lesions show less (i.e., <200 kPa) elasticity while cancers reach high levels (upto 300 kPa). Shearwave elastography has shown superiority as compared to B-mode ultrasound and mammogram in determining the nature of the breast lesions. It has shown high sensitivity in BIRAD 3 and 4 lesions to downgrade and helps in making accurate diagnosis. It has also shown potential in predicting response of neoadjuvant chemotherapy.

**Keywords:** breast shearwave elastography, scoring system, breast radiology, ultrasound, breast cancer imaging

## 1. Introduction

All the tissues of the body have some elasticity due to presence of variable amount of elastic tissue. Pathological insult of the tissues causes change in tissue architecture by disturbing elastic tissue proportion. These pathological insults invariably include chronic inflammatory conditions and cancers as well. Thus the physical examination of the body to make idea of the tissue architecture was the fundamental part of the diagnosis making from the ancient period. Palpation was the sole method of diagnosis in ancient period dates back to more than 5000 years ago during the era of Pharaoh. With advancements in technology, different modes of assessment have been introduced in clinical practice notably imaging techniques. Ultrasound and X-rays are the most commonly used economical, non-invasive and highly reliable techniques in clinical practice. Measurement of the stiffness is quite

old method, the same principal was followed by elastography which measures tissue stiffness and displays it in the output window. Initially strain elastography was introduced where tissue was displaced by applying pressure on tissue by using probe [1].

Shearwave elastography (SWE) is a relatively new (i.e., 2003) advancement of the ultrasound system which uses ultrafast shearwaves for assessment of elasticity of the tissue by using acoustic radiation force excitation and displays in real time [2]. Shearwave elastography has been used in combination with B-mode ultrasound in order to enhance its diagnostic accuracy. A number of studies have been conducted till date showing role of elastography notably assessment of liver fibrosis in chronic hepatitis patients, assessment of thyroid and breast lesions. In all organs it has shown its superiority than conventional B-mode ultrasound in determining the nature of the lesions. In breast diseases it has been studied for its role not only in differentiating benign and malignant lesions, but also investigated in predicting response to neoadjuvant chemotherapy in locally advanced breast cancers. The diagnostic significance of SWE has been studied since its introduction in clinical practice; nevertheless many aspects are still under investigation. In addition, most of the research works done till date has investigated its role in diagnostics; however its role in screening has not been studied yet. This book chapters looks at the basic mechanism of the shearwave elastography, technique of using shearwave elastography in breast, its clinical application in differentiating benign and malignant breast lesions.

## 2. Mechanism/physics of shearwave elastography

Shearwaves are ultrafast mechanical waves whose propagation is measured while it passes through tissues. The movement of the waves is influenced by the stiffness of the concerned tissue. The mechanism of the shearwaves follows Young's modulus, which has capability to assess difference in the characteristics of different biological tissues and secondly it quantitatively presents tissue stiffness [1]. This reproduction of the stiffness corresponds the palpation of the tissue on clinical examination.

The shearwave elastography is based on two mechanisms including a Mach cone, where different spherical waves in single plane make a Mach cone which allows propagation and rebuilding map of Young's modulus. Secondly the ultrafast mode allows up to 5000–30,000 frames per second depending on the nature of the tissue. In situations of smooth propagation of the waves the real time image generated tends to be clear and homogenous while the areas of stiff tissues show disturbances in the traveling and show high intensity colors with heterogeneous echo pattern. In the areas of extreme hardness the waves do not propagate at all resulting in back area known as *signal void area* or *punched out lesions*. The technique is implanted in Aixplorer (Supersonic Imagine, Aix-en-Province, France) equipment [1]. The equipment has wide acceptance for assessment of liver fibrosis stage in chronic hepatitis patients where this has largely replaced biopsy. However, for breast tissue it has not yet achieved due popularity among clinicians.

## 3. Elasticity differences of normal and pathological breast tissues

As the normal understanding the elasticity of the tissue varies with the disease progression. The particular diseases like chronic inflammation and cancers have higher tendency to show higher level of stiffness. It is also a general concept that

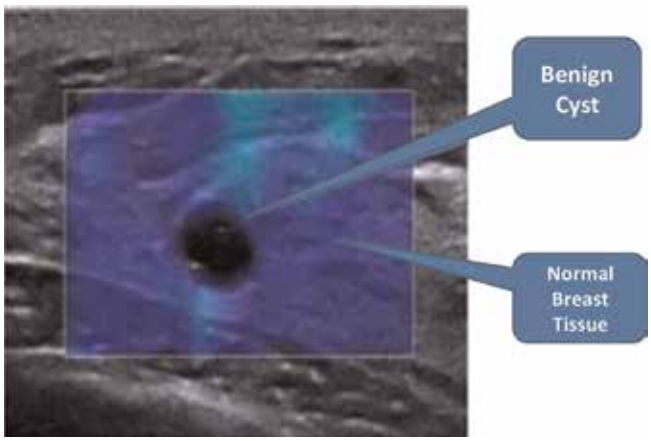


**Figure 1.**
*Qualitative appearance of normal breast tissue and benign cyst on shearwave elastography.*

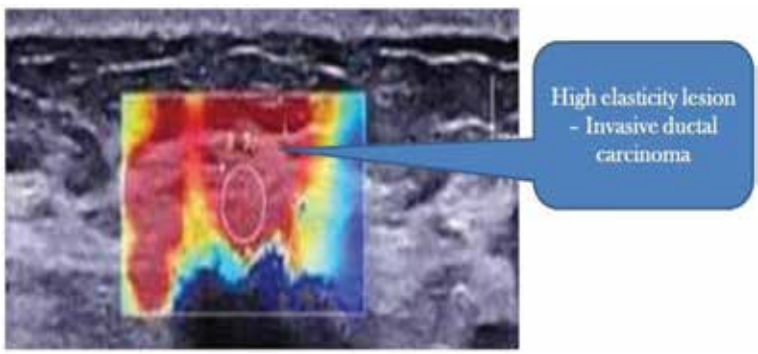


**Figure 2.**
*Invasive ductal carcinoma breast appearance on shearwave elastography.*

the cancers tend to be harder than the normal tissue and the benign lesions (**Figures 1** and **2**). Although it is not applicable in all situations as some benign conditions show harder consistency such as a cyst and some cancers show soft consistency like mucinous type. The study conducted on normal tissue showing the soft consistency with averagely blue color on qualitative assessment and normal tissue elasticity of the breast reported to be 30.68 ± 9.11 kPa in the four quadrants while in the nipple areola it was 31.35 kPa [3]. The stiffness shows negative relationship with the age of the patients. As the age advances in particular older women the breast parenchyma is largely replaced by fat. Fat is naturally much softer than the breast parenchyma thus understandably elasticity reduces. In contrast younger patients have more breast parenchyma and firmer breast thus relatively higher elasticity, though within limits of the normal range.

## 4. Breast shearwave probe and technique

A linear array probe with maximum frequency of 12–14 MHz is used for breast elastography (**Figure 3**). Technique of applying SWE is crucial. The application of probe for SWE is just to place it on the skin, no additional pressure is required. In the experience of the author if pressure is applied on breast tissues it causes false positive results. Thus just placing the probe and holding it perpendicular to the skin

**Figure 3.**
*Linear-array probe used for breast shearwave elastography.*

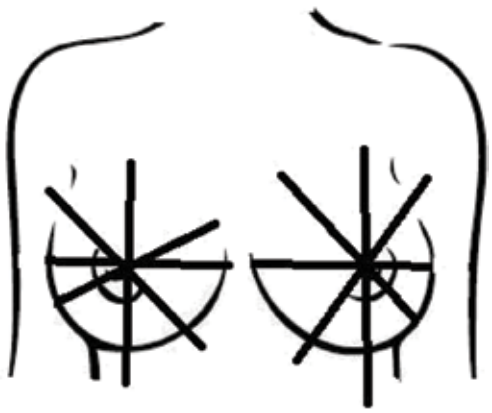

**Figure 4.**
*Clockwise fashion of assessing breast by shearwave elastography.*

is just appropriate. However, in deep seated lesions minimal compression may be applied without putting unnecessary pressure on the tumor.

The first stage and important stage is to get good quality homogenous B-mode images. The B-mode provides basis for generation of the SWE. Placing the probe parallel to the duct then moving it in clock wise fashion in all quadrants of the breast allows superficial assessment of whole breast (**Figure 4**). This is the general screening. In case if there is any lesion visible then detailed examination of the lesion is to be done in addition to the general assessment. The initial qualitative assessment is done followed by application of ROI for measurement of the elasticity.

## 5. Reliability of SWE as imaging modality in breast

### 5.1 SWE differentiating benign and malignant breast lesions

Since SWE was brought in clinical practice a number of studies have been conducted on its reliability and compared it with the conventional modes of imaging including ultrasound and mammograms. In addition to individual studies a number of meta-analysis has also been done [4–6]. Invariably all the studies showed superiority of SWE over ultrasound and mammograms alone in particular BIRAD 3 and 4 cases. However, SWE did not differentiate among molecular classes of breast cancer, though higher grades were associated with high elasticity [7]. Another study compared ultrasound and combined ultrasound with SWE to differentiate mastitis and malignancy. With addition of SWE specificity was increased from 11.5 to 96% [8].

There were studies available to suggest that SWE stiffness of the breast cancer has been linked with prediction of the poor survival [9, 10]. The harder the tumor, the poorer the survival. This can be biologically explained by having hard aggressive tumors with high grades and solid consistency resulting in poor survival [11]. A

| S. No | Author | Name of journal | Year of publication | Sample size | Conclusion |
|---|---|---|---|---|---|
| 1 | Doria [12] | European Journal of Radiology | 2019 | 396 | Malignant and benign breast lesions show significant difference in elasticity on SWE. Application of SWE reduces the rate of false positives by 25% in general while for BIRAD category four false negative rate was reduced by 54% |
| 2 | Choi [13] | British Journal of Radiology | 2019 | 428 | Combined approach with B-mode ultrasound and SWE significantly enhance diagnostic accuracy even in smaller tumors (≤2 cm) |
| 3 | Zhang [14] | Breast Cancer Research and Treatment | 2019 | 458 | BIRAD category four lesions were evaluated on B-mode Ultrasound and SWE. 90% were downgraded by SWE |
| 4 | Lin [15] | Cancer Management Research | 2018 | 2273 | Multi-center study compared B-mode ultrasound and SWE and compared with histopathology. SWE was superior in making diagnosis on BIRAD 3 and 4 category |
| 5 | Song [9] | Clinical Imaging | 2018 | 209 | Breast lesions were compared on B-mode with and without SWE. The addition of SWE improved specificity from 17 to 98% |
| 6 | Wang [16] | Ultrasound in Medicine and Biology | 2017 | 126 | Addition of SWE to conventional B-mode increases sensitivity and specificity in BIRAD 3 and 4 lesions |
| 7 | Choi [17] | European Radiology | 2016 | 116 | Non palpable breast lesions were evaluated. Addition of SWE increases sensitivity and specificity of diagnosis and differentiating benign and malignant non palpable breast lesions |
| 8 | Kim [18] | Medicine | 2015 | 177 | Addition of SWE to B-mode increases diagnostic accuracy in BIRAD 4 category |
| 9 | Lee [19] | European Journal of Radiology | 2015 | 140 | Complex cystic and solid masses showed that addition of SWE increases the chance of accurate diagnosis in BIRAD 3 and 4 category |
| 10 | Youk [20] | Ultrasound in Medicine and Biology | 2014 | 79 | Addition of SE or SWE improved the diagnostic performance of B-mode US, potentially reducing unnecessary biopsies |
| 11 | Kilic [21] | Journal of Breast Cancer | 2014 | 1 (a case report) | DCIS was detected within the fibroadenoma |
| 12 | Lee [22] | Radiology | 2014 | 159 | Shearwave increases sensitivity and specificity of US |
| 13 | Klotz [23] | Diagnostic and Interventional Imaging | 2014 | 167 | Shearwave elastography improves outcome of ultrasound |
| 14 | Zhou [24] | Radiology | 2014 | 137 | Addition of shearwave with stiff rim setting makes differentiation of the tumors better |
| 15 | Park [25] | Ultrasound in Medicine and Biology | 2014 | 64 | Excellent reproducibility |
| 16 | Mullen [26] | Clinical Radiology | 2014 | 86 | In smaller tumors ≤15 cm in size addition of the peri-tumoral rim on SWE in addition to the grayscale measurement make better comparability with the pathological size of the cancer |

| S. No | Author | Name of journal | Year of publication | Sample size | Conclusion |
|---|---|---|---|---|---|
| 17 | Cebi Olgun [27] | Diagnostic and Interventional Imaging | 2014 | 115 | Provides additional valuable quantitative information |
| 18 | Choi [11] | Ultrasound in Medicine and Biology | 2014 | 116 | Shearwave elastography correlated with the grade and stiffness |

**Table 1.**
*Summary of the studies evaluating role of shearwave elastography in differentiating benign and malignant lesions of the breast.*

summary of the studies reporting on role of SWE in differentiating benign and malignant lesions is given in **Table 1**.

## 5.2 SWE predicting response to neo-adjuvant chemotherapy in locally advanced breast cancer

Shearwave elastography was evaluated to assess its potential role in predicting response to chemotherapy in a number of studies (**Table 2**). Each tumor has cellular component and the tumor stroma. When there is compact cellular component the tumor tend to show hardness which appears as high elasticity on SWE. While with the action of the chemotherapy; cells start to die and there comes softness which appears as reduction in elasticity of the tumors. Those tumors show response to chemotherapy present with reduced stiffness earlier in the course of treatment (**Table 2**). Thus invariably all the studies showed that those tumor showing pathological complete response have also shown reduction in the elasticity on SWE earlier [33].

| S. No | Author | Name of journal | Year of publication | Sample size | Conclusion |
|---|---|---|---|---|---|
| 1 | Evan [28] | Clinical Radiology | 2018 | 80 | Out of 80 patients 26% achieved pathological complete response, which was assessed by reduction in elasticity of the cancer on SWE |
| 2 | Wang [29] | British Journal of Radiology | 2018 | Mouse model | Xenograph mouse models were used. Results showed reduced elasticity of the tumors achieving clinical benefit. This reduction was picked up by SWE |
| 3 | Jing [30] | Journal of Ultrasound in Medicine | 2016 | 62 | After 2 cycles of neoadjuvant chemotherapy and results showed that the tumors achieving clinical benefit showed reduction in the elasticity with 2 cycles |
| 4 | Chamming's [31] | Ultrasound in Medicine and Biology | 2016 | Mouse model | Xenograph mouse models were used. The SWE evaluation showed significant reduction in tumor stiffness after chemotherapy |
| 5 | Lee[32] | Annals of Surgical Oncology | 2015 | 71 | The response areas showed reduction in the elasticity while the areas of higher stiffness were corresponding areas with the residual tumors |

**Table 2.**
*Summary of the studies showing role of shearwave elastography in predicting response to neoadjuvant chemotherapy in locally advanced breast cancer.*

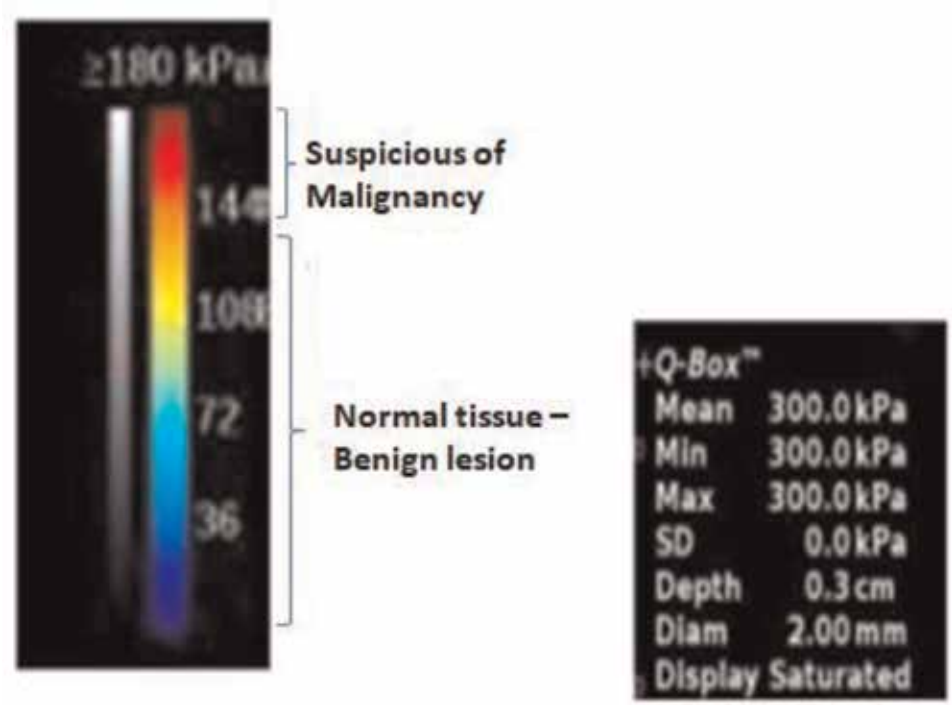


**Figure 5.**
*Qualitative parameter (a) and quantitative parameters (b) of breast lesion assessment on shearwave elastography.*

## 6. Reporting of breast SWE

The probe needs to be placed very gently on the breast without application of any pressure. For breast evaluation clockwise 12 measurements have to be taken. The reporting is to be done by using qualitative as well as quantitative findings of the breast tissue including color of the tissue and maximum elasticity values (**Figure 5a** and **b**). If there is any additional finding such as signal void area then it has to be described along with its location in the breast. The ROI is placed in all the areas with maximum elasticity level are to be taken into account. The size of the ROI is to be adjusted according to the size of the tumor and the proportion of the heterogeneous tissue including hard and soft parts. The cancers show more heterogeneity then the benign lesions. Thus the highest elasticity is taken as well as reading from heterogenous area to take the ratio of the low elasticity and high elasticity. The breast areas are to be reported followed by the detailed report of the lesion. The specific area report should include color, elasticity and the presence of signal void area.

## 7. Interpretation of shearwave elastography

Shearwaves are ultra-fast waves generated by acoustic force radiation travel transversely into the tissues and display output in qualitative and quantitative mode. The qualitative outcome is displayed in the form of color change that ranges from dark blue (i.e., normal tissue) to yellow, orange (i.e., benign) and finally red and dark red (i.e., malignancy) (**Figures 5a, 6–9**). The corresponding quantitative measurement ranges from 0 to 300 (**Figure 5b**). The tissue elasticity of the breast

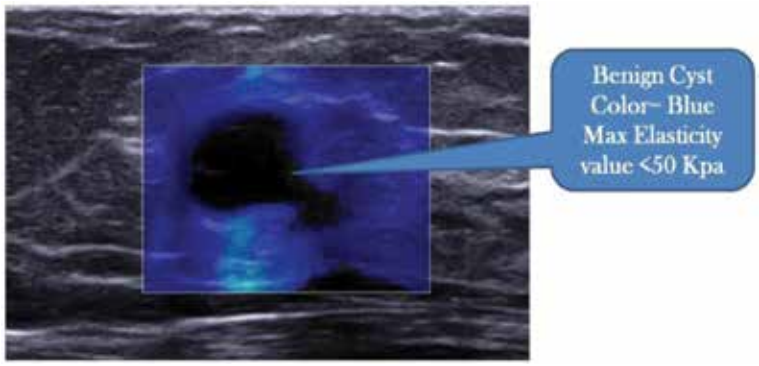


**Figure 6.**
*Benign breast cyst on shearwave elastography.*

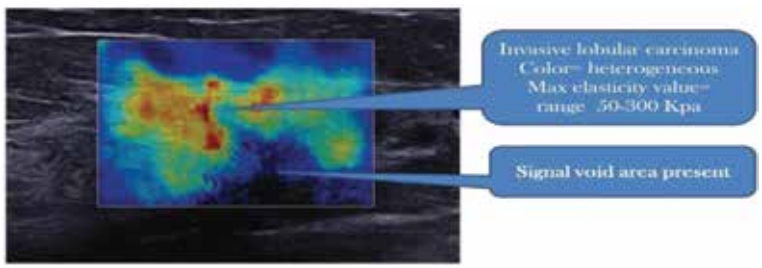


**Figure 7.**
*Invasive lobular carcinoma appearance on shearwave elastography.*

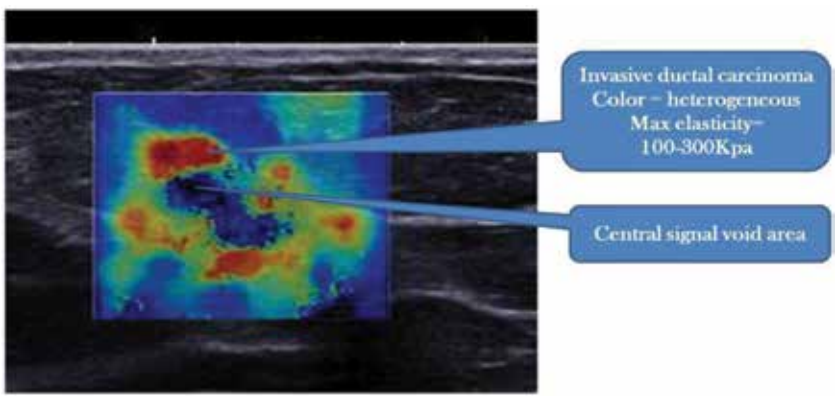


**Figure 8.**
*Invasive ductal carcinoma appearance with signal void area on shearwave elastography.*

showed negative correlation with the age i.e., as the age advances the tissue elasticity reduces [3]. This can be explained by natural evolution of the breast where with advancing age breast parenchyma replaced by fat tissue. This should always be borne in mind that high resolution good quality images can only be interpreted. In case if there is so much of background noise and the images are not giving a clear description it's better to avoid interpretation of such images. In this regard the best approach is to do a combine approach with B-mode first. With the B-mode imaging identify the lesion and its characteristics then SWE be applied on the lesion in order to avoid influence of artifacts.

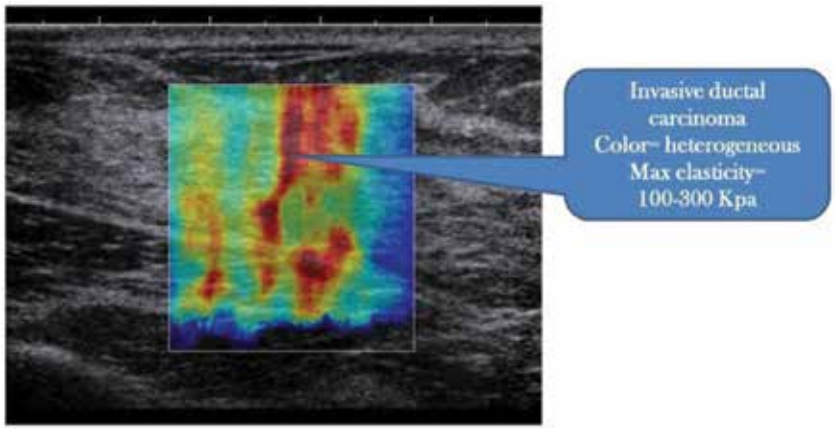


**Figure 9.**
*Invasive ductal carcinoma appearance on shearwave elastography—without signal void area.*

As the elasticity increases the kilopascal measurements also rises. However, in certain situations where intrinsic factors of the tumor show false negative results such as in situ cancers. While age of the patients, high risk lesions, tumors closer to the chest wall or overlying skin or deep seated tumors were likely to develop false positives results [13]. The study including 428 smaller tumor (≤2 cm) compared conventional B-mode ultrasound with SWE combined approach. The results showed that SWE combined approach was superior than B-mode alone, however in situ cancers showed false negative results [13]. Another study showed that presence of in situ tumor, calcifications and tumors near the nipple are likely to produce inaccurate results [34]. The study was conducted on non-palpable breast lesions including 79 malignant and 73 benign breast lesions. The smaller size of the lesion was also associated with inaccurate results in the study [34]. The inaccuracies in SWE interpretation could be explained by the nature of the lesion such as the case of in situ cancers, which has not yet produced that high reaction of the surrounding peri-tumoral tissue. The age of the patient and the location of the tumor potentially have influence of the breast tissue elasticity. The study including 1137 tumors to differentiate characteristics of the types of breast cancers on SWE. There was no characteristic difference in different histological types of cancers with exception of tubular type which showed less elasticity [35]. The fibroadenomas on the other hand show false positive expression if they were larger in size [36]. Interestingly lobular carcinoma has potential to display itself as benign or probably benign on B-mode ultrasound or mammogram but SWE showed higher rate of picking up lobular cancers [37].

The characteristics of the benign and malignant lesions were evaluated in a prospective cross-sectional study including 119 women. These patients underwent clinical breast examination, followed by conventional ultrasound then SWE and finally ultrasound guided tissue biopsy. The results showed that the benign lesions tend to be oval or round in shape with homogenous echopattern. Their color ranges from blue to yellow and green but reasonably homogenous with low elasticity. On the other hand malignant lesions were in contrast with irregular margins, heterogeneous echopattern and color from red to dark red in correlation with high elasticity [38].

The debatable issue lies with SWE is the operator dependency which is attached to B-mode ultrasound by default. The application of the probe is crucial with dependency on the operator; however there is less influence on the results if the technique of the probe application is correct.

In this regard, a study compared an operator with 15 years experience with that having 1 year [39]. The reproducibility of the results was high with SWE showing

less dependency on operator experience for interpretation, while intra-observer reproducibility has been reported to be 0.789 on SWE [25].

There are a number of parameters which could be utilized for interpretation such as mean elasticity value, minimum elasticity value and maximum elasticity. Most of the studies showed maximum elasticity value in kilopascals as the most reliable to be considered. However, all parameters need to be observed in cases of highly heterogeneous cancers.

## 8. Breast lesion scoring system

The authors have developed a scoring system for better diagnostic yield of shearwave elastography by combining qualitative and quantitative characteristics of the breast lesions. The scoring system takes into account the change of color, quantitative measurement of stiffness in kilopascals (kPa) and presence or absence of the signal void area (i.e., punched out lesion). A summary of the scoring system is given in **Table 3**.

Hard solid tumors showed dark color on qualitative measure, while benign soft tumors show natural color including blue, yellow orange. Normal breast tissue is blue in color. Fibrocystic lesion change color from blue to yellow or even orange but none of the benign lesions turn dark red. Similarly all the malignant lesion were red in different shades. Quantitative measurement of the kPa of benign lesions was low with less stiffness while solid tumor and cancers show score >200. Dark red color on qualitative scale and >250 kPa was invariably seen in cancers. When the cancer gets really hard and shear waves fail to penetrate resulting in signal void area punched out lesion. There was an exception of breast abscess which also showed signal void area due to cavity. The differing point of the breast abscess and the malignant breast lesion was based on color and mean kPa score while signal void area was seen in majority of both cases. **Figures 10–12** portray the breast lesion from benign to malignant pathologies.

| Parameter | Score 1 | Score 2 | Score 3 |
|---|---|---|---|
| Color | Blue, yellow, orange | Red, dark red | Dark red |
| Mean kPa range | <200 | >200 but <250 | >250 |
| Punched out lesion status | Absent | Present | May be present |

**Table 3.**
*Scoring system to interpret Shearwave elastography findings of breast lesions.*

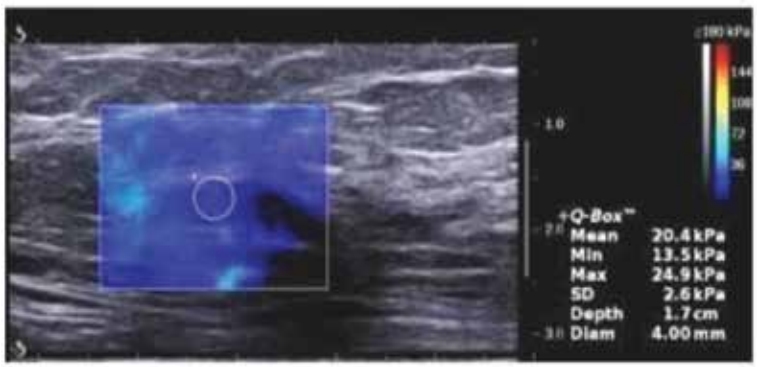


**Figure 10.**
*Benign breast disease on shearwave elastography.*

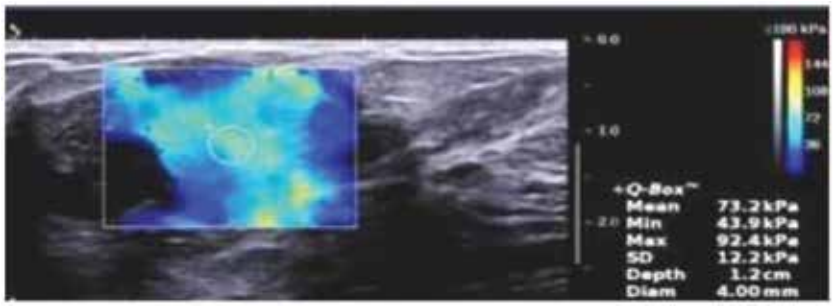


**Figure 11.**
*Fibrocystic disease on shearwave elastography.*

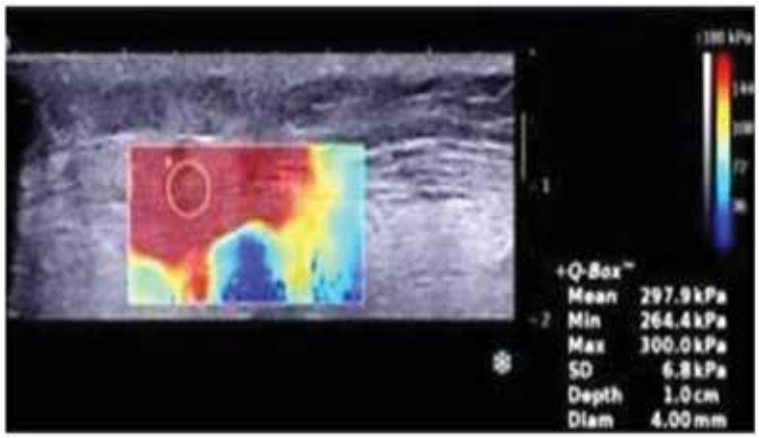


**Figure 12.**
*Invasive ductal carcinoma of breast on shearwave elastography.*

## 9. Conclusion

Shearwave elastography is a new advanced technique with ultrafast mode of shearwaves to assess elasticity of the tissue. It has established role in assessment of the liver fibrosis. The available literature favors use of shearwave elastography in combination with B-mode ultrasound to enhance diagnostic accuracy of the conventional ultrasound. However, it has not been widely used in clinical practice. Though it has shown great potential in differentiating BIRAD 3 and 4 categories and successfully avoiding negative biopsies.

## Author details

Binafsha Manzoor Syed[1*], Jawaid Naeem Qureshi[2] and Bikha Ram Devrajani[3]

1 Medical Research Center, Liaquat University of Medical and Health Sciences, Jamshoro, Pakistan

2 Department of Surgery, Indus Medical College, Tando Mohammad Khan, Pakistan

3 Department of Medicine, Liaquat University of Medical and Health Sciences, Jamshoro, Pakistan

*Address all correspondence to: drbinafsha@hotmail.com

## References

[1] Gennisson JL, Deffieux T, Fink M, Tanter M. Ultrasound elastography: Principles and techniques. Diagnostic and Interventional Imaging. 2013;**94**(5): 487-495

[2] Nakashima K, Shiina T, Sakurai M, Enokido K, Endo T, Tsunoda H, et al. JSUM ultrasound elastography practice guidelines: Breast. Journal of Medical Ultrasonics. 2013;**40**(4):359-391

[3] Sendur HN, Gultekin S, Salimli L, Cindil E, Cerit M, Sendur AB. Determination of normal breast and areolar skin elasticity using shear wave elastography. Journal of Ultrasound in Medicine. Jul 2019;**38**(7):1815-1822. DOI: 10.1002/jum.14877. Epub 2018 Nov 25

[4] Huang R, Jiang L, Xu Y, Gong Y, Ran H, Wang Z, et al. Comparative diagnostic accuracy of contrast-enhanced ultrasound and shear wave elastography in differentiating benign and malignant lesions: A network meta-analysis. Frontiers in Oncology. 2019;**9**:102

[5] Luo J, Cao Y, Nian W, Zeng X, Zhang H, Yue Y, et al. Benefit of shear-wave elastography in the differential diagnosis of breast lesion: A diagnostic meta-analysis. Medical Ultrasonography. 2018;**1**(1):43-49

[6] Xue Y, Yao S, Li X, Zhang H. Value of shear wave elastography in discriminating malignant and benign breast lesions: A meta-analysis. Medicine. 2017;**96**(42):e7412

[7] Ganau S, Andreu FJ, Escribano F, Martin A, Tortajada L, Villajos M, et al. Shear-wave elastography and immunohistochemical profiles in invasive breast cancer: Evaluation of maximum and mean elasticity values. European Journal of Radiology. 2015;**84**(4):617-622

[8] Liu SQ, Liu YP, Zhou BG, Deng XH, Li XL, Xiang LH, et al. Two-dimensional shear wave elastography for differential diagnosis between mastitis and breast malignancy. Clinical Hemorheology and Microcirculation. 2018;**70**(3):347-354

[9] Song EJ, Sohn YM, Seo M. Diagnostic performances of shear-wave elastography and B-mode ultrasound to differentiate benign and malignant breast lesions: The emphasis on the cutoff value of qualitative and quantitative parameters. Clinical Imaging. 2018;**50**:302-307

[10] Evans A, Sim YT, Pourreyron C, Thompson A, Jordan L, Fleming D, et al. Pre-operative stromal stiffness measured by shear wave elastography is independently associated with breast cancer-specific survival. Breast Cancer Research and Treatment. 2018;**171**(2): 383-389

[11] Choi WJ, Kim HH, Cha JH, Shin HJ, Kim H, Chae EY, et al. Predicting prognostic factors of breast cancer using shear wave elastography. Ultrasound in Medicine and Biology. 2014;**40**(2): 269-274

[12] Doria MT, Jales RM, Conz L, Derchain SFM, Sarian LOZ. Diagnostic accuracy of shear wave elastography—Virtual touch™ imaging quantification in the evaluation of breast masses: Impact on ultrasonography's specificity and its ultimate clinical benefit. European Journal of Radiology. 2019; **113**:74-80

[13] Choi HY, Seo M, Sohn YM, Hwang JH, Song EJ, Min SY, et al. Shear wave elastography for the diagnosis of small (≦2 cm) breast lesions: Added value and factors associated with false results. The British Journal of Radiology. 2019; **92**(1097):20180341

[14] Zhang Q, Song S, Xiao Y, Chen S, Shi J, Zheng H. Dual-mode artificially-intelligent diagnosis of breast tumours in shear-wave elastography and B-mode

ultrasound using deep polynomial networks. Medical Engineering and Physics. 2019;**64**:1-6

[15] Lin X, Chang C, Wu C, Chen Q, Peng Y, Luo B, et al. Confirmed value of shear wave elastography for ultrasound characterization of breast masses using a conservative approach in Chinese women: A large-size prospective multicenter trial. Cancer Management and Research. 2018;**10**:4447-4458

[16] Wang M, Yang Z, Liu C, Yan J, Zhang W, Sun J, et al. Differential diagnosis of breast category 3 and 4 nodules through BI-RADS classification in conjunction with shear wave elastography. Ultrasound in Medicine and Biology. 2017;**43**(3):601-606

[17] Choi JS, Han BK, Ko EY, Ko ES, Shin JH, Kim GR. Additional diagnostic value of shear-wave elastography and color doppler US for evaluation of breast non-mass lesions detected at B-mode US. European Radiology. 2016;**26**(10): 3542-3549

[18] Kim SJ, Ko KH, Jung HK, Kim H. Shear wave elastography: Is it a valuable additive method to conventional ultrasound for the diagnosis of small (≦2 cm) breast cancer? Medicine. 2015; **94**(42):e1540

[19] Lee BE, Chung J, Cha ES, Lee JE, Kim JH. Role of shear-wave elastography (SWE) in complex cystic and solid breast lesions in comparison with conventional ultrasound. European Journal of Radiology. 2015;**84**(7): 1236-1241

[20] Youk JH, Son EJ, Gweon HM, Kim H, Park YJ, Kim JA. Comparison of strain and shear wave elastography for the differentiation of benign from malignant breast lesions, combined with B-mode ultrasonography: Qualitative and quantitative assessments. Ultrasound in Medicine and Biology. 2014;**40**(10):2336-2344

[21] Kilic F, Ustabasioglu FE, Samanci C, Bas A, Velidedeoglu M, Kilicaslan T, et al. Ductal carcinoma in situ detected by shear wave elastography within a fibroadenoma. Journal of Breast Cancer. 2014;**17**(2):180-183

[22] Lee SH, Chang JM, Kim WH, Bae MS, Seo M, Koo HR, et al. Added value of shear-wave elastography for evaluation of breast masses detected with screening US imaging. Radiology. 2014;**273**(1):61-69

[23] Klotz T, Boussion V, Kwiatkowski F, Dieu-de Fraissinette V, Bailly-Glatre A, Lemery S, et al. Shear wave elastography contribution in ultrasound diagnosis management of breast lesions. Diagnostic and Interventional Imaging. 2014;**95**(9):813-824

[24] Zhou J, Zhan W, Chang C, Zhang X, Jia Y, Dong Y, et al. Breast lesions: Evaluation with shear wave elastography, with special emphasis on the "stiff rim" sign. Radiology. 2014; **272**(1):63-72

[25] Park HY, Han KH, Yoon JH, Moon HJ, Kim MJ, Kim EK. Intra-observer reproducibility and diagnostic performance of breast shear-wave elastography in Asian women. Ultrasound in Medicine and Biology. 2014;**40**(6):1058-1064

[26] Mullen R, Thompson JM, Moussa O, Vinnicombe S, Evans A. Shear-wave elastography contributes to accurate tumour size estimation when assessing small breast cancers. Clinical Radiology. 2014;**69**(12):1259-1263

[27] Cebi Olgun D, Korkmazer B, Kilic F, Dikici AS, Velidedeoglu M, Aydogan F, et al. Use of shear wave elastography to differentiate benign and malignant breast lesions. Diagnostic and Interventional Radiology. 2014;**20**(3):239-244

[28] Evans A, Whelehan P, Thompson A, Purdie C, Jordan L, Macaskill J, et al.

Identification of pathological complete response after neoadjuvant chemotherapy for breast cancer: Comparison of greyscale ultrasound, shear wave elastography, and MRI. Clinical Radiology. 2018;**73**(10):910.e1-910.e6

[29] Wang JW, Guo ZX, Lin QG, Zheng W, Zhuang SL, Lin SY, et al. Ultrasound elastography as an imaging biomarker for detection of early tumor response to chemotherapy in a murine breast cancer model: A feasibility study. The British Journal of Radiology. 2018;**91**(1085): 20170698

[30] Jing H, Cheng W, Li ZY, Ying L, Wang QC, Wu T, et al. Early evaluation of relative changes in tumor stiffness by shear wave elastography predicts the response to neoadjuvant chemotherapy in patients with breast cancer. Journal of Ultrasound in Medicine. 2016;**35**(8): 1619-1627

[31] Chamming's F, Le-Frere-Belda MA, Latorre-Ossa H, Fitoussi V, Redheuil A, Assayag F, et al. Supersonic shear wave elastography of response to anti-cancer therapy in a xenograft tumor model. Ultrasound in Medicine and Biology. 2016;**42**(4):924-930

[32] Lee SH, Chang JM, Han W, Moon HG, Koo HR, Gweon HM, et al. Shear-wave elastography for the detection of residual breast cancer after neoadjuvant chemotherapy. Annals of Surgical Oncology. 2015;**22**(Suppl 3):S376-S384

[33] Evans A, Whelehan P, Thompson A, Purdie C, Jordan L, Macaskill J, et al. Prediction of pathological complete response to neoadjuvant chemotherapy for primary breast cancer comparing interim ultrasound, shear wave elastography and MRI. Ultraschall in der Medizin. 2018;**39**(4):422-431

[34] Park SY, Choi JS, Han BK, Ko EY, Ko ES. Shear wave elastography in the diagnosis of breast non-mass lesions: Factors associated with false negative and false positive results. European Radiology. 2017;**27**(9):3788-3798

[35] Evans A, Sim YT, Thomson K, Jordan L, Purdie C, Vinnicombe SJ. Shear wave elastography of breast cancer: Sensitivity according to histological type in a large cohort. Breast. 2016;**26**:115-118

[36] Elseedawy M, Whelehan P, Vinnicombe S, Thomson K, Evans A. Factors influencing the stiffness of fibroadenomas at shear wave elastography. Clinical Radiology. 2016; **71**(1):92-95

[37] Sim YT, Vinnicombe S, Whelehan P, Thomson K, Evans A. Value of shear-wave elastography in the diagnosis of symptomatic invasive lobular breast cancer. Clinical Radiology. 2015;**70**(6): 604-609

[38] Hari S, Paul SB, Vidyasagar R, Dhamija E, Adarsh AD, Thulkar S, et al. Breast mass characterization using shear wave elastography and ultrasound. Diagnostic and Interventional Imaging. 2018;**99**(11):699-707

[39] Aslan H, Pourbagher A, Ozen M. The role of shear-wave elastography in the differentiation of benign and malign non-mass lesions of the breast. Annali Italiani di Chirurgia. 2018;**89**:385-391

Section 3

# Other Application of Ultrasound Elastography

Chapter 9

# Pancreatic Elastography

*Lidia Ciobanu*

## Abstract

Pancreatic elastography represents a challenging new procedure for inflammatory pathology or tumour masses. There are technical difficulties for accurate assessment of pancreatic stiffness due to deep localization. But the new software for both conventional and endoscopic ultrasound are promising techniques for differential diagnosis between malignant tumours and different forms of chronic pancreatitis (groove pancreatitis or autoimmune pancreatitis). Early diagnosis of chronic pancreatitis, noninvasively by transabdominal shear wave elastography, is actively studied nowadays. Elastography might offer a predictive tool for the occurrence of pancreatic fistula after pancreatoduodenectomy. This chapter introduces the recent innovation of pancreatic elastography and makes recommendations for its use.

**Keywords:** pancreas, elastography, pancreatic cancer, chronic pancreatitis

## 1. Introduction

The pancreatic pathology assessment represents a challenge even today when many imaging techniques are available. The differentiation between chronic pancreatitis and malignant lesions requires sometimes many imaging combined procedures, even histology, without an accurate assessment. The elastography development used the principle that the assessment of a tissue elasticity of tissue might differentiate a benign soft lesion from a malignant hard tissue. But the stiffness assessment and measurement of this small organ, deeply localised in the retroperitoneum, are difficult. High accuracy and reproducibility of pancreatic elastography are not easily obtained, as the histology is not always available [1].

Nowadays both transabdominal ultrasound (US) and endoscopic ultrasound (EUS) allow pancreatic elastography assessment. There are two types of pancreatic elastography: strain elastography and shear wave speed elastography [1]. In the case of strain elastography, the stiffness of pancreatic tissue is estimated by measuring the grade of strain generated by external pressure. For shear speed elastography, the stiffness is estimated by measuring the propagation speed of the shear wave (the transverse wave) generated by acoustic radiation force impulse (ARFI) [1].

The results of elastography can be the strain, which has a negative correlation with tissue stiffness, and the shear wave speed, which has a positive correlation with tissue stiffness [2].

Elastography that measures shear wave speed is classified into shear wave elastography, which uses ARFI as the method to excite shear waves, and transient elastography, in which shear waves are excited in a mechanical manner. Fibroscan™, the only transient elastography device, is not used for the pancreas due to its localization [2]. Shear wave speed might be displayed by two different methods: as

the average speed within a small region (target ROI) and as an image reflecting the distribution of the speeds in the ROI [2].

## 2. Transabdominal ultrasound: strain elastography

The stiffness of pancreatic tissue is estimated through transabdominal ultrasound by measuring the grade of strain generated by aortic pulsation [1–4]. The relationship between the grade of strain and the stiffness of target tissue is negative correlation: the greater the strain, the softer pancreatic tissue is. For a proper assessment, the target tissue should be located in line between the probe and the aorta [1]. A fine elastogram can be easily obtained in the pancreatic body, except for the patients with severe arteriosclerosis. The elastograms obtained in the pancreatic head and tail should be interpreted with caution [1].

Strain elastography of the pancreas can be obtained with transabdominal ultrasound (US) and with EUS.

First clinical application of US elastography had been reported with real-time tissue elastography™ (RTE) produced by Hitachi Aloka [5, 6]. In the conventional RTE, only qualitative diagnosis using colour map was possible. This technique measures compression-induced tissue deformation (strain) within a region of interest (ROI), which is visualised using a transparent colour overlaying on the B-mode image. In this colour map, the hardest tissue is displayed as blue, and the softest tissue is displayed as red. In RTE, pancreatic cystic lesions cannot be evaluated, due to artefacts, when fluid component of cyst was assessed.

The first report of the usefulness of US elastography for the pancreas in clinical practice was published by Uchida et al. in 2009 [7]. They defined typical colour map observed in US-RTE for different clinical scenarios: homogeneous colour in normal pancreas, markedly hard area with soft spots, was in pancreatic ductal adenocarcinoma, uniform and soft comparable to parenchyma in neuroendocrine tumour and mixture of various colours in chronic pancreatitis. The same authors reported the 70–80% diagnostic accuracy for pancreatic tumours of B-mode alone; when B-mode was combined with US-RTE, the diagnostic accuracy was more than 90% [7].

This qualitative diagnosis using colour map was subjective and highly operator dependent; quantitative diagnosis using strain ratio was established since the second generation of RTE. Strain ratio was defined as the ratio of the strain of reference tissue (B) divided by the strain of target tissue (A).

Strain ratio was adapted from the theory called “fat lesion ratio” reported in the breast, which means the ratio of the strain of fat around the mammary gland divided by the strain of target tissue. The initial principal considered that the stiffness of fat was almost equal in different individuals [1]. To date no consensus exists for the reference area, on non-tumorous area inside the pancreatic parenchyma [8, 9] or on red area around the pancreas, estimated to be fat [10, 11]. There is no evidence if red area around pancreas is really fat. The strain ratios calculated for the same target tissue quite differ according to wherever the reference area is set [1].

The cutoff levels of strain ratio for differential diagnosis between malignant and benign varied in reported studies [9–11], meaning that pancreatic RTE is highly operator dependent and lacks adequate reproducibility.

A fine B-mode image is required for a fine elastogram, and this is obtained within 6 cm in depth from the body surface in US. Therefore, pancreatic elastogram is quite difficult in the obese. Also B-mode image is easily affected by gastrointestinal gas in US. These problems will occur less frequently in EUS.

Recommendations to obtain a quality elastogram on B-mode US [2]:

- The most important is to obtain a quality B-mode images with as few artefacts as possible.

- Examination is made from the epigastric fossa in a dorsal position, (semi) sitting position, or left lateral decubitus position.

- No vibration should be caused by the probe, which should lightly touch the abdominal wall.

- The patient should hold his breath.

- Two settings for ROI are accepted [12]: (1) ROI is set only within the target area; (2) ROI is set both within the target area and the surrounding tissue. The second is recommended for neoplastic cancer assessment.

- The colours in an elastogram minutely vary with the passage of time according to cardiovascular pulsation. It is desirable that elastograms with good reproducibility are taken at every pulsation by recording the images of elastograms in a range of 5–10 pulsations.

## 3. Transabdominal ultrasound: shear wave elastography

For this type of elastography, emission of ARFI is possible for the entire pancreas. Virtual Touch™ quantification (VTQ) produced by Siemens is a representative instrument. VTQ displays the stiffness of pancreatic tissue digitally shear wave velocity being measured. SWV is expressed in m/s. If an error occurs, X,XX m/s is displayed on the right part of the screen instead of digits [1].

Even if this technique is very promising for the pancreas, there are some issue to be considered. There is a limit to the acoustic radiation force impulse that is certainly safe within the body [2]. Also, when the tissue in the ROI is hard, measurement error tends to occur, because it is difficult to generate sufficient shear waves. When SWV of a pancreatic tumour cannot be assessed, ROI should be placed on a tip of the tumour [2]. If the target area is far from the probe, the attenuation of the focused ultrasound reduces the acoustic radiation force impulse, which in turn reduces the amplitude of the shear waves, making it difficult to detect the shear waves [12]. The safety standards are accomplished by the focused ultrasound [2], but the transmission waveform and wavelength are different from the usual ultrasonic pulses. A concern is represented by its influence on the body, through a possible increase in temperature [13]. Its safety in simultaneous use with contrast media is not confirmed yet [14].

It is recommended to repeat three times the same measurement for the same site about if the reproducibility is high. If the reproducibility is low, a measurement should be repeated 10 times for the same site and the median is used [2].

New ARFI software are developed (ElastPQ™ (Philips), Virtual Touch™ IQ: VTIQ (Siemens)), but their use for the pancreatic pathology is still limited.

Instead the Shear Wave™ Elastography (SWE) (Super Sonic Imaging) uses a new approach. In SWE, ultrasonic beams are continuously emitted to different depths in the tissue, and thus a conically shaped wave surface of shear waves is formed [2]. By an ultrafast imaging method, the shear wave speed is measured. The transducers repeat outgoing/incoming transmissions of ultrasonic waves. A colour map is displayed in the ROI, which can be defined in any location [2]. The mean ± SD, the minimum value, and the maximum value of the shear wave speed

in the ROI are displayed. A ratio is calculated when two ROIs in different locations are compared. The study conducted by Arda et al. [15] reported measurement of stiffness for normal pancreas: 11.1 ± 3.2 kPa for males and 10.8 ± 3.1 kPa for females.

## 4. Echo-endoscopy elastography: strain elastography

The first report of EUS elastography was published in 2005 by Hirooka et al. [5]. Then many papers reported their experience using RTE for pancreatic EUS elastography, being for many years the only system available. In RTE obtained by EUS, the diagnosis is qualitative. It is recommended that the ROI to be set to include peripancreatic tissue [2]. Red colour corresponds to the softest tissue within ROI, and blue corresponds to the hardest tissue within ROI. The remaining tissue is displayed as a coordinated colour between red and blue according to its stiffness. As the colour map depends on the size of ROI in RTE, it is not an absolute one [1].

Some technique aspects should be kept in mind for a qualitative elastogram [2]. The EUS probe should be lightly touching the wall of the stomach or the duodenum. The selected image must be without artefacts. The ultrasonic beam should be towards the aorta, and the strain should be generated in the depth direction. The RTE image should be stably generated for a certain period (5 s or longer in normal cases). For the evaluation of vibration energy, it would be preferable to refer to a strain indicator or to a strain graph. A good-quality B-mode image should be obtained to suit the RTE image [2].

The main debated issue was the differentiation of benign vs. malignant. The diagnostic criteria to differentiate malignancy from benignancy considered two aspects: (1) the dominant colour within colour map and (2) the homogeneity of colour map [1].

In a multicentre study on 121 patients with pancreatic tumours (92 malignant and 29 benign), Giovannini et al. [16] proposed a scoring system: score 1, homogeneous green represents normal tissue; score 2, heterogeneous soft tissue (green, yellow, and red) corresponds to inflammatory tissue; score 3, mixed colour or honeycombed can be attributed to any pathology; score 4, small green central area surrounded by mainly blue; and score 5, mainly blue with heterogeneous green and red, represents advanced malignant lesion. Scores 1 and 2 were considered benign, and scores 4 and 5 were assigned to malignant pathology. The sensitivity and specificity for this score were 92.3 and 80% [16].

The (semi) quantitative evaluation is possible, being more objective, but the analytical procedure is complicated. The image quantitative analysis reported included strain ratio [9, 10, 17], strain histogram [18, 19], and neural network [20–22]. A comparison between different analysis methods has not been conducted, so there is no consensus about which of these methods is the best.

## 5. Clinical applications for pancreatic elastography

Uchida et al. [7] published the first report evaluating the usefulness of US elastography for the pancreas in 2009. They reviewed elastograms performed for 10 normal pancreas and reported the typical colour map for normal pancreas assessed by RTE as homogeneous colour.

The normal reference values of pancreas stiffness using ARFI elastography through Virtual Touch Tissue Quantification (Siemens) were reported by Zaro et al. in 2016 [23]: from the entire parenchyma—1.216 m/s ± 0.36 (head, 1.224 m/s; body, 1.227 m/s; and tail, 1.191 m/s) [23]. Another study found a significant correlation

between increasing age and elastographic parameters [24]. Using SWE (Super Sonic Imaging) Arda et al. [15] reported measurement of stiffness for normal pancreas: 11.1 ± 3.2 kPa for males and 10.8 ± 3.1 kPa for females.

## 6. Benign vs. malignant mass pancreatic lesions

The most frequent use of elastography in pancreatic pathology is for differential diagnosis between benign and malignant focal lesions.

The number of reports on strain elastography with US is extremely small in comparison with EUS.

Uchida et al. [7] used strain elastography with US to evaluate the colour patterns of the pancreatic cancers, pancreatic endocrine tumours, and chronic pancreatitis. They concluded that adding strain elastography to the B-mode observations the

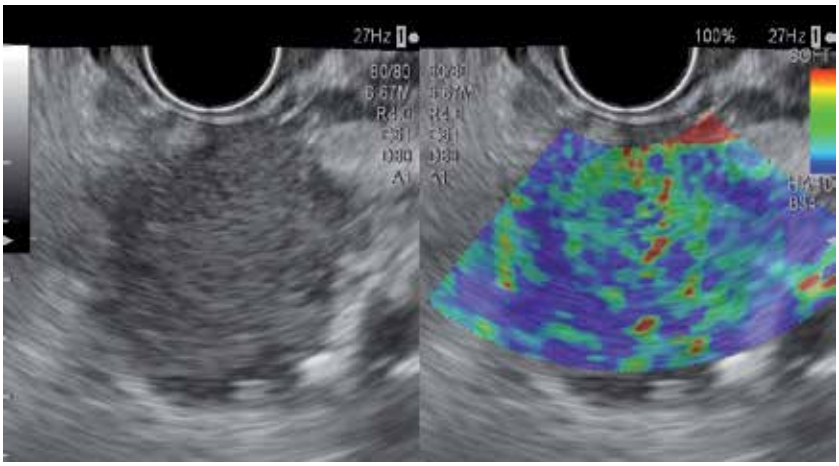


**Figure 1.**
*Advanced pancreatic adenocarcinoma assessed by EUS-RTE. Elastogram is mainly blue with heterogeneous green and red corresponding to score 5 from Giovannini classification.*

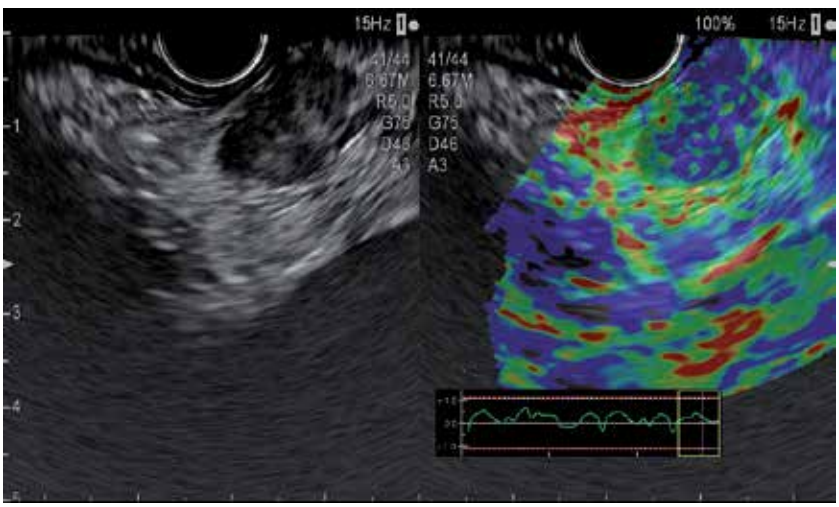


**Figure 2.**
*Small neuroendocrine tumour at the tail of the pancreas assessed by EUS-RTE. Elastogram depicts heterogeneous small points surrounded by mainly blue corresponding to score 4 from Giovannini classification.*

diagnosis sensitivity is improved [7]. Kawada et al. [8] reported the use of strain ratio to distinguish between malignancy and benignancy of pancreatic solid tumours. The evaluation of the pancreatic tumours by transabdominal shear wave elastography was reported by Zaro et al. [25] in a pilot studied. The mean SWV

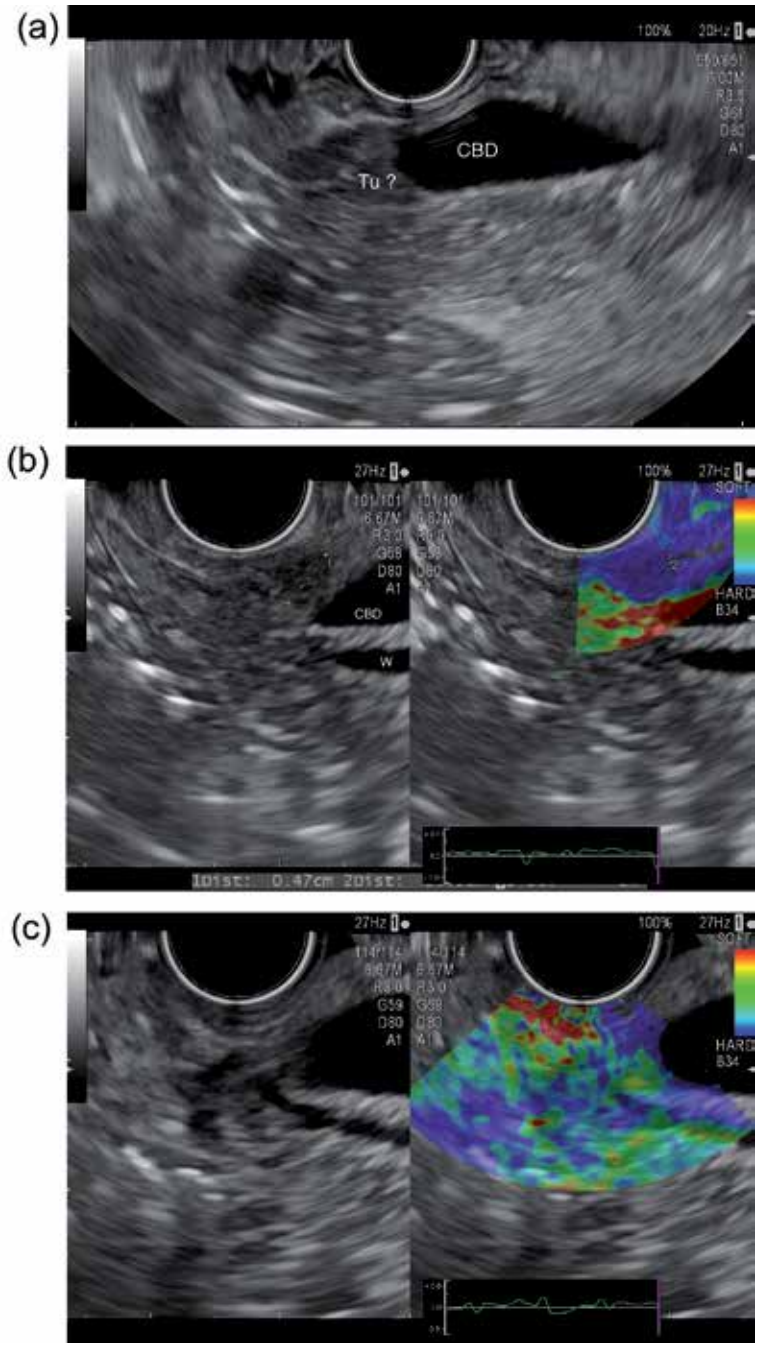


**Figure 3.**
*(a) EUS B-mode. Dilated common bile duct and suspicion of periampular tumour. (b) A "tumour-like image, suspected of malignancy" on elastogram, due to its blue (hard) appearance. This false elastogram is due to the angulations of distal tip of echo-endoscope. (c) A correct assessment of the stiffness of the ampular region displays a mixed inflamed tissue: heterogeneous soft tissue (green and red) corresponding to score 2 in Giovannini classification.*

of the pathological parenchyma indicated an increase of the SWV at the tumoral (cephalic) level corresponding to 1.54 ± 0.32 m/s compared to 1.21 ± 0.27 m/s for normal pancreas in the control group. Future research is needed to validate this data.

Most reports regarding EUS elastography for the pancreas are associated with the differential diagnosis between benign and malignant solid pancreatic tumours, being published several meta-analyses related to the differential diagnosis of pancreatic tumours [26, 27]. Elastograms for pancreatic adenocarcinoma and neuroendocrine tumours are displayed in **Figures 1** and **2**.

The sensitivity of EUS elastography for the differential diagnosis of pancreatic tumours is reported to be excellent ranging from 95 to 99%, while its specificity is reported to be inadequate ranging from 67 to 76% [1, 26, 27]. This low specificity is explained by the increased stiffness of benign nodule from chronic pancreatitis due to severe fibrosis. Fine needle aspiration through EUS is still mandatory even in cases with proper assessment of pancreatic tissue stiffness. There are few selective cases in which EUS-FNA cannot be performed, and the malignant diagnosis arguments include elastography [28]. But consensus criteria for differential diagnosis between malignant and benign pancreatic tumours were not established.

In clinical practice there are many challenging diagnosis. The images obtained with EUS elastography should be integrated in the clinical context of the patient, being complementary to other imaging techniques. Small tumour-like images, with suggestive malignant features at elastogram, should be interpreted with caution. To assess the quality and reproducibility of the elastography image, a consistent colour pattern obtained in a number of consecutive frames is indicated. If there are different elastograms obtained for the same tumour-like image (**Figure 3a**–**c**), all the technical adjustments should be rechecked.

## 7. Chronic pancreatitis

Chronic pancreatitis is frequently diagnosed in advance stages. Echo-endoscopy may be a useful method for the early diagnosis of chronic pancreatitis, even its diagnostic criteria are operator dependent.

Shear wave elastography using transabdominal US might be an objective and noninvasive method for the early diagnosis of pancreatic fibrosis. Yashima et al. [29] subjected 46 patients with chronic pancreatitis and 52 normal pancreas and measured SWV at the head, the body, and the tail of the pancreas for 10 times in each case and reported a sensitivity of 75% and a specificity of 72% for detection of chronic pancreatitis. They also determined the cutoff of SWV optimal for diagnosing chronic pancreatitis as 1.40 m/s by ROC analysis. Multivariate analysis detected that severe alcohol intake (OR = 3.87, p = 0.005) and deeper depth of the pancreas from the body surface ≥4.2 cm (OR = 0.10, p = 0.002) were associated with the stiffness of the pancreas (>1.40 m/s) [12]. Kuwahara et al. [30] reported that chronic pancreatitis might be diagnosed noninvasively and objectively using SW-EG without performing EUS, the diagnosis accuracy being 77%.

Many reports evaluated the accuracy of EUS elastography for the diagnosis of pancreatic fibrosis. An elastogram in a patient with chronic pancreatitis is displayed in **Figure 4**. Itoh et al. [18] performed EUS elastography preoperatively for the proximal side of the pancreatic tumour and compared the elastograms with microscopic findings of the resected specimens. They found significant correlation between objective parameters assessed by elastography (mean, standard deviation, skewness, kurtosis) and the grade of fibrosis evaluated by histology. Iglesias-Garcia

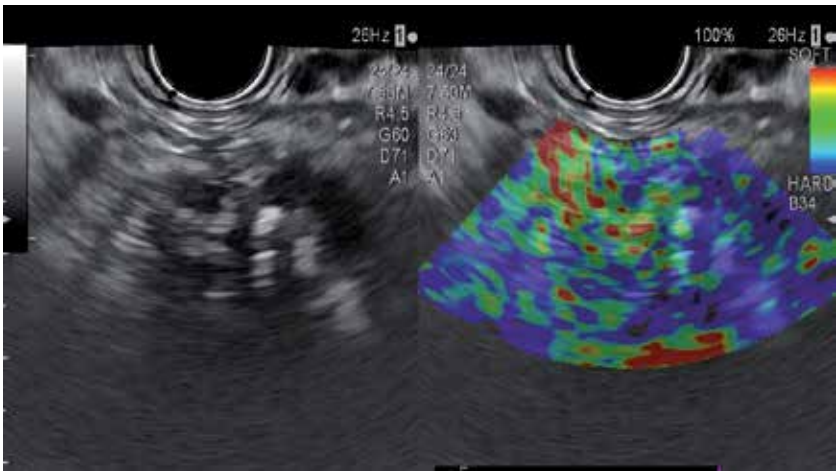


**Figure 4.**
*An elastogram of chronic pancreatitis: heterogeneous soft tissue (green, yellow, and red) corresponding to score 2 in Giovannini classification.*

et al. [31] reported a positive correlation between strain ratio and Rosemont classification ($r = 0.813$, $p < 0.0001$).

EUS elastography could predict pancreatic exocrine dysfunction in patients with chronic pancreatitis [32]. Iglesias-Garcia et al. [31] found significant correlation between strain ratio and pancreatic exocrine dysfunction evaluated by 13C-mixed triglyceride breath test.

In autoimmune pancreatitis the specific elastogram detected in five cases was homogenous stiffness of the whole organ, different from the circumscribed mass lesion in ductal adenocarcinoma [33].

## 8. Prediction of pancreatic fistula after pancreatic surgery

There are studies reporting that the stiffness of the pancreas measured preoperatively could predict the incidence of postoperative pancreatic juice fistula [34–36]. The postoperative fistula was observed more frequently in patients with lower stiffness of the pancreas (SWV < 1.54 m/s) than in patients with higher stiffness of the pancreas (63 vs. 17%, $p < 0.001$) [34].

## 9. Conclusions

The aim of pancreatic elastography for the pancreas is to reflect accurately the histological structure. The pancreatic elastography is challenging, as the access to this small organ is not easy, deep in the centre of the body. Also the biopsy specimens are difficult to obtain for direct comparison. Many of the challenges were resolved by the new technical achievements in the recent years. Both transabdominal US and EUS elastography might offer the clinicians an important tool for depiction of early chronic pancreatitis and a reliable tool for differential diagnosis between malignant and benign pancreatic masses.

## Author details

Lidia Ciobanu
Iuliu Hatieganu University of Medicine and Pharmacy, Regional Institute of Gastroenterology and Hepatology, Cluj-Napoca, Romania

*Address all correspondence to: ciobanulidia@yahoo.com

## References

[1] Kawada N, Tanaka S. Elastography for the pancreas: Current status and future perspective. World Journal of Gastroenterology. 14 Apr 2016;**22**(14):3712-3724

[2] Hirooka Y, Kuwahara T, Irisawa A, Itokawa F, Uchida H, Sasahira N, et al. JSUM ultrasound elastography practice guidelines: Pancreas. Journal of Medical Ultrasonics (2001). 2015;**42**:151-174. DOI: 10.1007/s10396-014-0571-7

[3] Shiina T, Doyley MM, Bamber JC. Strain imaging using combined RF and envelope autocorrelation processing. In: Proceeding of the 1996 IEEE Int Ultrasonics Symposium. San Antonio: IEEE; 1996. DOI: 10.1109/ULTSYM.1996.584292

[4] Shiina T, Yamakawa M, Nitta N. Recent prognosis of ultrasound elasticity imaging technology. International Congress Series. 2004;**1274**:59-63. DOI: 10.1016/j.ics.2004.07.054

[5] Hirooka Y, Itoh A, Hashimoto S. Utility of EIS: Elastography in the diagnosis of pancreatic diseases. Gastrointestinal Endoscopy. 2005;**61**:AB282. DOI: 10.1016/S0016-5107(05)01447-1

[6] Uchida H, Hirooka Y, Ito A, Hashimoto S, Kawashima H, Hara K, et al. Utility of elastography in the diagnosis of pancreatic diseases using transabdominal ultrasonography. Gastroenterology. 2005;**128**:A536

[7] Uchida H, Hirooka Y, Itoh A, Kawashima H, Hara K, Nonogaki K, et al. Feasibility of tissue elastography using transcutaneous ultrasonography for the diagnosis of pancreatic diseases. Pancreas. 2009;**38**:17-22. DOI: 10.1097/MPA.0b013e318184db78

[8] Kawada N, Tanaka S, Uehara H, Takakura R, Katayama K, Fukuda J, et al. Feasibility of second-generation transabdominal ultrasound-elastography to evaluate solid pancreatic tumors: Preliminary report of 36 cases. Pancreas. 2012;**41**:978-980. DOI: 10.1097/MPA.0b013e3182499b84

[9] Itokawa F, Itoi T, Sofuni A, Kurihara T, Tsuchiya T, Ishii K, et al. EUS elastography combined with the strain ratio of tissue elasticity for diagnosis of solid pancreatic masses. Journal of Gastroenterology. 2011;**46**:843-853. DOI: 10.1007/s00535-011-0399-5

[10] Iglesias-Garcia J, Larino-Noia J, Abdulkader I, Forteza J, Dominguez-Munoz JE. Quantitative endoscopic ultrasound elastography: An accurate method for the differentiation of solid pancreatic masses. Gastroenterology. 2010;**139**:1172-1180. DOI: 10.1053/j.gastro.2010.06.059

[11] Dawwas MF, Taha H, Leeds JS, Nayar MK, Oppong KW. Diagnostic accuracy of quantitative EUS elastography for discriminating malignant from benign solid pancreatic masses: A prospective, single-center study. Gastrointestinal Endoscopy. 2012;**76**:953-961. DOI: 10.1016/j.gie.2012.05.034

[12] Kawada N, Tanaka S, Uehara H, et al. Potential use of point shear wave elastography for the pancreas: A single center prospective study. European Journal of Radiology. 2014;**83**:620-624

[13] Herman BA, Harris GR. Models and regulatory considerations for transient temperature rise during diagnostic ultrasound pulses. Ultrasound in Medicine & Biology. 2002;**28**:1217-1224

[14] Barnett SB, Duck F, Ziskin M. Recommendations on the safe use of ultrasound contrast agents. Ultrasound in Medicine & Biology. 2007;**33**:173-174

[15] Arda K, Ciledag N, Aktas E, et al. Quantitative assessment of normal soft-tissue elasticity using shear-wave ultrasound elastography. AJR. American Journal of Roentgenology. 2011;**197**:532-536

[16] Giovannini M, Thomas B, Erwan B, Christian P, Fabrice C, Benjamin E, et al. Endoscopic ultrasound elastography for evaluation of lymph nodes and pancreatic masses: A multicentre study. World Journal of Gastroenterology. 2009;**15**:1587-1593. DOI: 10.3748/wjg.15.1587

[17] Mayerle J, Simon P, Dickson EJ, et al. The role of EUS guided elastography to diagnose solid pancreatic mass lesions. Pancreas. 2010;**39**:1334

[18] Itoh Y, Itoh A, Kawashima H, et al. Quantitative analysis of diagnosing pancreatic fibrosis using EUS-elastography (comparison with surgical specimens). Journal of Gastroenterology. 2014;**49**:1183-1192

[19] Janssen J, Papavassiliou I. Effect of aging and diffuse chronic pancreatitis on pancreas elasticity evaluated using semiquantitative EUS elastography. Ultraschall in der Medizin. 2014;**35**:253-258

[20] Saftoiu A, Vilmann P, Gorunescu F, et al. Accuracy of endoscopic ultrasound elastography used for differential diagnosis of focal pancreatic masses: A multicenter study. Endoscopy. 2011;**43**:596-603

[21] Saftoiu A, Vilman P, Gorunescu F, et al. Neural network analysis of dynamic sequences of EUS elastography used for the differential diagnosis of chronic pancreatitis and pancreatic cancer. Gastrointestinal Endoscopy. 2008;**68**:1086-1094

[22] Saftoiu A, Iordache S, Gheonea DI, et al. Combined contrast-enhanced power doppler and real-time sonoelastography performed during EUS, used in the differential diagnosis of focal pancreatic masses (with videos). Gastrointestinal Endoscopy. 2010;**72**:739-747

[23] Zaro R, Lupsor-Platon M, Cheviet A, Badea R. The pursuit of normal reference values of pancreas stiffness by using acoustic radiation force impulse (ARFI) elastography. Medical Ultrasonography. 2016;**18**(4):425-430

[24] Chantarojanasiri T, Hirooka Y, Kawashima H, Ohno E, Sugimoto H, Hayashi D, et al. Age-related changes in pancreatic elasticity: When should we be concerned about their effect on strain elastography? Ultrasonics. 2016;**69**:90-96

[25] Zaro R, Dina L, Pojoga C, Vesa S, Badea R. Evaluation of the pancreatic tumors by transabdominal shear wave elastography: Preliminary results of a pilot study. Medical Ultrasonography. 2018;**20**(3):285-291

[26] Mei M, Ni J, Liu D, et al. EUS elastography for diagnosis of solid pancreatic masses: A meta-analysis. Gastrointestinal Endoscopy. 2013;**77**:578-589

[27] Pei Q, Zou X, Zhang X, et al. Diagnostic value of EUS elastography in differentiation of benign and malignant solid pancreatic masses: A meta-analysis. Pancreatology. 2012;**12**:402-408

[28] Popescu A, Săftoiu A. Can elastography replace fine needle aspiration? Endosc Ultrasound. 2014;**3**:109-117. DOI: 10.4103/2303-9027.123009

[29] Yashima Y, Sasahira N, Isayama H, Kogure H, Ikeda H, Hirano K, et al. Acoustic radiation force impulse elastography for noninvasive assessment of chronic pancreatitis. Journal of

Gastroenterology. 2012;**47**:427-432. DOI: 10.1007/s00535-011-0491-x

[30] Kuwahara T, Hirooka Y, Kawashima H, Ohno E, Ishikawa T, Yamamura T, et al. Usefulness of shear wave elastography as a quantitative diagnosis of chronic pancreatitis. Journal of Gastroenterology and Hepatology. Mar 2018;**33**(3):756-761

[31] Iglesias-Garcia J, Domínguez-Muñoz JE, Castiñeira-Alvariño M, Luaces-Regueira M, Lariño-Noia J. Quantitative elastography associated with endoscopic ultrasound for the diagnosis of chronic pancreatitis. Endoscopy. 2013;**45**:781-788. DOI: 10.1055/s-0033-1344614

[32] Domínguez-Muñoz JE, Alvarez-Castro A, Lariño-Noia J, Nieto L, Iglesias-García J. Endoscopic ultrasonography of the pancreas as an indirect method to predict pancreatic exocrine insufficiency in patients with chronic pancreatitis. Pancreas. 2012;**41**:724-728. DOI: 10.1097/MPA.0b013e31823b5978

[33] Dietrich CF, Hirche TO, Ott M, Ignee A. Real-time tissue elastography in the diagnosis of autoimmune pancreatitis. Endoscopy. 2009;**41**:718-720

[34] Harada N, Ishizawa T, Inoue Y, Aoki T, Sakamoto Y, Hasegawa K, et al. Acoustic radiation force impulse imaging of the pancreas for estimation of pathologic fibrosis and risk of postoperative pancreatic fistula. Journal of the American College of Surgeons. 2014;**219**:887-894.e5. DOI: 10.1016/j.jamcollsurg.2014.07.940

[35] Hatano M, Watanabe J, Kushihata F, Tohyama T, Kuroda T, Koizumi M, et al. Quantification of pancreatic stiffness on intraoperative ultrasound elastography and evaluation of its relationship with postoperative pancreatic fistula. International Surgery. 2015;**100**:497-502. DOI: 10.9738/INTSURG-D-14-00040.1

[36] Lee TK, Kang CM, Park MS, Choi SH, Chung YE, Choi JY, et al. Prediction of postoperative pancreatic fistulas after pancreatectomy: Assessment with acoustic radiation force impulse elastography. Journal of Ultrasound in Medicine. 2014;**33**:781-786. DOI: 10.7863/ultra.33.5.781

Chapter 10

# Assessment of De Quervain Tenosynovitis Patients with Strain-Based Elastography

*Ahmad Mohammad Ghandour*

## Abstract

Elastography was introduced to clinical practice almost two decades back, to further enhance ultrasound imaging for illustrating the difference in mechanical properties between diseased and healthy tissues, i.e., difference in tissue stiffness, in a qualitative and quantitative way. In the nineteenth century, Fritz De Quervain reported patients with pain and swelling at the wrist. It is an entrapment condition of the tendons within the first extensor compartment. The advantages of ultrasound (U/S), in general, is being a rapid bed-side test, low cost, availability, and great patient compliance all of which elastography makes use of. Elastography imaging for liver fibrosis assessment is a well-known technique; yet recent territories for tissue elasticity assessment are emerging. One of these large territories is muscle tendons elasticity assessment in different pathologic conditions. One of these areas is changes in tendons stiffness. Fifty-two subjects were studied, 30 diseased and 22 healthy. The main complaint of the diseased group was pain at the radial side of the wrist, while healthy subjects were symptom free. Sensitivity was 92%, while specificity was 93%. From my work, I reached the conclusion of that the disease can be diagnosed with strain-based elastography in a quantitative way with confidence and reliability.

**Keywords:** ultrasound, elastography, strain-based elastography, strain elastography, wrist joint, De Quervain tenosynovitis

## 1. Introduction

Elastography was introduced to clinical practice almost two decades back, to further enhance ultrasound imaging [1] and illustrate the difference in mechanical properties between diseased and healthy tissue [2], i.e., difference in tissue stiffness, in a qualitative and quantitative way. The basic idea of elastography is to take advantage of the changed tissue elasticity/stiffness during tissue disease as compared to adjacent similar normal tissues.

The advantages of ultrasound (U/S)—in general—is being a rapid bed-side test, low cost, availability, and great patient compliance all of which elastography makes use of.

Elastography imaging for liver fibrosis assessment is a well-known technique; yet recent territories for tissue elasticity assessment are emerging. One of these large territories is muscle tendons elasticity assessment in different pathologic conditions. One of these areas is changes in tendons stiffness.

In the nineteenth century, Fritz De Quervain reported patients with pain and swelling at the wrist. It is an entrapment condition (tendon inflammation) of the

tendons within the first extensor (dorsal) compartment of the wrist back of the wrist; patients suffered pain during motion of the thumb. The tenosynovitis affects the abductor pollicis longus (APL) and the extensor pollicis brevis (EPB) tendons-muscle tendons at the back of the wrist [3].

Anatomically, the first extensor compartment of wrist joint is lying between the radial styloid process and the base of the thumb, containing two muscle tendons: the abductor pollicis longus (APL).

De Quervain disease is considered the second most common tendon entrapment condition after trigger finger. Because of repeated trauma, the first dorsal extensor compartment tendons thicken, hindering their gliding through the tight fibro-osseous tunnel.

In B-mode ultrasound scan of the first dorsal compartment, we can find one or more of the following criteria: fluid collection, thickening of tissues, or tissue edema. Colored Doppler application to the tissue under investigation shows increased blood flow to the area.

## 2. Elastography techniques

Tissue elasticity is assessed with ultrasound tissue elastography. Elasticity of a tissue is its tendency to resist deformation when applying force the tissue in question, or regaining its original shape after cessation of the force. The idea of elastography is based on assuming that the tissue under examination is entirely elastic and has no viscosity [4].

Two main techniques are developed to measure tissue elasticity quantitatively using ultrasound machines:

1. Strain technique: apply normal stress to the tissue and the normal strain of the tissue is calculated; where tissue strain is its ability to expand after removal of the stress [4].

2. Shear-wave technique: a dynamic stress applied to the tissue under examination using different techniques to apply such a dynamic stress, and the tissue strain is calculated [4].

## 3. Strain technique

Strain technique is first to evolve between the two techniques mentioned above, and it uses two methods for strain calculation: either strain elastography or acoustic radiation force impulse (ARFI). What we are concerned here is about the first method, i.e., strain elastography.

Strain elastography can be achieved by two methods of excitation:

1. Manual compression by the operator using the ultrasound transducer; provided that the examined tissue is superficial.

2. No manual compression; where tissue displacement occur physiologically with internal organs as cardiovascular or respiratory systems, hence deeper structures could be studied.

What we are concerned with here is manual compression that is explained in details later on.

## 4. Tsukuba score for tissue elasticity

Tsukuba elasticity score is a 1–5 score scale; built upon a map of stiffness of tissues in and around the pathologically affected segment, and the score calculated based upon the stiffness of the lesion in relation to the surrounding tissues.

a. Lesions scored (1): lesion has less or equal stiffness to surrounding tissues;

b. Lesions scored (2): lesion has mixed areas of stiffness;

c. Lesions scored (3): lesion is stiffer than surrounding tissue, and on elastogram has lesser size than B-mode ultrasound;

d. Lesions scored (4): lesion is stiffer than the surrounding tissue, and on elastogram has same size as B-mode ultrasound; and

e. Lesions scored (5): lesion is stiffer than the surrounding tissue, and larger on elastogram than B-mode ultrasound.

## 5. Study goal

My hypothesis was that with the pathological changes in the first extensor compartment tendons of the wrist by virtue of the disease, we could use the Tsukuba score for tissue elasticity [5] to quantitatively assess the elasticity or hardness of the affected tendons.

## 6. Ultrasound and strain-based elastography examination technique

Ultrasound examinations performed using Philips IU22 xMatrix machine (Philips Ultrasound, Bothell, WA, USA) with linear transducer (12–15 MHz). Advanced small parts option and elastography QLAB were used.

The patient positioned in sitting at the edge of the examination couch with legs dependent, i.e., both knees flexed at right angle with forearm under examination positioned over the ipsilateral thigh in pronation with a clean plastic sheet in between the thigh and forearm of the patient.

B-mode ultrasound examination of the compartment retinaculum and tendons performed at the start to scrutinize the full spectrum of the lesion in transverse and longitudinal views.

Strain-based elastography was then performed by applying controlled pressure over the compartment guided by colored column on screen of ultrasound machine to achieve the proper pressure amount for strain-based elastography calculation by the machine.

Strain-based elastography mean and standard deviation calculations readings are then displayed.

Three strain-based elastography readings are taken for the patient and averaged to calculate the final reading, which will be used to diagnose the condition.

## 7. The problem

The condition is an entrapment syndrome.

## 8. Anatomy

The first extensor compartment of wrist joint is lying between the radial styloid process and the base of the thumb, containing two muscle tendons: the abductor pollicis longus (APL), which is inserted into the base of the first metacarpal bone, or into trapezium bone and extensor pollicis brevis (EPB), which is inserted into the proximal phalanx of the thumb [6].

The APL and EPB muscle tendons with their synovial sheets travel under the extensor retinaculum, which are attached to radial styloid forming tight fibro-osseous tunnel.

## 9. Epidemiology

De Quervain tenosynovitis is considered the second most common tendon entrapment condition after stenosing tenosynovitis-trigger finger [7].

The condition occurs in middle-aged persons with 3:1 female to male ratio [7].

The condition occurs by the virtue of repetitive wrist movement associated with thumb radial abduction with wrist extension and radial wrist deviation [8].

The classic populations are mothers and childcare workers; however, secretaries and nurses much presented [7, 8]. Other populations affected are golf players or frequent hammer users [9, 10].

Modern life style escalated the incidence of De Quervain tenosynovitis because of computer and cellular phones excessive use [11].

## 10. Clinical presentation

Main patient complaint is pain and swelling over the styloid process of the radius [12].

On examination, swelling and tenderness over radial styloid found. Crepitus and triggering may be also found [12].

Finkelstein's test, the clinical test examination, involves flexion of the meta-carpophalangeal joint of the thumb in a closed hand followed by ulnar deviation passively of the wrist joint can replicate the pain at radial styloid [9, 12].

## 11. Pathology

Because of repeated trauma, the APL and EPB tendons thicken, hindering their gliding through the tight fibro-osseous tunnel [13, 14].

Pathologically, the tendons are thickened by virtue of degenerative changes such as myxoid degeneration, deposition of mucopolysaccharides, and fibrocartilag-enous metaplasia [13, 14].

Hence, it is a misnomer to call the condition tenosynovitis, as the pathological changes do not involve tendons inflammation [15].

## 12. B-mode ultrasound findings

Several findings could be detected in B-mode ultrasound scan of the first dorsal compartment prior to strain-based elastography application; these findings include [16]:

- Fluid collection in the tendon sheaths (**Figure 1**).
- Thickened overlying retinaculum.
- Thickened synovial sheaths (**Figure 2**).
- Thick edematous tendons of APL and EPB (**Figure 3**) at level of styloid process of the radius (compared with contralateral side).
- Halo sign; due to edema in the tissues surrounding the tendons.
- Doppler application reveals hyperemia surrounding the tendons.

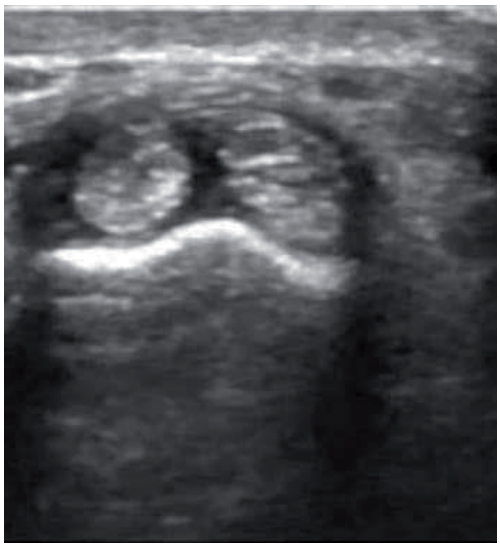

**Figure 1.**
*Fluid collection in the synovial sheaths of APL and EPB muscle tendons in transverse ultrasound image of a patient with De Quervain tenosynovitis.*

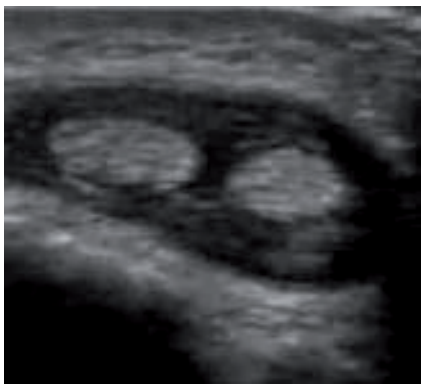

**Figure 2.**
*Thickened synovial sheaths of APL and EPB muscle tendons with fluid collection in tendon sheath in transverse ultrasound image of a patient with De Quervain tenosynovitis.*

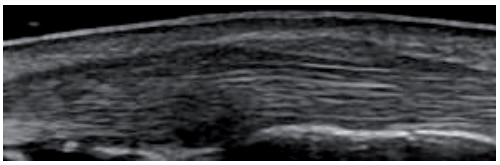

**Figure 3.**
*Thick edematous tendon of APL muscle in longitudinal ultrasound image of a patient with De Quervain tenosynovitis.*

| Index | Percentage (%) |
|---|---|
| PPV | 95 |
| NPV | 90 |
| Sensitivity | 92 |
| Specificity | 93 |

**Table 1.**
*Strain-based elastography indices.*

| Number of subjects | Strain-based elastography ratio |
|---|---|
| 28 patients | 1–3.5 |
| 2 patients | 4.2–6 |
| 20 volunteers | 6.1–9.2 |
| 2 volunteers | 2–3.9 |

**Table 2.**
*Strain-based elastography ratios in De Quervain tenosynovitis patients and volunteers.*

## 13. Current study

Fifty-two subjects were studied; 30 diseased comprised group 1 and 22 healthy comprised group 2.

The main complaint of the diseased group was pain at the radial side of the wrist with positive Finkelstein test, while healthy subjects were symptom-free with negative Finkelstein test.

There was no significant difference ($p > 0.01$) between groups in regards to age and sex.

Strain-based elastography indices are illustrated in **Table 1**.

The mean elastography value for the diseased was 2.3; while for healthy subjects, it was 6.1 with statistically significant difference between the two groups ($p < 0.001$). For strain ratio details, refer to **Table 2**.

The threshold for diagnosing De Quervain disease was 4.

B-mode ultrasound findings displayed in **Table 2** [3].

## 14. Discussion

In De Quervain tendinopathy tendon increased cross section, increased water content of the tendons, abnormal degenerative materials deposited, and changes in collagen fibers properties all lead to changes of the elastic characteristics of the tendons with consequent softening of the affected tendons [17].

In my work, I found lower sensitivity (92%) than specificity (93%) for the quantitative assessment of the disease, in accordance with the remarks of Sébastien Aubry studying the Achilles tendinopathy with shear-wave elastography [18].

De Zordo et al. [19] stated that normal Achilles tendons show hard consistency as compared to diseased tendons, going with my work results of 6.1 elastography mean value for healthy subjects and 2.3 for diseased. Moreover, Dirrichs et al. [20] studied epicondylar, Achilles, and prepatellar pathologic tendons and found that the diseased tendons returned decreased elastography values as compared to healthy volunteers regardless of anatomical location.

In my study, I found statistically significant difference ($p < 0.001$) between healthy and diseased subjects in regards to elastography readings in accordance with Chen and coworkers concluding that elastography is an important tool for mechanical information assessment of Achilles function [21].

In two healthy subjects, we found low strain ratio, which could be explained by the fact that they were having subclinical tenosynovitis as postulated by De Zordo et al. [22].

Moreover, not possibly to explain the three diseased tendons showing high elastography values except for one patient with cyst formation under the retinaculum raising the tension inside the compartment.

More study is needed for the true benefit of strain-based elastography of the condition comparing the results with histopathological specimens—if possible—of the affected tendons, for a definitive proof of the presence or absence of the disease and the state of progression of the disease.

## 15. Conclusion

We can conclude that the disease can be diagnosed with strain-based elastography in a quantitative way with confidence and reliability.

## Conflict of interest

The author declares no conflict of interest financially or personally with any institution, organization, or persons.

## Author details

Ahmad Mohammad Ghandour
Department of Radiology, Faculty of Medicine, Ain Shams University Cairo, Egypt

*Address all correspondence to: ahmed_ghandour@med.asu.edu.eg

## References

[1] Prker KJ, Huang SR, Musulin RA, Lerner RM. Tissue-response to mechanical vibrations for sonoelasticity imaging. Ultrasound in Medicine & Biology. 1990;**16**:241-246

[2] Doyley MM, Parker KJ. Elastography: General principles and clinical applications. Ultrasound Clinics. 2014;**9**(1):1-11. DOI: 10.1016/j.cult.2013.09.006

[3] Ghandour AM, Ghandour TM. Strain-based elastography assessment of patients with De Quervain tenosynovitis: A preliminary study. The Egyptian Journal of Radiology and Nuclear Medicine. 2018;**49**:415-418

[4] Sigrist RMS, Liau J, El Kaffas A, Chammas MC, Willmann JK. Ultrasound elastography: Review of techniques and clinical applications. Theranostics. 2017;**7**(5):1303-1329. DOI: 10.7150/thno.18650

[5] Itoh A, Ueno E, Tohno E, Kamma H, Takahashi H, Shiina T, et al. Breast disease: Clinical application of US elastography for diagnosis. Radiology. 2006;**239**:341-350

[6] Hazani R, Engineer NJ, Cooney D, Wilhelmi BJ. Anatomic landmarks for the first dorsal compartment. Eplasty. 2009;**8**:6-11

[7] Zanzoni A. Mint: A molecular interaction database. Journal of Microbiology. 2002;**513**:135-140. DOI: 10.1016/s0014-5793(01)03293-8

[8] Satteson E, Shruti C. Tannan: De Quervain tenosynovitis. In: StatPearls. Treasure Island (FL): StatPearls Publishing; 2019

[9] Ritu G, Abzug Joshua M. De Quervain's tenosynovitis: A review of the rehabilitative options. Hand (N Y). 2015;**10**(1):1-5

[10] Jaworski CA, Krause M, Brown J. Rehabilitation of the wrist and hand following sports injury. Clinics in Sports Medicine. 2010;**29**(1):61-80. DOI: 10.1016/j.csm. 2009.09.007

[11] Ali M, Asim M, Danish SH, et al. Frequency of De Quervain's tenosynovitis and its association with SMS texting. Muscles Ligaments Tendons Journal. 2014;**4**(1):74

[12] Stoller DW, Tirman PF, Bredella MA. Diagnostic imaging, Orthopaedics. Amirsys Inc; 2004. ISBN: 0721629202

[13] Cyriac P-V, van der Windt DAWM, Winters Jan C, Betty M-d J, Cochrane Musculoskeletal Group. Corticosteroid injection for de Quervain's tenosynovitis. Cochrane Database of Systematic Review; 2009. DOI: 10.1002/14651858. CD005616.pub2

[14] Min CJ, Jae-Kyung W, Kyoung-Bun L, In Ae P, Ann Y, Kyung MW. Comparison of shear-wave and strain ultrasound elastography in the differentiation of benign and malignant breast lesions. AJR. 2013;**201**:W347-W356

[15] Clarke MT, Lyall HA, Grant JW, Matthewson MH. The histopathology of de Quervain's disease. Journal of Hand Surgery (British). 1998;**23**(6):732-734

[16] Diop AN, Ba-Diop S, Sane JC, et al. Role of US in the management of de Quervain's tenosynovitis: Review of 22 cases. Journal de Radiologie. 2008;**89** (9 Pt 1):1081-1084

[17] Cortes Daniel H, Suydam Stephen M, Grävare SK, Buchanan Thomas S, Elliott Dawn M. Continuous shear wave elastography: A new method to measure in-vivo viscoelastic properties of tendons. Ultrasound in Medicine & Biology. 2015;**41**(6):1518-1529

[18] Sébastien A, Jean-Philippe N, Mickaël T, Fabio B, Chrystelle V, Fabrice M. Viscoelasticity in achilles tendinopathy: Quantitative assessment by using real-time shear-wave elastography. Radiology. 2015;**274**(3)

[19] Tobias DZ, Christian F, Feuchtner Gudrun M, Vinzenz S, Markus R, Sabine KA. Real-time sonoelastography findings in healthy achilles tendons. AJR. 2009;**193**:W134-W138

[20] Dirrichs T, Quack V, Gatz M, et al. Shear wave elastography (SWE) for the evaluation of patients with tendinopathies. Academic Radiology. 2016;**23**(10):1204-1213

[21] Chen XM, Cui LG, He P, et al. Shear wave elastographic characterization of normal and torn achilles tendons a pilot study. Journal of Ultrasound in Medicine. 2013;**32**(3):449-455

[22] De Zordo T, Chhem R, Smekal V, et al. Real-time sonoelastography: Findings in patients with symptomatic achilles tendons and comparison to healthy volunteers. Ultraschall in der Medizin. 2010;**31**(4):394-400

*Edited by Monica Lupsor-Platon*

Elastography, the science of creating noninvasive images of mechanical characteristics of tissues, has been rapidly evolving in recent years. The advantage of this technique resides in the ability to rapidly detect and quantify the changes in the stiffness of soft tissues resulting from specific pathological or physiological processes. Ultrasound elastography is nowadays applied especially on the liver and breast, but the technique has been increasingly used for other tissues including the thyroid, lymph nodes, spleen, pancreas, gastrointestinal tract, kidney, prostate, and the musculoskeletal and vascular systems. This book presents some of the applications of strain and shear-wave ultrasound elastography in hepatic, pancreatic, breast, and musculoskeletal conditions.

Published in London, UK


IntechOpen

ISBN 978-1-83880-015-4
9 781838 800154